University of Cyprus

**DEPARTMENT OF CIVIL AND ENVIRONMENTAL ENGINEERING**

# INVESTIGATION OF THE EFFECT OF SOIL DEFORMABILITY ON THE PEAK SEISMIC RESPONSE OF CONVENTIONAL AND BASE-ISOLATED BUILDINGS THROUGH SAP2000 OAPI PARAMETRIC ANALYSES

MASTER OF SCIENCE (M. Sc.) THESIS in EARTHQUAKE ENGINEERING

**CHRISTOS ANASTASIOU**

B. Sc. in Civil and Environmental Engineering, University of Cyprus

2022

**DEPARTMENT OF CIVIL AND ENVIRONMENTAL ENGINEERING**

# INVESTIGATION OF THE EFFECT OF SOIL DEFORMABILITY ON THE PEAK SEISMIC RESPONSE OF CONVENTIONAL AND BASE-ISOLATED BUILDINGS THROUGH SAP2000 OAPI PARAMETRIC ANALYSES

By

**Christos Anastasiou**

**Examination Committee:**

**Dimitrios Loukidis**, Associate Professor
Department of Civil and Environmental Engineering, University of Cyprus

**Dimos C. Charmpis**, Associate Professor
Department of Civil and Environmental Engineering, University of Cyprus

**Petros Komodromos**, Associate Professor
Department of Civil and Environmental Engineering, University of Cyprus

**Thesis supervisor:**

**Petros Komodromos**, Associate Professor
Department of Civil and Environmental Engineering, University of Cyprus

# ABSTRACT

The earthquake resistant design of a structure is implemented according to the relevant provisions of the seismic codes of each country. Most seismic codes, including the Eurocodes, assume that the structure is fixed-supported to a rigid ground. This ''conservative'' simplification is based on the assumption that potential contribution of soil deformability in the seismic response of a structure is considered as beneficial, compared to the response of the corresponding fixed-supported. Therefore, the influence of soil deformability is ignored, assuming that it can be only beneficial. However, in some cases, it has been observed that the peak seismic response of a structure founded on a rigid ground, without the effect of soil deformability, may lead to a lower estimation of the actual peak seismic response. In addition, taking into account the soil deformability, the structure's fundamental eigenperiod may increase. Consequently, significant differences in the seismic response of structures, may emerge due to the soil deformability, which should not be always neglected.

In this thesis, the behaviour of a spatial conventionally supported reinforced concrete building, as well as the corresponding base-isolated structure, are examined, taking into account the soil deformability. For the conventionally supported structure, linear time-history analysis is conducted, while non-linear time-history analysis is performed for the base-isolated structure, in order to take into account, the nonlinear behavior of the seismic isolation system. The soil deformability can be simulated using six springs. Specifically, one translational spring in each horizontal direction X and Y, one in the vertical Z direction, and one rotational spring in each direction (X, Y and Z). The stiffnesses of the springs are calculated in accordance with the foundation characteristics and the mechanical properties of the supporting soil. In order to examine the influence of the soil deformability in the peak seismic response, the buildings are assumed to be founded on three different soil types: rock (which represents the fixed support to a rigid ground), sand and soft clay. Moreover, both the conventionally fixed-supported building and the base-isolated building are subjected to both near-fault (NF) and far-fault (FF) seismic excitations, in order to investigate the effect of the earthquake characteristics, in addition to the soil deformability, on their peak seismic responses.

Furthermore, in this thesis the entire procedure of configuration and parametric analysis of the structural models are conducted through the SAP2000 software, using the SAP2000 Open Application Programming Interface (OAPI) in combination with the Python language. Basically, the OAPI is the interface tool that allows access to SAP2000 to perform parametric analyses, using a programming language, such as Python. More specifically, the data and parameters that are required to perform dynamic analyses and parametric studies are written in the Python programming language and then transferred to SAP2000, by its OAPI. It is remarkable that the operation of SAP2000 is done entirely in the background, through the OAPI, without any need for intervention by the user. Consequently, parametric analyses can be easily conducted with great flexibility and efficiency. Also, computed results can be efficiently and effectively postprocessed through the OAPI interactions, in order to compare them through the parametric studies.

# ΠΕΡΙΛΗΨΗ

Ο αντισεισμικός σχεδιασμός ενός οικοδομήματος πραγματοποιείται βάσει των σχετικών προνοιών των κανονισμών και κωδικών αντισεισμικού σχεδιασμού. Οι περισσότεροι αντισεισμικοί κανονισμοί, συμπεριλαμβανομένου του Ευρωκώδικα, θεωρούν ότι το υπό εξέταση οικοδόμημα εδράζεται σε ακλόνητο και απαραμόρφωτο έδαφος. Η παραμορφωσιμότητα του εδάφους παραλείπεται θεωρώντας ότι η συνεισφορά της παραμορφωσιμότητας του εδάφους στη σεισμική απόκριση των κατασκευών είναι ευνοϊκή σε σύγκριση με τη θεώρηση άκαμπτου και απαραμόρφωτου εδάφους. Εντούτοις, σε κάποιες περιπτώσεις διαφάνηκε ότι η σεισμική απόκριση μιας κατασκευής σε άκαμπτο και απαραμόρφωτο έδαφος, αγνοώντας την παραμορφωσιμότητα του εδάφους, μπορεί να οδηγήσει σε λανθασμένη εκτίμηση, σε σχέση με την πραγματική μέγιστη σεισμική απόκριση. Επιπλέον, λαμβάνοντας υπόψη την παραμορφωσιμότητα του εδάφους, η αναμενόμενη αύξηση της θεμελιώδους ιδιοπεριόδου της υπό σχεδιασμού κατασκευής ακολουθείται από σημαντική διαφοροποίηση στη σεισμική απόκριση της κατασκευής. Για το λόγο αυτό, ίσως να είναι σημαντικό να λαμβάνεται υπόψη στον αντισεισμικό σχεδιασμό των κατασκευών και η παραμορφωσιμότητα του εδάφους.

Στην διατριβή αυτή μελετήθηκε η συμπεριφορά ενός συμβατικά θεμελιωμένου κτιρίου από οπλισμένο σκυρόδεμα και του αντίστοιχου σεισμικά μονωμένου, λαμβάνοντας υπόψη την παραμορφωσιμότητα του εδάφους. Για το συμβατικό κτήριο διενεργήθηκαν γραμμικές αναλύσεις χρονοϊστορίας, ενώ για το σεισμικά μονωμένο κτίριο μη γραμμικές αναλύσεις χρονοϊστορίας για να ληφθεί υπόψη η μη γραμμικότητα του συστήματος σεισμικής μόνωσης. Η παραμορφωσιμότητα του εδάφους λήφθηκε υπόψη χρησιμοποιώντας συνολικά έξι ελατήρια. Ένα μεταθεσιακό ελατήριο σε κάθε οριζόντια διεύθυνση (Χ και Υ) και στην κατακόρυφη διεύθυνση Z, και ένα στροφικό ελατήριο σε κάθε διεύθυνση (Χ, Υ, και Z). Οι δυσκαμψίες των ελατηρίων υπολογίστηκαν σύμφωνα με τα χαρακτηριστικά της θεμελίωσης και τις μηχανικές ιδιότητες του εδάφους. Για την εξέταση της επιρροής της παραμορφωσιμότητας του εδάφους στη σεισμική απόκριση, οι κατασκευές θεωρούνταν ότι εδράζονται σε τρεις τύπους εδάφους. Συγκεκριμένα, σε βράχο ο οποίος αντιπροσωπεύει ακλόνητο και απαραμόρφωτο έδαφος, σε άμμο και σε άργιλο. Επίσης, τα δυο κτίρια υποβλήθηκαν σε σεισμικές διεγέρσεις κοντινού και

μακρινού πεδίου, ώστε να μελετηθεί η επιρροή τους, στη μέγιστη σεισμική απόκριση των κτιρίων σε συνδυασμό με την παραμορφωσιμότητα του εδάφους.

Επιπρόσθετα, στη διατριβή αυτή, ολόκληρη η διαδικασία σύνθεσης και ανάλυσης των κατασκευαστικών μοντέλων έγινε μέσω του λογισμικού μηχανικής SAP2000, όμως παρακάμπτοντας την κλασσική χειρωνακτική διαδικασία αφού, χρησιμοποιήθηκε η διεπαφή προγράμματος εφαρμογής (Open Application Programming Interface-OAPI) του λογισμικού SAP2000 και η γλώσσα προγραμματισμού Python. Βασικά, η διεπαφή προγράμματος εφαρμογής είναι το εργαλείο που ‘’ενώνει’’ και ‘’μεταφέρει’’ τα δεδομένα και τα αποτελέσματα μεταξύ του προγράμματος που αναπτύχθηκε στη γλώσσα προγραμματισμού Python και του λογισμικού SAP2000. Συγκεκριμένα, στη γλώσσα Python έχει γραφεί ο κώδικας με τον οποίο εκτελείται ολόκληρη η διαδικασίας ανάλυσης στο παρασκήνιο, μέσω του λογισμικού SAP2000, χωρίς να χρειάζεται οποιαδήποτε παρέμβαση από τον χρήστη. Με αυτό τον τρόπο μπορούν να διενεργηθούν πολύ αποδοτικά και με εξαιρετική αποτελεσματικότητα παραμετρικές αναλύσεις και να γίνει η επεξεργασία και η σύγκριση μεταξύ των αποτελεσμάτων.

# ACKNOWLEDGMENTS

With the accomplishment of this thesis, the 7th year of studies at the University of Cyprus has been completed. These seven years, I manage to obtain the bachelor's degree in civil and Environmental Engineering and the master's science degree in Civil Engineering with specialization in Earthquake Engineering. Except from the above, I have gained a lot of experiences and knowledge that changed my way of thinking and made me a better person and as well as, I made new friends that helped me at difficult moments.

Firstly, I would like to thank my supervisor, Prof. Petros Komodromos. His guidance, persistent help and great patience made this master thesis possible. My sincere thanks to my thesis examination committee members: Prof. Dimitrios Loukidis and Prof. Dimos Charmpis, for reviewing my thesis and serving on the examination committee.

Furthermore, special thanks and gratefulness goes to my best friend L., for his constant support and help throughout all of my personal hard situations. In addition, his advice made me to get over many difficulties.

Last but not least, I would like to express my biggest thank and love to my family. I am very grateful to born in this family and I am very proud for each one of them. We have been always acted together like a big punch and we faced the worst moments of our lives, always united. Therefore, this thesis is dedicated to my father Yiannis, my mother Vasoulla, my sister Petrina, my brothers Kiriakos and Marios, the angel of the family Raphael and my beloved nephew Nikolas. I hope the rest of our life would be full of health and happiness.

My motto in life by C.P. Cavafy '' As you set out for Ithaka hope your road is a long one, full of adventure, full of discovery… Keep Ithaka always in your mind. Arriving there is what you're destined for. **But don't hurry the journey at all**. Better if it lasts for years, so you're old by the time you reach the island, **wealthy with all you've gained on the way**, **not expecting Ithaka to make you rich**…''

# TABLE OF CONTENTS

# LIST OF FIGURES

# LIST OF TABLES

# Chapter 1 – INTRODUCTION

## 1.1 Motivation and Objectives

In recent years, the design of civil engineering structures in Cyprus has to be conducted according to the provisions of the relevant European earthquake resistant design code. Typically, by following the regulations of the Eurocodes for earthquake resistant buildings, the design is implemented under the assumption of a rigid ground. According to EN 1998-1:2004§4.3.1, soil deformability has to be taken into account in those cases, where it is possible to develop unfavourable effects on the structure's response. Traditionally, soil deformability is customarily assumed to be beneficial for the seismic response of structures compared to the rigid ground assumption. Thus, in many seismic codes this assumption has been adopted as a most likely conservative simplification (Mylonakis and Gazetas, 2000).

However, in some cases it has been shown that assuming an infinitely rigid support and ignoring the soil flexibility, may lead to lower estimation of the peak seismic response. Moreover, soil deformability, in general, increases the fundamental eigenperiod of the building by the decrease in the overall structural system's stiffness (Narayana, Sharada Bai and Manish, 2010). Therefore, the seismic response of a structure while taking into account the soil deformability, may significantly differ from that of the same structure with the rigid base assumption (Gowda, Narayana and Narandra, 2015). Hence, it is essential to examine how soil deformability may influence the peak seismic response of conventionally supported, as well as base-isolated, buildings.

In this thesis, the seismic response of a typical two-story concrete building is examined both as conventionally fixed-supported and as base-isolated, founded under three different soil types: rock, sand and soft clay, in order to assess the potential soil deformability effects. Linear elastic time-history analyses are performed for the conventionally fixed-supported structure, while nonlinear time-history analyses are conducted for the base-isolated building. Additionally, the influence of soil deformability on the peak seismic response, in conjunction with the impact of near-fault (NF) and far-fault (FF) ground motions, is also examined. The whole configuration, design and analysis procedure of each model under consideration, is conducted using the SAP2000 OAPI, from the beginning till the end. Specifically, the proper commands are provided in the Python

programming language. Subsequently, the connection with the SAP2000 software is achieved through its OAPI, which is the interface that conveys the given data from Python to the SAP2000 software and vice versa. In this way, it is very effective and efficient to automatically conduct parametric analyses with minimal user interventions. In addition, the postprocess of the computed results is available through the OAPI interactions, in order to effectively compare them through the parametric studies.

## 1.2 Consideration of soil deformability

The assumption that is widely used while examining and analysing a structure under an earthquake excitation, is that the structure is considered to be fixed-supported to an infinitely rigid ground. Hence, the deformability of the supporting ground is ignored, while the structure might develop tensile stresses at its supports without, partially or entirely detaching from the ground. Therefore, it might be essential to take into account the influence of soil deformability in the seismic response of structures (Kostopoulou, 2016), since the peak seismic response of a structure founded on a rigid base, may vary significantly from the same structure resting on a deformable soil (Patel et al., 2011). A relevant research work on the deformability of soil by Casolo, Diana and Uva (2016) identified that the assumption of a fixed base constraint is untrustworthy.

The soil deformability leads to the lengthening of the lateral natural eigenperiod of a building due to the overall decrease in its lateral stiffness. Such lengthening of the fundamental eigenperiod, could alter remarkably the seismic response of structures, especially for stiff and massive structures constructed on relatively soft soil (Bhattacharya, Dutta and Dasgupta, 2004; Gowda, Narayana and Narandra, 2015). A more recent study by Bayraktar and Hökelekli (2020) tried to investigate the influence of soil deformability, where it was observed that soil deformability increased the number of damaged elements. Furthermore, according to Tengali and Suman (2017), the influence of soil deformability becomes dangerous for heavy structures founded on soft soils. In addition, according to Mylonakis and Gazetas (2000), it might be very likely for a structure to be detrimentally affected due to the increase of its fundamental eigenperiod. Hence, the common assumption of solely beneficial effects of soil deformability may lead to unsafe design. However, some authors concluded that the influence of soil deformability is negligible (Hatzigeorgiou and Beskos, 2010; Rodriguez and Montes, 2000). For assessing how soil

deformability may influence the seismic response of a structure, the structure can be conveniently simulated using a set of elastic springs (Narayana, Sharada Bai and Manish, 2010), which represents the soil deformability. The Winkler approach to simulate the soil deformability, by using elastic spring, was utilized also by Roopa *et al.* (2015).

According to the literature review provided by Mahmoud, Austrell and Jankowski (2012), several studies disregarded the effects of soil deformability on the dynamic response of base-isolated structures. Thus, they examined the influence of soil deformability on the seismic response of base-isolated buildings, where it was observed that the soil deformability might remarkably affect the seismic response of base-isolated buildings. Specifically, the superstructure's response was affected, especially for structures with longer natural periods or for seismic excitations with high Peak Ground Acceleration (PGA). Furthermore, previous observations (Gazetas and Dobry, 1984; Kavvadas and Gazetas, 1993; Nikolaou *et al.*, 2001) had demonstrated that the seismic response of large structures founded on soft soil conditions, might be affected by the soil deformability. Another research by Wu and Chen (2001), showed that the increase in an soil flexibility led to an increase of the base shear values. Additionally, the interstorey drifts were increasing with the soil's deformability. Last, but not least, a more recent research work by Aden *et al.* (2019), concluded that the soil deformability reduced the efficiency of the base isolation due to the provided additional flexibility to the system, which led to an increase in the deformations of the structure.

## 1.3 Open Application Programming Interface (OAPI) of SAP2000 and Python

Since we need to perform a large number of parametric studies with time-history dynamic analyses, the Open Application Programming Interface (OAPI) of SAP2000, through the Python programming language, are utilized.

Specifically, the OAPI is a mediator between the components of two applications, which works in the background and provides the means for their interactions through simple commands. In addition, APIs act like 'messengers' that deliver requests and return responses between applications. In particular, in each interaction there is a server and a client. The first provides the resource and the latter makes the request. Since the server is able to implement the request of the client, the API will return the relevant resource. For

the current thesis, the structural analysis and design software SAP2000 is accessed through its OAPI, to conduct parametric analyses.

The SAP2000 OAPI is a powerful tool that makes feasible for the users to automate numerous processes that are related to the configuration, analysis and design of structural models. Additionally, through the use of the OAPI, the link of the SAP2000 software with third-party software, can be achieved. Furthermore, it allows the users to obtain customized analysis and design results. For the performed simulations, the required data, functions and parameters for the configuration of the examined model and for the implementation of the dynamic analysis, are written in Python and transferred to SAP2000, by its OAPI. Subsequently, the SAP2000 software, taking into account the given data, creates and designs the model and executes the dynamic analysis, in the background. Hence, the standard point-and-click manual procedure is by-passed. Moreover, by using SAP2000 OAPI, easy control and access to the analysis data is facilitated. With this approach, parametric analyses can be effectively conducted with great flexibility and efficiency. Several major and popular programming languages can be used to implement parametric analyses by accessing SAP2000 through its OAPI, but the chosen one for this thesis is Python.

Python is an interactive, interpreted and object-oriented programming language. Despite the fact that Python is a high-level programming language with significant power, it has a very clear and simple syntax, which is similar to English language writing. Moreover, its syntax provides the ability for developers to write programs with fewer lines, in comparison with other programming languages. Furthermore, Python's syntax and dynamic typing in combination with its interpreted nature, make it an ideal language for scripting and rapid application development, for many circumstances. Hence, it is easy to read and understand the written code and, generally, it is easy to learn how to utilize the Python language. Additionally, the variables and their data types used in a code, have not to be pre-declared since Python automatically assigns the data type during the execution of the code. Also, Python runs on an interpreter system, which means that the code can be executed simultaneously, while it is written but at a significant computational cost, since it is much slower than compiled programming languages. Finally, Python is a free of charge and open-source language, which comes under the Open-Source Initiative (OSI) approved open-source license.

## 1.4 Outline

A brief overview of how the parametric analyses will be conducted through the SAP2000 OAPI for the examination of the effect of the soil deformability, for conventional and base-isolated structures, is introduced in this chapter. Subsequently, the theoretical background, via the available literature review, is provided in chapter 2.

Chapter 3 summarises the basic characteristics of the Python programming language and discusses its advantages, compared to other programming languages. Moreover, the utilization of the SAP2000 OAPI is briefly explained, in order to perform parametric analyses.

The following chapter, Chapter 4, outlines the conventional structure models' configuration and design, which include the soil deformability simulation, the superstructure characteristics and the applied seismic excitations. In addition, it provides some information about the dynamic time-history analysis, as well as the results of the conventional structure's modal analysis supported on the three considered soil types.

Linear time-history analyses through the SAP2000 OAPI are performed in Chapter 5 for the conventionally supported building considering soil deformability. More precisely, the maximum interstorey drifts and the peak absolute floor accelerations of the conventional structure founded on rock, sand and soft clay are illustrated and discussed, in order to investigate the influences of soil deformability. Furthermore, the effects of the selected near-fault (NF) and far-fault (FF) seismic ground motions are investigated, by performing parametric analyses under 5 pairs of NF and 5 pairs of FF seismic records, in combination with the soil deformability.

Chapter 6 begins with a description of the available seismic isolation options and then, the configuration and the design of the seismic isolation system that is used with the considered two-story R/C building, is described. Then, the potential effect of soil deformability on the considered seismically isolated building is assessed in Chapter 7. Specifically, a similar study to that conducted to investigate the potential soil deformability influences on the peak seismic response of the conventionally supported structure, is implemented for the base-isolated structure, too. Therefore, the peak seismic response of the base-isolated structure founded on rock, sand and soft clay is computed and discussed.

Finally, Chapter 8 summarizes the main conclusions and contributions of this research work and notes its potential future research extensions.

# Chapter 2 – LITERATURE REVIEW

The literature review begins by looking at how soil deformability might be influencing the peak seismic responses of conventional structures, followed by its potential effects on base-isolated structures. In addition, the potential impact of near- *vs.* far-fault seismic ground motions on structures, is discussed.

## 2.1 Soil Deformability on Conventionally Supported Structures

A common practice, while examining and analysing a structure under an earthquake excitation, is the assumption that the structure is considered to be fixed-supported to rigid ground. Hence, the deformability of the supporting ground is completely ignored, while the structure might develop tensile stresses at its supports without the ability to detach from the ground. Nevertheless, both the soil is deformable and the transferring of tensile forces between the foundation and the ground are practically impossible.

Therefore, it might be essential to take into account the influence of soil deformability in the seismic response of buildings (Kostopoulou, 2016), since the peak seismic behaviour of a structure founded on a rigid base might remarkably differ from the same structure resting on a deformable soil (Patel *et al.*, 2011). In addition, the deformability of soil causes lengthening of fundamental eigenperiods due to the decrease in the overall stiffness of the system. Such lengthening of the fundamental eigenperiods could alter the seismic response of buildings significantly, especially for stiff and massive structures constructed on relatively soft soils (Bhattacharya, Dutta and Dasgupta, 2004; Gowda, Narayana and Narandra, 2015). The soil deformability can be conveniently simulated using a set of elastic springs (Narayana, Sharada Bai and Manish, 2010).

Manos, Naxakis and Soulis (2015) have conducted a relevant research study considering the soil deformability. More specifically, a two-story reinforced concrete frame building, with masonry infills located in Kefalonia – Greece, was designed and constructed according to the old seismic code regulations. After an intense seismic excitation that had occurred in the area, the building exhibited low to medium levels of damage, regardless of the earthquake's intensity. Therefore, the effects of the mat foundation with a thickness of 0.5 m lying on flexible soil, were investigated. Due to the lack of suitable geotechnical data of the considered area, the examination of soil-foundation deformability was strived in a

parametric way in order to define the soil's elastic properties. Three different types of soil were assumed: hard soil, medium stiffness soil and soft soil. Additionally, the simulation of the soil layers was done with two different ways. In conclusion, it was observed that soil deformability had not a notable affect to all cases. However, the fundamental eigenperiods had been slightly increased. Lastly, the radiation damping of the soft soil reduced the structural damage, especially in the case of having a mat foundation, where destructive differential displacements were restricted.

An additional research work on the deformability of soil by Casolo, Diana and Uva (2016) identified that the assumption of a fixed base constraint was untrustworthy. The specific research case concerned a bell tower without the consideration of vicinity buildings. When the soil deformability was increased, the damage at the belfry level was reduced. However, the base of the tower demonstrated local damage. Regarding the soil, different deformability profiles were assumed, which were modelled with linear elastic properties according to Kramer (1996).

A more recent study by Bayraktar and Hökelekli (2020) tried to investigate the influence of soil deformability on the damage mechanisms of brick and stone masonry bridge arches. Specifically, the Winkler spring supports method was used to simulate the soil. Three different foundation soil conditions were considered: hard, soft and an intermediate situation between them. It had been observed that the smallest tensile damage happened in medium soil conditions. However, a reduction in soil deformability had been found to cause an increase to tensile damage levels in the case of brick arches. Additionally, most and least damaged elements found to be in the case of medium soil condition and hard soil condition, respectively. Consequently, switching the soil condition from hard to medium increased the number of the damaged elements.

Roopa *et al.* (2015), also used the Winkler approach to simulate the soil deformability for the analysis, too. Specifically, the springs had been applied to a mat foundation of a 13-storey R/C building. Moreover, the springs' stiffnesses values had been calculated by using the Richart and Lysmer expressions. As a result, higher interstorey drifts had been observed, especially in the middle storeys. Furthermore, the response of the structure assuming soil flexibility, was more unfavorable than considering a rigid base. In contrast, Zanwar and Hosur (2016), had examined the soil flexibility, following the FEMA

356 guidelines to calculate the stiffnesses of the springs representing the soil deformability, which were modelled using the ETABS software. The outcome of that research study was that soil deformability led to an increase in the fundamental eigenperiod of the structure. The same had been observed by Upadhaya (2018). Also, Zanwar and Hosur (2016), also stated that storey displacements were larger when soil flexibility had been considered, although the base shear was smaller.

According to Tengali and Suman (2017), the influence of soil deformability becomes dangerous for heavy structures founded on soft soils. Specifically, two different kinds of foundation had been assumed for an 8-storey R/C structure. A model with a mat foundation and a model with pile foundations, were analyzed using the SAP2000. While, for the case of mat foundation the maximum displacement was reduced, when soil deformability had been considered, it was increased for the model of pile foundations.

In accordance with low-rise frame structures, it had been observed that the seismic response could remarkably be increased, taking into account soil flexibility, whereas, the response of medium to tall height buildings tend to decrease (Dutta, Bhattacharya and Roy, 2004). Expressions by Gazetas (1991) were used for the calculation of soil deformability parameters. In addition, Farghaly's and Ahmed's (2013) research, concluded that taking into account soil flexibility leads to a more conservative seismic response of tall buildings, too.

It is worth to mention that, some authors concluded that the influence of soil deformability is negligible (Hatzigeorgiou and Beskos, 2010; Rodriguez and Montes, 2000). However, according to Mylonakis and Gazetas (2000), it might be very likely for a structure to be detrimentally affected due to the increase of its fundamental eigenperiod. Hence, the common view of beneficial effects of soil deformability may lead to unsafe design.

Conclusively, several studies presented and explained alternative models to consider soil deformability (Chen and Yang Shi, 2013; Patel *et al.* 2011; Dutta and Roy, 2002).

## 2.2 Soil Deformability on Base-Isolated Structures

According to the literature review provided by Mahmoud, Austrell and Jankowski (2012), several studies disregard the effects of soil deformability on the dynamic response of base-isolated structures. By ignoring the soil deformability, unreliable results might be obtained, since the earthquake-resistance design for buildings is based on fixed supports to infinitely stiff ground. Previous observations (Gazetas and Dobry, 1984; Kavvadas and Gazetas, 1993; Nikolaou *et al.*, 2001) had demonstrated that the seismic response of large structures founded on soft soil conditions, might remarkably be affected by soil deformability. Furthermore, a significant number of studies, that examined the effects of soil deformability for seismically isolated bridge structures (Vlassis and Spyrakos, 2001; Tongaonkar and Jangid, 2003; Kunde and Jangid, 2006; Soneji and Jangid, 2008) have been published. However, very limited research studies have been conducted, considering the effect of soil deformability on the peak seismic response of seismically isolated buildings. According to Spyrakos *et al.* (2009), considering the soil deformability is important for a single degree of freedom (SDOF) system. Thus, they investigated how soil flexibility might influence a base-isolated structure under harmonic ground motions.

In addition to the above, Mahmoud, Austrell and Jankowski (2012) examined the influence of soil deformability on the seismic response of base-isolated buildings. Laminated rubber bearings (LRBs) and high damping rubber bearings (HDRBs) had been used for the base-isolation systems. Specifically, buildings with different fundamental eigenperiods were considered, as well as different soil types and seismic motions, had been used. Additionally, the buildings were modelled both as SDOF and MDOF. Moreover, the expressions that had been used to calculate the spring stiffnesses and damping coefficients of the foundation, in order to consider the soil deformability, were proposed by Whitman and Richart (1967). It is worth to mention that the ordinary consideration for the soil material is to be a homogeneous elastic half-space. Whereas, other researchers recommended lumped-parameter models (Wolf and Somaini, 1986; Wu and Chen, 2001) for the soil material.

Mahmoud, Austrell and Jankowski (2012) observed that the soil deformability might remarkably affect the seismic response of base-isolated buildings. The superstructure's response was affected, especially for structures with longer fundamental eigenperiods or

for seismic excitations with a high peak ground acceleration (PGA). In addition, greater accelerations, velocities and displacements values were observed considering soil flexibility for the LRBs system. Lastly, HDRBs led to higher structural peak responses, considering soil deformability, in comparison with the LRBs.

Another research study by Wu and Chen (2001), tried to examine the above issue. Specifically, three soil conditions had been assumed: hard soil, medium soil and soft soil. The analysis was conducted using the ETABS software. As a result, the increase in the soil flexibility led to an increase of the base shear values. Additionally, the interstorey drifts were increasing with the soil's deformability. Hence, development of largest drifts arised in the case of soft soil conditions. The same could be observed for the values of story shears. Finally, Wu and Chen (2001) concluded that, multi-storey base-isolated structures were more suitable to be founded on hard soil conditions and on medium soil conditions, based on the computed seismic responses.

The SAP2000 software was utilised by Aden *et al.* (2019), to study the seismic response, considering the soil deformability of a base-isolated building. They concluded that the soil deformability lessened the efficiency of base isolation due to the provided additional flexibility to the system, which led to an increase in the deformations of the structure. Furthermore, Karabork, Deneme and Bilgehan (2014) used SAP2000 software to study a base-isolated building with HDRBs. It had been concluded that, soil deformability was a significant factor to be considered for the selection of the appropriate base isolation system, for a structure. The same was highlighted by Stehmeyer and Rizos (2008) research. For instance, when soil deformability was taken into account, stiff isolators tended to decrease the effects of the seismic excitation. In addition, structure's performance was found to be directly proportional to the isolator's stiffness. Therefore, Karabork, Deneme and Bilgehan (2014) stated that an isolation system could be ideal for a rigid base support. However, the effectiveness of the same isolation system considering soil deformability as well, decreases. On the other hand, Forcellini (2018) used the OpenSeesPL computational interface to examine the effect of soil deformability in relation to the seismic response of base-isolated structures. Consequently, Forcellini mentioned that the eigenperiod of the structure increased when the soil deformability increased. The same happened to the displacements, although, the base shear was reduced. Lastly, an increase in soil deformability led to a reduction in the effectiveness of the base-isolation.

Tongaonkar and Jangid (2003) investigated the influence of soil deformability on the seismic response of seismically isolated span-continuous deck bridges. Elastomeric bearings were used for the seismic isolation. It was observed that, soil flexibility influenced the bearing displacements at the abutment. Thus, according to Tongaonkar and Jangid (2003), disregarding the effects of soil deformability led to uncertainties in the design. Furthermore, the effects of soil deformability tended to be more intense for stiff bridges compared to the corresponding seismically isolated bridges.

The research by Krishnamoorthy and Anita (2016), proposed a numerical model of a seismically isolated structure, using a friction pendulum system (FPS) considering soil deformability in order to assess the structure's response. The results of that study indicated that soil deformability influenced the seismic response of the structure. More specifically, considering soil flexibility, turned out to be harmful for near-fault and low-frequency earthquakes. However, for far-fault and high-frequency earthquakes, it was beneficial. Moreover, the friction coefficient of FPS influenced the soil deformability effects. The larger the former, the smaller would be the latter and vice versa. In addition, the fundamental eigenperiod of the seismically isolated structure with FPS, influenced the soil deformability effects. While the fundamental eigenperiod was small, the soil deformability effects were either trivial or beneficial. Whereas, at high fundamental eigenperiods, soil deformability was detrimental.

## 2.3 Near Fault vs. Far Fault Ground Motions

According to Mavroeidis, Dong and Papageorgiou (2004), the first time that a structural damage was linked to the impulsive character of the near-fault ground motion, was in 1971. More specifically, the damage took place at Olive View Hospital in San Fernando, California. Although, the disastrous consequences of near-fault ground motions, when causative faults were in the region of large metropolitan areas, started to be realised after 1995. Forward directivity and the fling effect are the main characteristics of the near-fault ground motions. Thus, the seismic response of structures in the near field of a rupturing fault could be remarkably different from the seismic response of similar structures in the far field. Furthermore, one of the most important characteristics of near-fault ground motions is the impulsive character of the velocity and displacement affecting at long periods. The fault normal (FN) components of ground motions, in contrast with the fault parallel (FP)

components, are often composed by high displacements and velocity pulses. Specifically, the pulses are affected by the rupture mechanism, the slip direction in relation to the site and the directivity effect. The directivity effect is the position of the recording station in relation to the fault, due to the propagation of the rupture toward the recordings. There are three types of directivity effects: forward, reverse and neutral (Zhang and Wang, 2013).

Furthermore, forward directivity effects refer to strike-slip and dip-slip events. The former leads to larger forward directivity conditions for sites near the end of the fault, when the rupture front is moving towards the site. In the case of the latter, forward directivity conditions take place for sites located in the up-dip projection of the fault plane. Moreover, reverse directivity effects, where longer duration and lower amplitude ground motions are developed, are demonstrated when the rupture propagates away from the site. Lastly, when the site is less or more perpendicular to the fault from the hypocentre, refers to neutral directivity effects. Commonly, the phrase ''directivity effects'' is used to describe the forward directivity effects because they are more crucial (Zhang and Wang, 2013).

Zhang and Wang (2013), stated that the fling effect is *''a result of a permanent ground displacement due to the static deformation field of the earthquake, occurring over a discrete time interval of several seconds as the fault slip is developed''.* The study of the abovementioned authors, investigated the dynamic behaviour of concrete gravity dams subjected to near-fault and far-fault ground motion excitations. As a result, near-fault earthquake ground motions caused severe damage to concrete gravity dams compared to the far-fault. Hence, they highlighted that the effects of near-fault ground motions should be considered.

Pulse-type motions, which are ground motions close to a ruptured fault that developed from forward-directivity, are called near fault ground motions, and can cause severe damage on certain structures. Forward-directivity motions typically leads to the most severe loading of structural and earth systems. Therefore, Bray and Marek (2004) focused on the characterization of these ground motions. Their research mentioned the conditions that could lead to forward and backward directivity. Specifically, the parameters that they had used were the angle between the direction of the rupture propagation and the direction of waves traveling from the fault to the site and the fraction of the fault

rupture surface that lies between the hypocentre and the site. Smaller angles and larger fractions led to forward directivity. It is worth to mention that, Bray and Marek (2004) noted that conditions for forward directivity could be satisfied, although forward directivity could not occur. In that case, the station was at the end of a fault and rupture occurred towards the station, but slip was concentrated near the end of the fault where the station was located.

According to Liao, Loh and Wan (2001), in the case when the fundamental eigenperiod is smaller than the width of the acceleration pulse, the structure could develop more damage. Moreover, in near-fault ground motions the peak ground velocity (PGV) / peak ground acceleration (PGA) ratio and velocity pulse duration, were found to be higher than those from far-field ground motions. When the structure was subjected to near-fault ground motion, the ductility demand was higher than expected.

Somerville *et al.* (1997) had mentioned that rupture directivity effects caused spatial variations in ground motion amplitude and duration around faults and differences between the strike-normal and strike-parallel components of horizontal ground motion amplitudes, which also have spatial variations around the fault. These variations became significant at an eigenperiod of 0.6 seconds and generally grew in size with increasing fundamental eigenperiod. However, Somerville (2005) mentioned that forward rupture directivity caused the fault-normal component to be systematically larger than the fault-parallel component at eigenperiods longer than about 0.5 seconds. Therefore, in order to accurately characterize near-fault ground motions, it was suggested that it might be necessary to specify separate response spectra and time histories for both fault-normal and fault-parallel components. Additionally, the propagation of rupture toward a site at a velocity that was almost as large as the shear wave velocity, caused most of the seismic energy from the rupture to arrive in a single large pulse of motion, which occurred at the beginning of the record. This pulse of motion represented the cumulative effect of almost all of the seismic radiation from the fault (Somerville *et al.*, 1997).

The study by Alavi and Krawinkler (2004), investigated the response of frame structures excited to near-fault ground motions. It had been observed that, the response of structures with longer fundamental eigenperiods than the pulse period was way different from those with shorter fundamental eigenperiods. The former, developed early

yielding in the higher stories. Whereas high ductility demands migrate to the bottom stories as the ground motion become more severe. The latter, developed the maximum demand in the bottom stories.

Furthermore, the research by Mazza and Vulcano (2011), examined the effectiveness of base-isolated framed structures with HDRBs, taking into account the horizontal and vertical components of near-fault ground motions. The buildings were designed according to the Eurocodes. Firstly, the acceleration ratio (aPGA) was defined as the ratio between the peak value of the vertical acceleration (PGAV) and the corresponding value of the horizontal acceleration (PGAH). It was noted that, high values of aPGA is a characteristic of a strong near-fault ground motion and could be significantly modify the axial forces of the columns. In addition, it was highlighted that for the designing of base-isolated structures, the vertical component of the ground motion must be considered, in order to avoid potential underestimation of the response.

It is worth to mention that there have been very limited research publications that consider the effects of near-fault ground motions on the peak structural response in conjunction with the soil deformability. Although, a study by Bray and Rodriguez-Marek (2004) showed that lower magnitude events led to longer fundamental eigenperiods of the structures founded at soil sites than at rock sites. Consequently, the structures that had higher stiffness could developed more damage, compared to the structures with lower stiffness. The difference decreased as magnitude enlarged and ceased to exist for large magnitudes. Regarding the structural design, as longer is the fundamental eigenperiod of the structure, at soil sites, for earthquakes of low to moderate magnitudes, might need an alternative design methodology to handle the seismic event, in the case of near-fault ground motions. Hence, in regards to the ground motion, it could be very important to take into account the local site effects in the examination of near-fault ground motion due to the high probability of influences (Bray and Rodriguez-Marek, 2004).

# Chapter 3 - UTILISATION OF THE SAP2000 OAPI THROUGH PYTHON

This chapter outlines the basic characteristics of the Python language and discuss its advantages, compared to other programming languages. Additionally, it explains the utilization of the Open Application Programming Interface (OAPI) of the structural analysis program SAP2000, to perform parametric analyses, using the Python programming language. Specifically, the utilisation of the SAP2000 OAPI through Python enables the efficient and effective performance of large number of parametric analyses, where certain parameters should be automatically varied, without any interventions from the user and the overhead from the usage of the graphical user interface (GUI). Therefore, the parametric analyses are done programmatically and not interactively.

## 3.1 PYTHON

Python is an interactive, interpreted, and object-oriented programming language. It embodies a lot of capabilities, such as modules, exceptions, dynamic typing, high level of dynamic data types and classes. Furthermore, it supports several programming paradigms apart from the object-oriented programming, such as procedural and functional programming. Despite the significant power of Python, it has a very clear and simple syntax. In addition, it interfaces to various system calls and libraries, as well as to many window systems, and it is extensible in C, or C++, programming language. Moreover, it can be used as an extension language for applications that need a programmable interface.

Furthermore, Python's syntax and dynamic typing in combination with its interpreted nature, make it an ideal language for scripting and rapid application development, for many cases. For example, YouTube had been originally written in Python and a large part of Dropbox was written in Python, too.

Python can be utilised extensively for the efficient accomplishment of a lot of activities, such as the following:

- Automation of tasks
- Handling big data and performing complex mathematic calculations
- Creating user interfaces and website backends
- Developing web (server-side) and software applications

- Accessing database systems
- Reading and modifying files
- Downloading from the internet

Python is widely used due to its compatibility with most operating systems. Additionally, its syntax provides the ability for developers to write programs with fewer lines in comparison with other programming languages. Added to that, Python runs on an interpreter system, which means that the code can be executed simultaneously, while it is written. This means that prototyping can be very quick. It is often said that *'Python comes with batteries included',* which is used to highlight the 'richness' and the complete base library that supported by Python language. This is augmented with hundreds of thousands of external packages. Overall, by using Python every task can be accomplished relatively easy. Last but not least, Python is a versatile language that is easy to be learned and utilized. It is ideal for beginning programmers, however, it is also useful and powerful for seasoned professionals.

### 3.1.1 Indentation

One of the most important characteristics of the Python language is the use of indentations to group the blocks of the code. Indentation refers to the spaces at the beginning of a code line. While in other programming languages the indentation of code is for readability purposes only, in Python it is very significant. Without proper indentation, the written code will not run, thus all code blocks must be indented to the appropriate level. In addition, due to the mandatory use of indentation, the use of accolades to group the blocks of the code is not useful.

### 3.1.2 Dynamic Typing

In a strongly typed language, the declaration of the exact type of each variable, before its usage like *string, int, float* etc., is required. However, in Python, which is a completely object-oriented language, it is not necessary (table 3.1). More specifically, when running the code in Python the types of the variables are determined dynamically. While the code is running, Python considers the values given to variables, in order to accordingly declare their data types. For example, as showing in Table 3.1, the value of the *myNum* variable is integer type, and thus *myNum* variable is considered as an integer type.

***Table 3.1: Variable declaration in a strongly typed language and in Python***

| Strongly typed language (e.g. Java) | Python |
|---|---|
| string myName=”Christos” | myName=”Christos” |
| int myNum=2 | myNum=2 |

### 3.1.3 Garbage collection

Python incorporates the concept of variables. A variable has the ability to store any value, such as a number, a string of characters, or even bigger objects. Each declared variable, reserves the necessary amount of space in the computer’s memory. Therefore, useless variables have to be cleaned up to prevent memory leaks and to avoid possible errors related to this issue. In some programming languages, the clean-up has to be explicitly performed. Nevertheless, Python’s garbage collector manages this situation by automatically cleaning unused variables.

### 3.1.4 Integrated Development Environment (IDE) for Python

The usage of an IDE provides many benefits to the user. Firstly, it speeds up the code development as it offers autocompletion of words, syntax highlighting, and it suggests the available options to be used, based on the code context. Furthermore, an IDE supports the concept of a project. Specifically, opening a code project in an IDE, every project remains under the same directory and all projects’ settings are stored by the IDE. Last but not least, an IDE integrates the debugging process, which is very useful for a project. Basically, errors (bugs) are identified automatically during the code writing process, and they can be fixed easily. Overall, an IDE helps from setting up a project to debugging and running it.

For the current thesis, the IDE that is used to write the code in, is Spyder (Spyder IDE, 2020). Spyder is a powerful, free and open-source scientific environment written in Python, to be used for Python. It has been designed by and for scientists, engineers and data analysts. Spyder attributes a unique combination of advanced editing, analysis and debugging. In addition, it features profiling functionality of a comprehensive development tool with the data exploration, interactive execution, deep inspection and user-friendly

visualization capabilities of a scientific package. Furthermore, it offers built-in integration with many popular scientific packages like *NumPy, SciPy* etc., and it can be easily extended with plugins.

### 3.1.5 Advantages of Python

Firstly, Python is a high-level programming language whose syntax is simple and clear, similar to the English language. Thus, it is easy to read and understand the written code and, generally, it is easy to learn how to utilize the Python language. This leads to greater productivity and efficiency. The fact that Python is an interpreted language means that it directly executes the code, line by line. When an error occurs, the execution stops, and the error is reported back. It is worth to mention that, when the code has several errors, Python illustrates only one error at a time. Hence, debugging is easier. Moreover, the variables and their data types used in a code, are not to be pre-declared. Python automatically assigns the data type during execution of the code.

Furthermore, Python is a free of charge and open-source programming language. It comes under the Open System Interconnection (OSI) approved open-source license. Anyone can download it hassle free and start directly using it. In addition, Python has a huge number of additional packages and standard libraries facilitating every task. Therefore, a Python user does not need external libraries. Also, it is not necessary to change a Python code to run it at different platforms than the platform where the code is originally created.

However, the fact that it is not a compiled programming language, but it is interpreted, means that software developed in Python are relatively slower than corresponding software in compiled programming languages, such as C++, which are compiled in machine code.

### 3.1.6 Python Vs. Other Programming Languages

The tables (Tables 3.2 - 3.4) demonstrate the differences of Python programming language compared to Java, PHP and C++, respectively.

***Table 3.2: Python language differences compared to the Java language***

| Python | Vs | Java |
|---|---|---|
| Interpreted and dynamically typed: does not need to be compiled before execution | | Compiled and statically typed: needs to be compiled from source code (readable by humans) to machine code |
| Faster launch time – slower run time | | Slower launch time – faster run time |
| Building a project with Python takes few weeks and the whole project can be completed in a matter of months | | Building a project with Java can take months due to its high code complexity and volume |
| A development in Python is faster and less expensive | | A development in Java needs more time and money |
| Indentation is used to group the blocks of a code | | Semicolons and curly braces are obligatory to group blocks of a code |
| Less code lines | | More code lines |
| Supports various types of programming models such as imperative, object-oriented and procedural programming | | Completely based on the object-oriented and class-based programming models |

***Table 3.3: Python language differences compared to the PHP language***

| Python | Vs | PHP |
|---|---|---|
| Object-oriented scripting language | | Server-side scripting language |
| Utilised for many purposes (full-stack programming language) | | Utilised for web development purposes |
| Provides functional programming techniques | | Functional programming is not available |
| More organized, secure, and easier to maintain | | Not much maintainable |
| Proper provision for exception handling | | Does not properly support exception handling |

***Table 3.4: Python language differences compared to the C++ language***

| Python | Vs | C++ |
|---|---|---|
| Memory efficient due to its garbage collection | | Does not support garbage collection |
| It is easy to learn how to use and write codes | | It is more difficult to understand how to develop and reuse code, due to its complex syntax |
| An interpreter is used for the execution of the code, which makes it easy to run on any platforms and operating systems | | The code will not run-on other computers unless it is compiled on the specific computer |
| It can be used for rapid application development, since the code has smaller size | | It is difficult to be used for rapid application development because of its large code fragments |
| Better readability since the code is similar to the English language | | Hard to read due to the complex syntax and structures |
| The variables that are defined in Python are easily accessible outside the loop | | The scope of each variable is limited within the loop that it is used |

## 3.2 Application Programming Interface (API)

The Application Programming Interface (API) is an intermediary software that provides the ability to the components of two applications, to interact to each other by using a set of simple commands. APIs work quietly in the background making that interactivity possible. More specifically, APIs are 'messengers' that deliver requests and return responses between applications. In each interplay, there is a server, which is the app providing the resource, and a client, which is the app that makes the request. While the server can implement the request of the client, the API will return the respective resource. However, in the case that the client asks for a resource that does not exist on the server or a resource that is prohibited to be accessed, the API will provide an error message. Hence, APIs enforce selective access control to the server. Furthermore, using an app such as Facebook to send a message, or check the weather on a phone, an API is being used. Generally, APIs are responsible for nearly everything.

### 3.2.1 API example

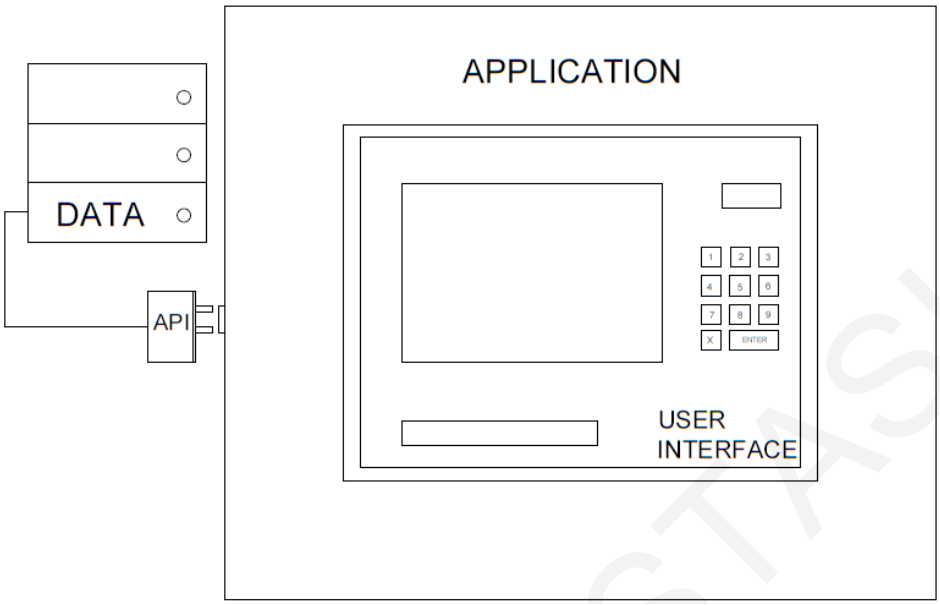


***Figure 3.1: Graphic representation of an ATM as an API example***

For better understanding of what is the API, an example is provided, representing, the withdrawal and the deposit of cash from/to an Automated Teller Machine (ATM). Basically, as illustrated in the Fig 3.1, the application is the ATM and the user interface is how the user interacts with the application. To complete a transaction, the user has to be allowed by the ATM to access his/her account. Similarly, an application provides a function and the interaction with the user is needed to communicate both with each other. This interaction is done through an API, which, in the case of the ATM, will allow the ATM to communicate with the bank. As shown in Fig 3.1, the bank is represented by the data. Hence, the API translates the request for cash to the bank's database and the relevant actions take place in the background, for the completion of the transaction. In a nutshell, an API is the interface that a software uses to access whatever it is needed such as, data, server software, or other applications.

## 3.3 OAPI of the SAP2000

The OAPI provided with the current version of SAP2000 (SAP2000, 2020), is a powerful tool that provides the ability to the users, to automate many of the processes required to configure, analyze, and design structural models. Additionally, it allows to user to obtain

customized analysis and design results. Furthermore, the fact that users are permitted to link SAP2000 with third-party software leads to a path for two-way exchange of model information with other programs. SAP2000 can be accessed through the OAPI by several major and popular programming languages such as MATLAB, C#, Visual Basic for Applications (VBA) and Python, which is the one that is used in the current thesis.

### 3.3.1 SAP2000 OAPI operation

The following flowchart (see Figure 3.2) illustrates how the SAP2000 OAPI is utilized, for the current thesis, using the Python programming language, in order provide access during run-time to the analysis software. Basically, the OAPI is the interface tool that translates the given data from Python to SAP2000. More specifically, the required data, functions and parameters for the configuration of the examined model and for the implementation of the dynamic analysis, are written in Python and transferred to SAP2000, by its OAPI. Hence, the SAP2000 software, taking into account the provided data, creates the model and executes the dynamic time-history analysis. It is worth to mention that the operation of SAP2000 is done entirely in the background. This fact completely overrides the standard point-and-click procedure, saving a lot of time. In addition, by using the SAP2000 OAPI, easy control and access to the analysis data is provided. Therefore, it is very easy and effective to make changes to the analysis data without any restrictions.

With this approach, parametric analyses can be easily conducted with great flexibility and efficiency. Furthermore, computed results can be efficiently and effectively postprocessed through the OAPI interactions, in order to compare them through the parametric studies that are automatically performed.

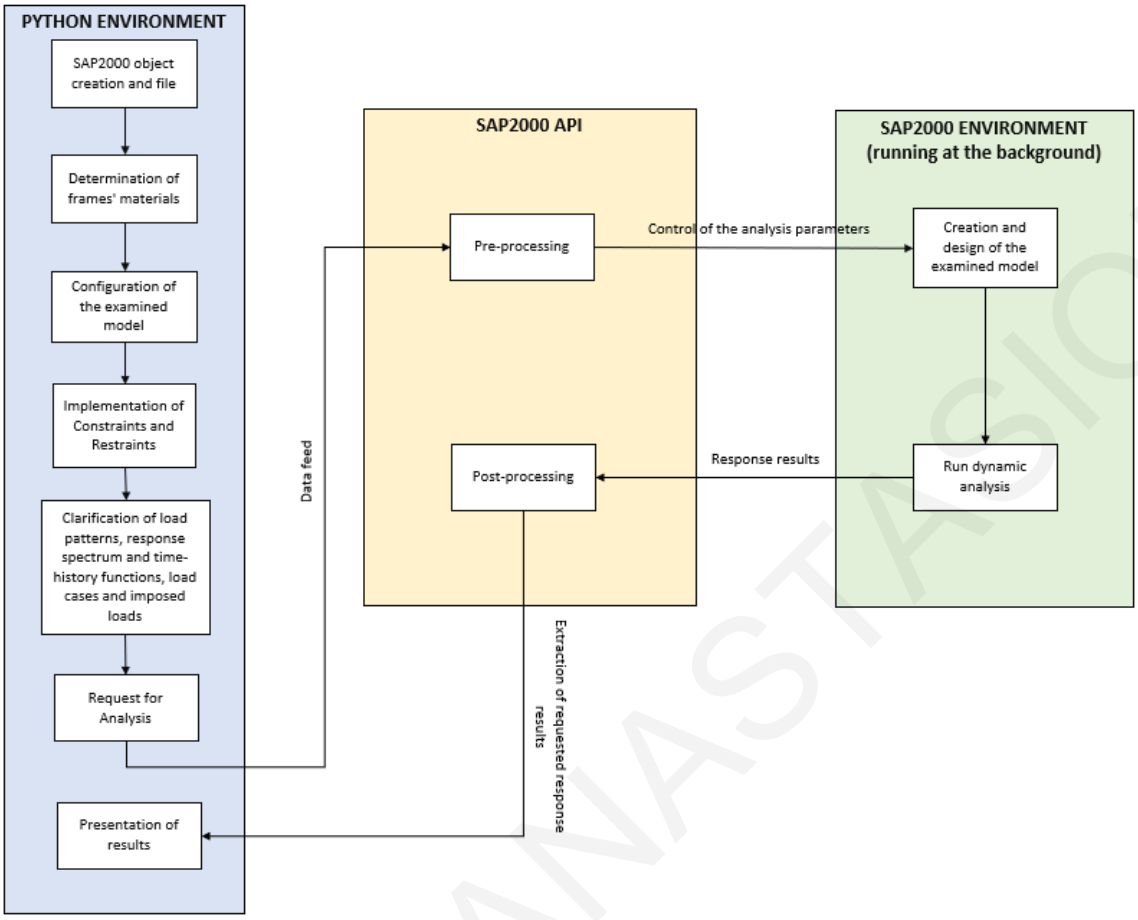


***Figure 3.2: Flowchart of how SAP2000 OAPI is utilised through Python***

### 3.3.2 Accessing SAP2000 through its OAPI using Python

Firstly, the user has to download and install Python. Secondly, it is required to install the Python package "*comtypes*". The easiest way to be implemented, is by opening a command prompt with administrative privileges and enter the command: *C:\>python -m pip install comtypes*. After that, the user is able to create a Python file. While using the SAP2000 OAPI through Python, the code has to begin with the following three commands:

```
import os

import sys

import comtypes.client
```

Then, in order to attach to an existing instance of the program the flag *AttachToInstance* has to be stated as *True*. Otherwise, it has to be defined as *False* and a new instance of the program will be started. For example:

```
AttachToInstance = False
```

In addition, the following flag must be equal to *True* to manually specify the path to *SAP2000.exe*, for a connection to a version of SAP2000 other than the latest installation. To launch the latest installed version of SAP2000, the flag *SpecifyPath* has to be equal to *False*, as follows:

```
SpecifyPath= False
```

In the case that the above flag is set to *True*, the path to the SAP2000 has to be specified, as well as the full path to the model. For instance:

```
ProgramPath = 'C:\Program Files\Computers and Structures\SAP2000 22\SAP2000.exe'

APIPath = 'C:\CSiAPIexample'
```

Next, the commands below check if the desired folder for saving exists. If it does not exist, then it is created. Otherwise, the program continues.

```
if not os.path.exists(APIPath):
    try:
        os.makedirs(APIPath)
    except OSError:
        pass
```

After that, determination of a variable that includes the full path with the specific name of the file is required. Moreover, it is very important to create a SAP2000 OAPI helper object, as follows:

```
ModelPath = APIPath + os.sep + 'fileName'

helper = comtypes.client.CreateObject('SAP2000v1.Helper')
```

```
helper = helper.QueryInterface(comtypes.gen.SAP2000v1.cHelper)
```

Furthermore, the *if-else* statements below, checks if there is an active case of SAP2000 to get the active SAP2000 OAPI object. If an active case does not exist, then the command *SpecifyPath* determines how the program should continue. More specifically, if it is equal to true, an instance of the pre-specified SAP2000 OAPI object is created. Otherwise, a case of the SAP2000 OAPI object, from the latest installed SAP2000 version, is created.

```
if AttachToInstance:
    try:
        mySapObject = helper.GetObject("CSI.SAP2000.API.SapObject")
    except (OSError, comtypes.COMError):
        print("No running instance of the program found or failed to attach.")
        sys.exit(-1)
else:
    if SpecifyPath:
        try:
            mySapObject = helper.CreateObject(ProgramPath)
        except (OSError, comtypes.COMError):
            print("Cannot start a new instance of the program from " + ProgramPath)
            sys.exit(-1)
    else:
        try:
            mySapObject = helper.CreateObjectProgID("CSI.SAP2000.API.SapObject")
```

```
except (OSError, comtypes.COMError):
    print("Cannot start a new instance of the program.")
    sys.exit(-1)
```

In order to create the SAP2000 OAPI object and specify the path of the file, the above-mentioned command instructions have to be followed. Afterwards, the SAP2000 application can start with the command *mySapObject.ApplicationStart()*. At this point, the user can open an existing model or create a new one and perform whatever actions are required. This can be done by using the corresponding commands from the OAPI documentation, which can be obtained with the installation of the SAP2000 software. Generally, the OAPI commands are accessed through *mySapObject.SapModel*. It may be helpful to define a *SapModel* variable to assign the latter. Hence, the OAPI commands could be accessed through the *SapModel* command only, instead of *mySapObject.SapModel*.

A brief example of the written algorithm in Python programming language for the utilization of the parametric analyses, is provided in the Appendix A.

# Chapter 4 - DESCRIPTION OF STRUCTURAL MODELLING

The current chapter provides information about different types of soils and describes how the soil deformability is taken into consideration for the purposes of this parametric study. Moreover, the examined building's characteristics are presented and the fundamental eigenperiods of the structure founded on the assumed soil types, are illustrated.

## 4.1 Foundations

According to Bowles (1997), foundation is an interface element between the supporting soil and an engineering structure, which transfers its self-weight and the loads from the superstructure to the earth. This transfer results in additional soil stresses than the existing stresses in the earth, which arise from its self-weight and its geological history. Consequently, it's one of the most important parts of an engineering system.

Foundations can be categorized as shallow or deep foundations, based on how they transfer the loads to the ground. Commonly, the loads are transmitted from the superstructure to the soil interface by column type members. In addition, columns have a relatively small cross-sectional area. The supporting capacity of the soil either from strength or deformation considerations, usually varies between 200 to 250 KPa and rarely exceeds 1000 KPa. Hence, the soil can be loaded up to such a level so that its limiting strength is not reached. Shallow foundations accomplish that by spreading the loads laterally, thus, the definition spread footing. In contrast, deep foundations distribute the load vertically. The main issue for both shallow and deep foundations is how the stresses are distributed, in the stress influence zone underneath the foundation.

Foundation elements must be designed to interface with the soil at a safe stress level and to manage settlements to a tolerable level. However, a significant factor that perplex the foundation design is the uncertainties of the soil parameters. Therefore, it is an ordinary practice to be conservative in designing the foundation elements as a consequence of the uncertainties in soil properties.

There are 3 types of shallow foundations: isolated footings, strip footings and mat foundations. Isolated footings with tie-beams are used in the current thesis. Their dimensions are calculated according to the structure's applied loads and considering a

supporting capacity equal to 200 KPa. In the considered case, the foundations' length, width and height are equal to 0.75m, 0.75m, and 0.5m, respectively.

## 4.2 Soil

Soil materials are classified as follows:

- Bedrock
- Boulders
- Gravels and sand
- Silt
- Clay

More specifically, bedrock is used to describe a rock formation at a depth in the ground on which a structure can be erected. Any other rocks and soils emanate from the original bedrock, which is formed by cooled molten magma and subsequent weathering. It mainly extends downward to molten magma while at the bottom, igneous rock can be found. In addition, one or more layers of more recently formed sedimentary rocks such as sandstone, limestone etc. formed by indurated soil deposits, could be over bedrock. Metamorphic rocks constitute the interface layers between igneous and sedimentary rocks, which are formed by increased heat and pressure acting on sedimentary rocks. Additionally, igneous, sedimentary and metamorphic rocks are subdivided into several groups and types based on various factors, which the most important are chemical, mineralogical, and textural attributes (Klein *et al.*, 2021). Overall, bedrock compose a satisfactory foundation (Bowles, 1997).

Boulders are massive chunks of rock detached from the parent material or erupted from volcanoes. Their volume could be up to about $10m^3$ and weigh between one-half to some hundreds of tons. Moreover, boulders are creating problems related to excavation and exploration of soil. Due to perplexing determination of their size, it would be destructive for a huge structure to be founded on them.

Pieces of rock with smaller size than boulders are referred to as cobbles, pebbles, gravels, sand, silt and colloids in descending order as illustrated in table 4.1. According to Bowles (1997), the diameter of the sand material varies from 0,074mm to 5mm. Whereas, Augustyn *et al.* (2019) stated that sand ranges in diameter between 0,02 and 2 mm.

Concerning the silts and clays, both require attentiveness when they are considered for the design of foundations, because they are more vulnerable in terms of strength and displacements. The main difference between silt and clay is that a clay mineral consists of hydro-aluminum silicate, thus, is not inert. Generally, clays have the ability to absorb water at high levels, which contributes to significant strength and volume changes. Furthermore, the particles of clay have high coupling forces between each other, therefore, a dry lump of clay has high strength. Nonetheless, due to the uncertainty of varying types of clay minerals that are contained to a clay, the latter is responsible for arising problems (Bowles, 1997).

***Table 4.1: Soil material classification with upper and lower possible size for each soil material (Bowles, 1997)***

| Material | Upper size (mm) | Lower size (mm) |
|---|---|---|
| Boulders, cobbles | 1000 | 75 |
| Gravel, pebbles | 75 | 2-5 |
| Sand | 2-5 | 0.074 |
| Silt | 0.074-0.05 | 0.006 |
| Rock flour | 0.006 | 0.002 |
| Clay | 0.002 | 0.001 |
| Colloids | 0.001 | - |

On the other hand, according to the EN 1998-1:2004, the soil should be classified by taking into account the value of the shear wave velocity $V_{s,30}$, which is the average shear-wave velocity (Vs) for the upper 30 m of the soil profile. However, if there is lack of determining the value of the shear wave velocity, then the value of $N_{SPT}$ can be used (Figure 4.1). Specifically, the $N_{SPT}$ is the number of blows (N), in the Standard Penetration Test (SPT), that are necessary to achieve a penetration of the sampler of 300 mm into the examined soil media. The purpose of the SPT is the determination of the resistance of the soil (EN 1997-2:2007).

| Ground type | Description of stratigraphic profile | Parameters | | |
|---|---|---|---|---|
| | | $v_{s,30}$ (m/s) | $N_{SPT}$ (blows/30cm) | $c_u$ (kPa) |
| A | Rock or other rock-like geological formation, including at most 5 m of weaker material at the surface. | > 800 | – | – |
| B | Deposits of very dense sand, gravel, or very stiff clay, at least several tens of metres in thickness, characterised by a gradual increase of mechanical properties with depth. | 360 – 800 | > 50 | > 250 |
| C | Deep deposits of dense or medium-dense sand, gravel or stiff clay with thickness from several tens to many hundreds of metres. | 180 – 360 | 15 - 50 | 70 - 250 |
| D | Deposits of loose-to-medium cohesionless soil (with or without some soft cohesive layers), or of predominantly soft-to-firm cohesive soil. | < 180 | < 15 | < 70 |
| E | A soil profile consisting of a surface alluvium layer with $v_s$ values of type C or D and thickness varying between about 5 m and 20 m, underlain by stiffer material with $v_s$ > 800 m/s. | | | |
| $S_1$ | Deposits consisting, or containing a layer at least 10 m thick, of soft clays/silts with a high plasticity index (PI > 40) and high water content | < 100 (indicative) | – | 10 - 20 |
| $S_2$ | Deposits of liquefiable soils, of sensitive clays, or any other soil profile not included in types A – E or $S_1$ | | | |

***Figure 4.1: Ground types (EN 1998-1:2004)***

Undoubtedly, the mechanical characteristics of soils are difficult to be understood and explained. This happens due to the wide variety of soil types and the complexity of their mechanical behaviour. In fact, soils that have the same physical and chemical properties could exhibit quite different mechanical behaviour (Miura *et al.*, 1997). Hence, averages of values are chosen for the characteristics and the mechanical properties of soils.

More specifically, in the current thesis a major objective is the consideration of the soil deformability and how that can affect the peak seismic response of a typical low-rise R/C building. Therefore, three different types of soil: rock, sand and soft clay, are considered in the parametric analyses. It is noted that the soft clay is considered deliberately, in order to examine the soil deformability effects in a relatively extreme case. For the rock's soil type, the Poisson's ratio (v) is determined according to Bowles (1997), whereas the Young's Modulus (E) is estimated according to Fjaer *et al.* (2008). Moreover, for the sand and soft clay soil types, both parameters are estimated according to Bowles (1997). The value of the shear modulus (G) for each soil type, is calculated using the following expression: $G = E/(2 \times (1 + v))$, as stated by Bowles (1997). The parameters' values for each soil type are tabulated in Table 4.2.

***Table 4.2: Values of the soil types parameters***

| Soil Type | Young's Modulus E (GPa) | Poisson's ratio v | Shear Modulus G (KN/m$^2$) |
|---|---|---|---|
| Rock | 60 | 0.25 | 24000000 |
| Sand | 0.02 | 0.35 | 7407.4 |
| Soft clay | 0.005 | 0.4 | 1785.7 |

## 4.3 Soil deformability and simulation with the SAP2000 OAPI

In order to ensure an appropriate earthquake resistant design, the regulations of the Eurocodes for earthquake resistant buildings should be followed, where the design is usually implemented under the assumption of a rigid ground. According to EN 1998-1:2004§4.3.1, soil deformability should only be considered in those cases where it would develop unfavourable effects on the structural response. Traditionally, soil deformability is supposed to be beneficial for the seismic response of structures, compared to the rigid ground assumption. Thus, in many seismic codes it has been suggested and adopted as a conservative simplification (Mylonakis and Gazetas, 2000).

However, in some cases it has been shown that the seismic response of a fixed base condition structure, ignoring soil flexibility, may lead to lower estimation of the actual peak seismic response. Added to that, soil deformability may increase the fundamental eigenperiod of the building (Narayana, Sharada Bai and Manish, 2010). Therefore, the

response of a structure taking into account the soil deformability, may significantly differ from the seismic response of the same structure with the rigid base assumption (Gowda, Narayana and Narandra, 2015).

Recent versions of SAP2000 software (version 22.0.0 and later), provides the ability to define parametrically, detailed foundations properties. The detailed foundations properties can be used to generate parametric foundation assemblies, which can be added to the model. Specifically, the term "assembly" refers to a collection of component objects (points, lines, areas, and links) that are created to represent the foundation. The available foundation properties are isolated footing, combined footing, pile group, pile pier and pile shaft. Furthermore, another ability that is provided by newer versions of the SAP2000 software, is the determination of soil profiles. Using the above enhancements that offered by SAP2000, soil deformability can be taken into consideration in the analysis more easily.

Nevertheless, in the current thesis the above-mentioned methodology to consider the soil deformability could not be used in the analysis as it is not yet supported by the OAPI of SAP2000, which has been utilized to perform parametric analyses. Therefore, an alternative methodology is used to consider the soil deformability in the analysis as explained below.

Soil deformability can be taken into account using six springs, one on each support joint. The springs correspond to three translational and three rotational springs, one at each direction. Commonly, the soil springs are considered to behave linearly. Springs' coefficients, which represent the stiffness of each spring, can be calculated based on the dimensions of the structure's foundation and the mechanical properties of the soil. Through the SAP2000 OAPI, it is possible to implement the aforementioned methodology, to take into account the soil deformability in the conducted dynamic analyses.

As already stated above, the examined model is assumed to be founded on isolated foundations with tie beams. The foundations' length, width and height are equal to 0.75m, 0.75m, 0.5m, respectively. In addition, each column of the building is assumed to be perfectly connected at the center of the corresponding isolated footing to eliminate possible eccentricities.

Taking into consideration the mechanical properties of each soil type, as stated in Table 4.2, and the dimensions of the isolated footings, the stiffnesses of the springs are calculated according to Gazetas (1991). More specifically, Gazetas (1991) proposed certain expressions for the calculation of the springs' stiffnesses, depending on the soil characteristics and the type and the shape of the foundation. In the current thesis, the isolated footings are assumed to be founded on the surface of a homogeneous halfspace. Therefore, the calculation of the springs coefficients is implemented by the following expressions, which refer to square shape foundations, as tabulated in Table 4.3. It is worth to mention that:

- B refers to the half of the dimension of the foundation
- G is the shear modulus of the assumed soil
- v is the poisson's ratio

***Table 4.3: Expressions used for the calculation of soil springs coefficients***

| Spring Direction | | Coefficient |
|---|---|---|
| Vertical (Z) | Translational | $Kz = \frac{4.54GB}{1-v}$ |
| Horizontal Y (lateral) | | $Ky = \frac{9GB}{2-v}$ |
| Horizontal X (longitudinal) | | $Kx = \frac{9GB}{2-v}$ |
| Around longitudinal (RX) | Rotational | $Krx = \frac{3.6GB^3}{1-v}$ |
| Around lateral (RY) | | $Kry = \frac{3.6GB^3}{1-v}$ |
| Around vertical (RZ) | | $Krz = 8.3\mathrm{G}B^3$ |

Tables 4.4 - 4.6, provide the computed values for the springs' stiffnesses for each soil type considered in this thesis. It is worth to highlight that, rock soil type essentially represents the rigid base support since, they lead to the same seismic responses.

***Table 4.4: Springs' stiffnesses for rock***

| Soil Type: Rock | |
|---|---|
| Translational | **Stiffness (MN/m)** |
| Vertical (Z) | 54480 |
| Horizontal Y (lateral) | 46286 |
| Horizontal X (longitudinal) | 46286 |
| Rotational | **Stiffness (MN/m/rad)** |
| Around longitudinal (RX) | 6075 |
| Around lateral (RY) | 6075 |
| Around vertical (RZ) | 10505 |

***Table 4.5: Springs' stiffnesses for sand***

| Soil Type: Sand | |
|---|---|
| Translational | **Stiffness (MN/m)** |
| Vertical (Z) | 19.4 |
| Horizontal Y (lateral) | 15.1 |
| Horizontal X (longitudinal) | 15.1 |
| Rotational | **Stiffness (MN/m/rad)** |
| Around longitudinal (RX) | 2.16 |
| Around lateral (RY) | 2.16 |
| Around vertical (RZ) | 3.24 |

***Table 4.6: Springs' stiffnesses for soft clay***

| Soil Type: Soft clay | |
|---|---|
| Translational | **Stiffness (MN/m)** |
| Vertical (Z) | 5.07 |
| Horizontal Y (lateral) | 3.77 |
| Horizontal X (longitudinal) | 3.77 |
| Rotational | **Stiffness (MN/m/rad)** |
| Around longitudinal (RX) | 0.565 |
| Around lateral (RY) | 0.565 |
| Around vertical (RZ) | 0.782 |

## 4.4 Superstructure

The three-dimensional (3D) model that is used throughout the thesis corresponds to a reinforced concrete building. The structure consists of two storeys with 15m length in the main horizontal axis X and 16m width in the secondary horizontal axis Y. Moreover, the area plan of the building (Figure 4.2) is 240m$^2$ and the height of each floor is 3m. The frame in the X direction has three equal spans of 5m each and the frame in the Y direction has 4 equal spans of 4m each. Furthermore, both in the X and Y directions, there are moment resisting frames with the beams rigidly connected to the columns (Figures 4.3 – 4.4). It is noted that in the current chapter, the building refers to a conventionally supported building. The corresponding base-isolated building is examined in Chapter 7.

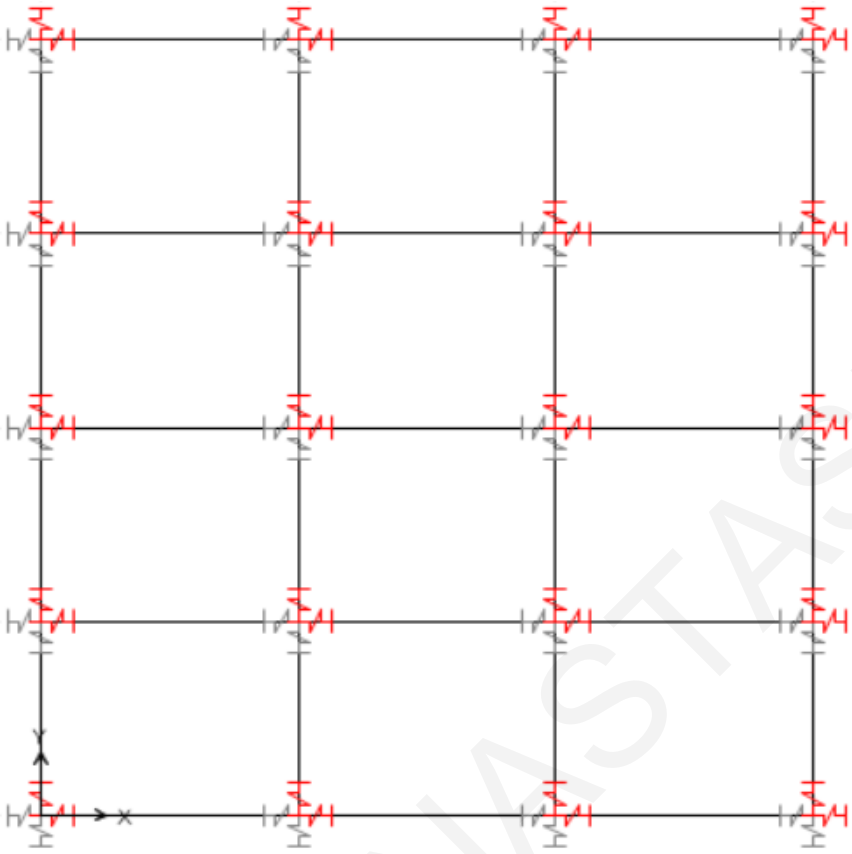


*Figure 4.2: Plan area of the considered model*

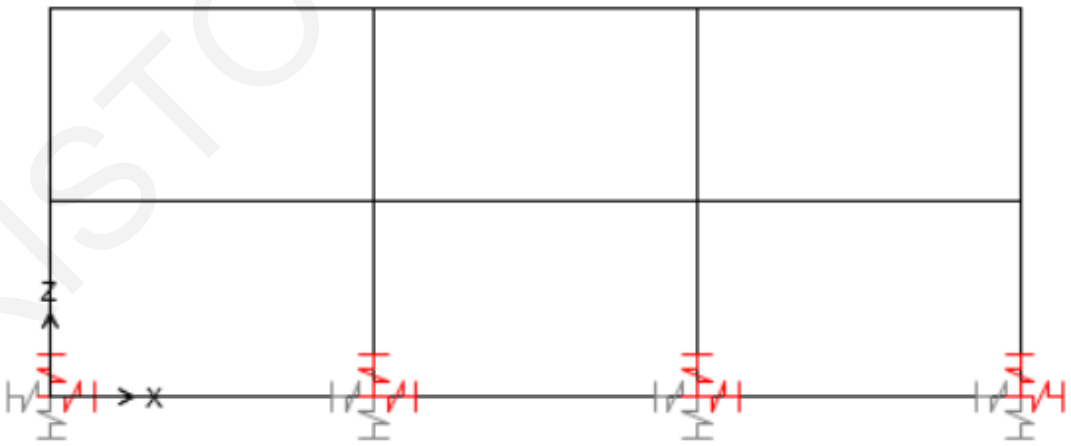


*Figure 4.3: Typical frame in the XZ direction of the considered model*

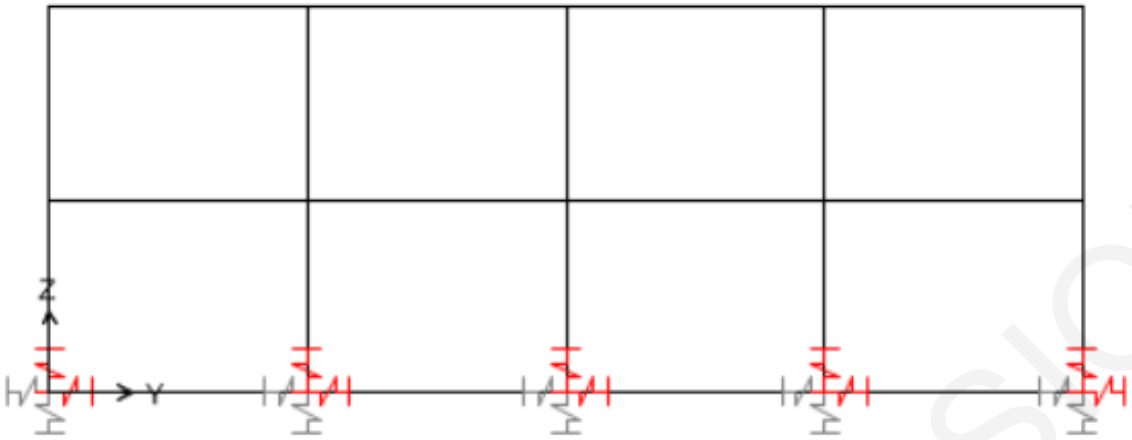


***Figure 4.4: Typical frame in the YZ direction of the considered model***

In extend of the above, all columns have square cross-section with 0.5 m sides. The material is assumed to be concrete with grade C30/37, according to the regulations of (Eurocode) EN 1992-1-1 per EN 206-1. There are two defined cross-sections for the beams: T and Γ. Depending on the location and the orientation, beams' cross-section dimensions vary as shown in Table 4.7. The columns' and beams' reinforcement, is implemented automatically by SAP2000 software. The default steel grade that is utilised by the program is S355, in accordance to EN 1993-1-1 per EN 10025-2. It is worth to mention that the slabs are not explicitly simulated, but they are implicitly taken into consideration through the following procedure: The applied loads on the slabs, are imposed on the respective adjacent beams. In addition, the geometric elements of the beams are modified to be considered as T or Γ cross-section beams. Specifically, the effective widths of beams' flanges are calculated considering the provision of EN 1992-1-1:2004§5.3.2.1. In addition, the diaphragm constraint of the slabs at each floor, is taken into account through the SAP2000 software.

***Table 4.7: Beams' cross-sections***

| | | | |
|---|---|---|---|
| T cross-section beam | Parallel to Direction X | Parallel to Direction Y | 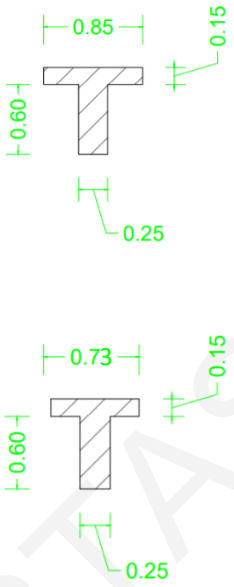 |
| Outside stem (m) | 0.6 | 0.6 | |
| Outside flange (m) | 0.85 | 0.73 | |
| Flange thickness (m) | 0.15 | 0.15 | |
| Stem Thickness (m) | 0.25 | 0.25 | |
| Γ cross-section beam | Parallel to Direction X | Parallel to Direction Y | 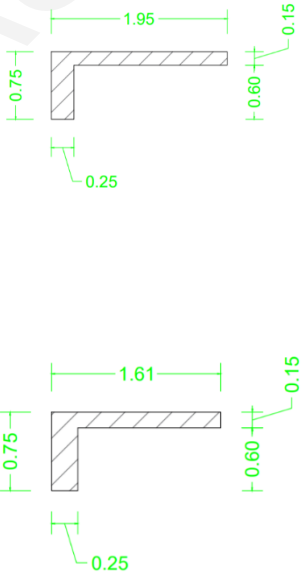 |
| Outside vertical leg (m) | 0.6 | 0.6 | |
| Outside Horizontal leg (m) | 1.95 | 1.61 | |
| Horizontal leg thickness (m) | 0.15 | 0.15 | |
| Vertical leg thickness (m) | 0.25 | 0.25 | |

A 3D view of the conventionally supported building is shown in Figure 4.5, where each different type of sections is presented with a different colour, as shown in Table 4.8.

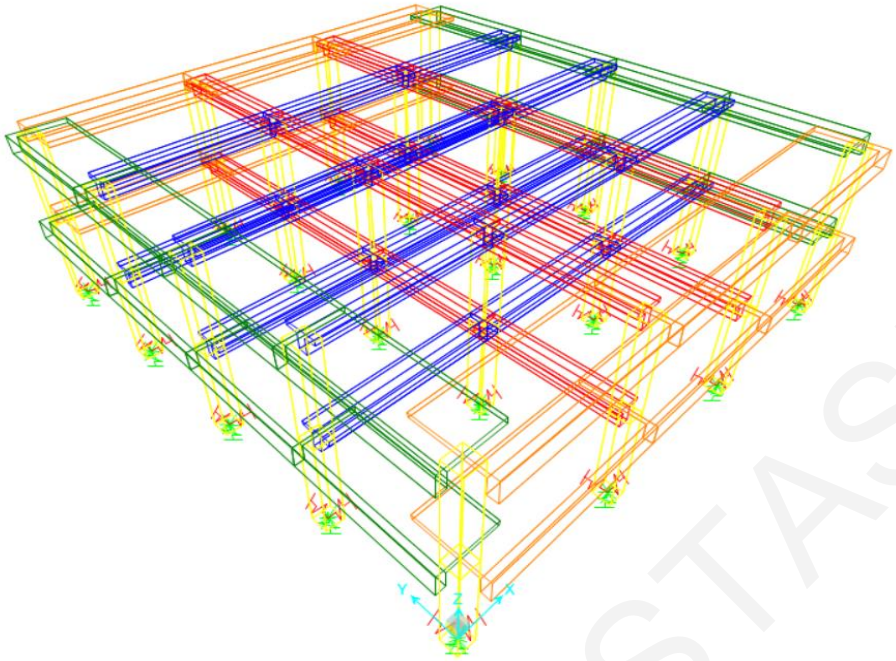

***Figure 4.5: Simulation model***

***Table 4.8: Beams and different colours according to each cross-section***

| | T cross-section beam | Γ cross-section beam |
|---|---|---|
| Parallel to Direction X | Blue colour | Orange colour |
| Parallel to Direction Y | Red colour | Green colour |

It should be highlighted that due to the need of comparing the same model under different circumstances, the same superstructure is used to examine the seismic response, considering the soil deformability for different soil profiles.

## 4.5 Applied Loads

According to the EN 1991 regulations, where is necessary, the adverse effects from loads such as wind, snow, fire and earthquake, shall be taken into account when designing a structure. However, it is not mandatory that all of the above have to be assumed acting simultaneously. Due to the location of the building (Paralimni, Cyprus) it is a rare phenomenon to snow and if so, it would not be much. Thus, snow loads are not significant.

In addition, to simplify the analysis of the examined building, loads that developed from wind and fire are neglected. Besides, the most unfavourable loads are almost always developed by seismic ground motions, which are the most critical actions considered in Cyprus.

In the current thesis, the loads of interest are:

- Selfweight of slabs
- Live loads of slabs
- Dead loads on slabs, such as floorings loads
- Dead loads on beams, such as external and internal masonries

The self-weight, dead and live loads on the surfaces of the slabs are considered to be uniformly distributed over the beams. The floors are classified in category A in regards to EN 1991-1-1: 2002, which refers to areas for residential and domestic activities. Hence, the corresponding live load for floors, which is defined by the Cyprus National Standards CYS EN 1991-1-1: 2002, is equal to 2kN/$m^2$. More specifically, Tables 4.9 - 4.10 present in detail all the applied loads that are considered for the analysis.

***Table 4.9: Slabs surface loads***

| | Self-weight (kN/$m^2$) | Dead Loads (kN/$m^2$) | Live Loads (kN/$m^2$) |
|---|---|---|---|
| 1st floor slabs | 3.75 | 1.50 | 2 |
| 2nd floor slabs | 3.75 | 2.50 | 2 |

***Table 4.10: External and internal masonry loads***

| | External Masonry (kN/m) | Internal Masonry (kN/m) |
|---|---|---|
| 1st floor beams | 10.35 | 6.30 |
| 2nd floor beams | 10.35 | 6.30 |

## 4.6 Dynamic time-history analyses

The time-history analyses aim to calculate the exact dynamic response of structures under seismic excitations, in terms of time. More specifically through a time-history dynamic analysis, the values of the structure's response, are computed at every time step of the seismic action until its end. Two methods for solving the differential motion equations can be used in the SAP2000 software: modal time-history analysis and time-history analysis with direct integration, assuming linear elastic behaviour.

SAP2000 implements the solution of the differential equations of motion with several numerical methods. For instance, Newmark, Wilson, Collocation, Hilber-Hughes-Taylor and Chung and Hulbert methods are used. The default method of SAP2000 for time-history analysis with direct integration, is the Hilber-Hughes-Taylor method, although the user has the ability to change the method to be used.

The method that is used to implement the linear time-history analyses in the current thesis, is the Newmark method. Specifically, the Newmark method is widely used for the solution of direct integrate time-history analyses due to the numerical stability that it provides. The coefficients γ and β that are required to be defined for the Newmark method, are considered as 0.5 and 0.25, respectively.

## 4.7 Seismic load combinations

The seismic load combinations (see Table 4.11) are set up according to the CYS EN 1990:2002. Each combination consists of two parts; the first, is the dynamic time-history analysis considering seismic loads and the second part is the static analysis under dead and live loads. Both directions X and Y, are taken into consideration and each part of the combination is multiplied by the proper coefficients. Furthermore, both horizontal components of the seismic action are considered to happen simultaneously. Specifically, in combinations 1-4, direction X is considered to be the primary component thus, the coefficient that multiplies the horizontal component of X direction is 1. In contrast, the seismic component in direction Y is considered to manifest only the 30% of it. The reverse applies for the combinations 5-8. Regarding the signs plus (+) and minus (-), they simply denote the direction in which each seismic component acts.

***Table 4.11: Seismic load combinations***

| Seismic Load Combinations | |
|---|---|
| 1 | **1.00G + 0.30Q+ 1.00Ex + 0.30Ey** |
| 2 | 1.00G + 0.30Q + 1.00Ex - 0.30Ey |
| 3 | 1.00G + 0.30Q - 1.00Ex + 0.30Ey |
| 4 | 1.00G + 0.30Q - 1.00Ex - 0.30Ey |
| 5 | **1.00G + 0.30Q + 0.30Ex + 1.00Ey** |
| 6 | 1.00G + 0.30Q + 0.30Ex - 1.00Ey |
| 7 | 1.00G + 0.30Q - 0.30Ex + 1.00Ey |
| 8 | 1.00G + 0.30Q - 0.30Ex - 1.00Ey |

In this thesis, only the combinations 1 and 5 are taken into account for observation, which can be considered sufficient when studying the response of a symmetric building in terms of the direction of action of the major seismic components. Since, the building model is symmetrical with respect to the two horizontal orthogonal axes, passing through the geometric center of the plan of the building, the assumption is considered as reasonable. Due to the symmetric plan of the structure, combinations 2 to 4 and 6 to 8 are producing absolute values of the same intensity and deformation, as combinations 1 and 5, respectively. The only difference that occurs is the plus (+) and minus (-) signs of the forces and deformations (Varnava, 2012). Hence, in order to limit the number of computations, seismic combinations 2 to 4 and 6 to 8 are omitted for this research work.

## 4.8 Modal Analysis

The natural eigenperiods of the conventional building for each soil type: rock, sand and soft clay, are calculated by the SAP2000 software API. Fajfar, Marusic and Perus (2005) highlighted that on a stiff, symmetrical and conventionally supported structure, the first and second eigenmodes are expected to be translational. Whereas the third one is expected to be torsional. Therefore, the eigenperiods that correspond to the translational eigenmodes have to be larger in comparison to the eigenperiod with the corresponding torsional eigenmode. This fact is confirmed by the performed eigenvalue analysis for each

model of the conventionally supported building, for the examined soil types. Figures 4.6 – 4.8 illustrates the 1st, 2nd and 3rd eigenmodes for rock, sand and soft clay, respectively.

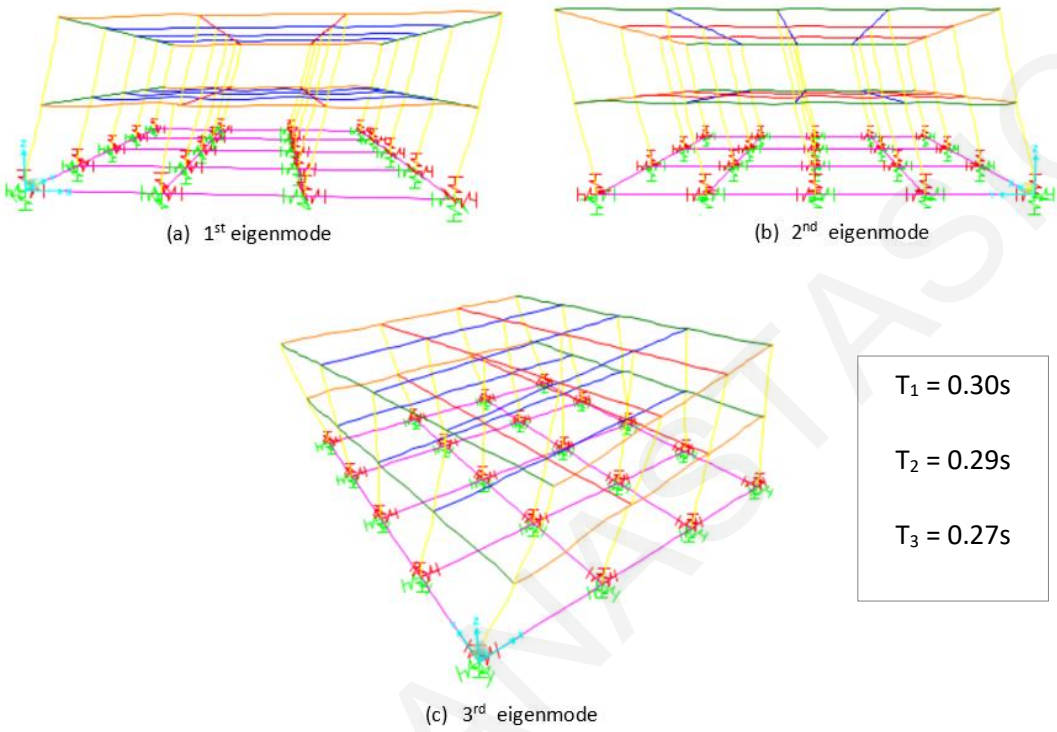


***Figure 4.6: (a) 1st, (b) 2nd and (c) 3rd eigenmodes corresponding to rock soil type***

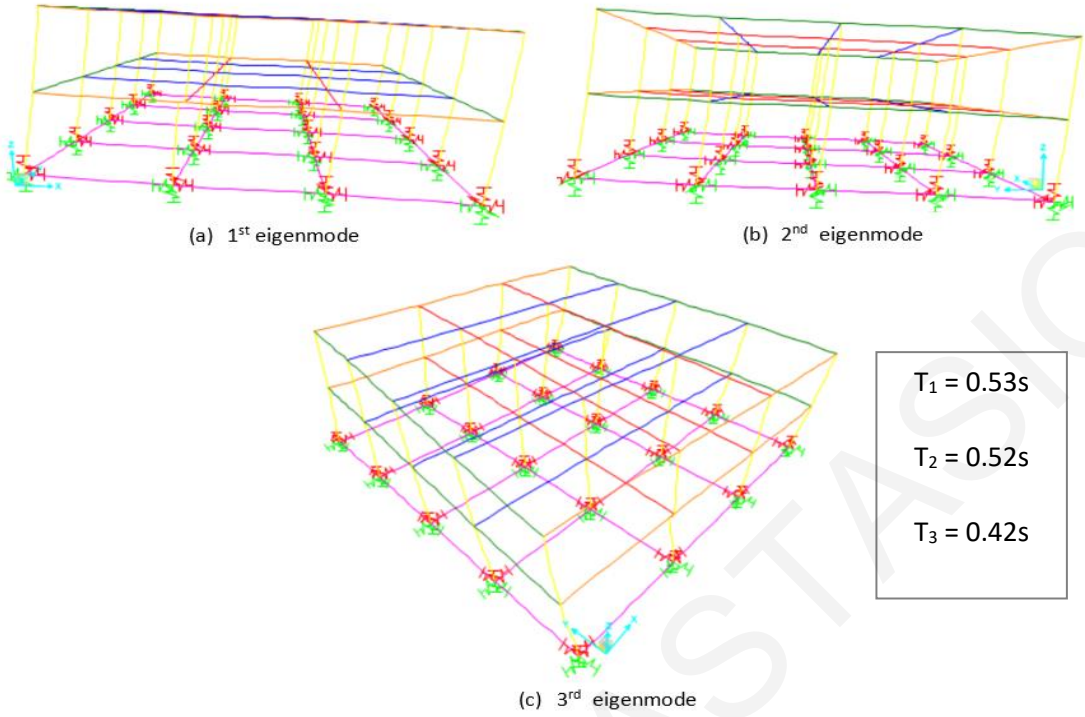


***Figure 4.7: (a) 1st, (b) 2nd and (c) 3rd eigenmodes corresponding to sand soil type***

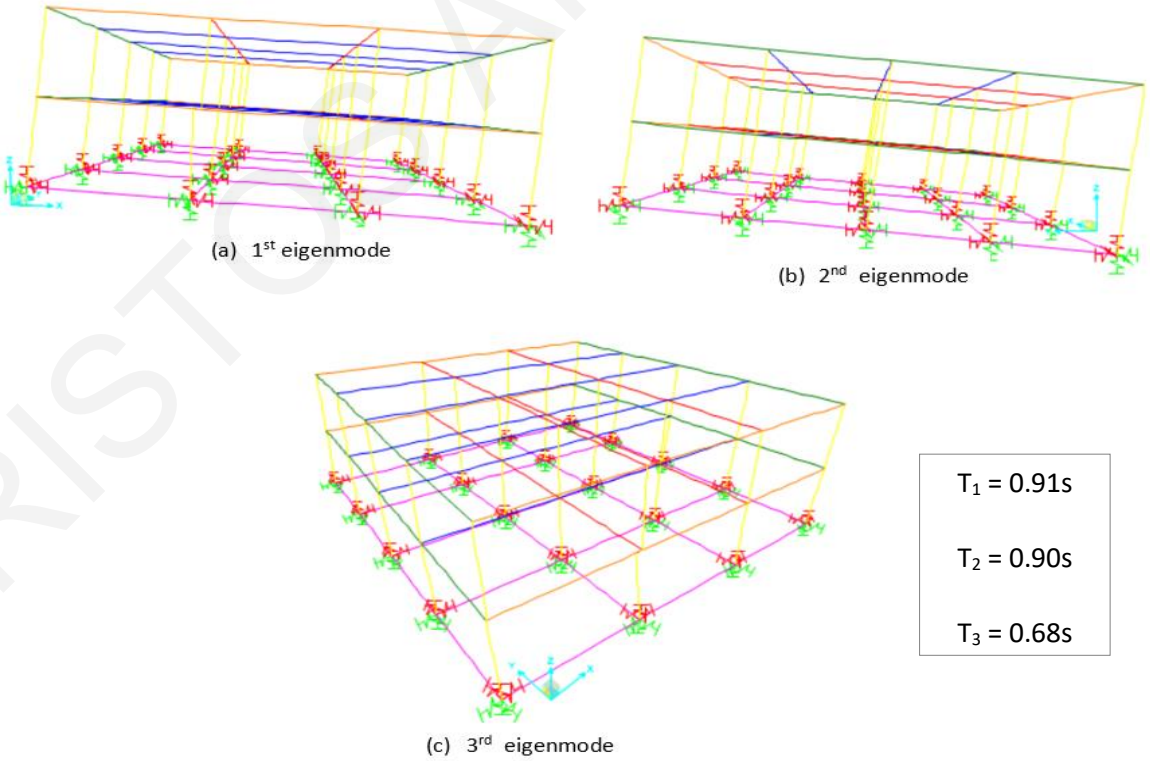


***Figure 4.8: (a) 1st, (b) 2nd and (c) 3rd eigenmodes corresponding to soft clay soil type***

In particular, the first eigenmode of the building on each examined soil type is translational in the primary horizontal X direction, while the second eigenmode is translational in the secondary horizontal Y direction. As expected, the third eigenmode is torsional in all of the three cases. The first, second and third eigenperiods of the building for the three examined soil types are shown in Table 4.12.

Specifically, the fundamental eigenperiod for the structure founded on rock, which is essentially equivalent to the fixed supported structure to a rigid ground, is 0.30 s. For the case of sand, the fundamental eigenperiod is increases to 0.53 s and for the structure founded on soft clay the fundamental eigenperiod is reaches the value of 0.91 s. Such lengthening of the fundamental eigenperiods, can remarkably affect the seismic response of the structures, which is examined in the following chapters.

***Table 4.12: 1st, 2nd and 3rd eigenperiods (T1, T2 and T3) and eigenmodes (Φ1, Φ2 and Φ3) of the conventionally supported building for rock, sand and soft clay***

| Soil Type | $T_1$ (s) | $\Phi_1$ | $T_2$ (s) | $\Phi_2$ | $T_3$ (s) | $\Phi_3$ |
|---|---|---|---|---|---|---|
| Rock | 0.30 | Translational in (horizontal) X direction | 0.29 | Translational in (horizontal) Y direction | 0.27 | Torsional around Z (vertical) axis |
| Sand | 0.53 | | 0.52 | | 0.42 | |
| Soft clay | 0.91 | | 0.90 | | 0.68 | |

# Chapter 5 - PEAK SEISMIC RESPONSE OF CONVENTIONALLY SUPPORTED BUILDING

## 5.1 Introduction

Selected results from the time-history analyses of the previously described typical conventionally supported building are presented in this chapter, providing the peak seismic responses under the selected seismic excitations. More specifically, the influence of soil deformability in the peak seismic response of the typical conventionally supported building, are presented and discussed. Additionally, the effects of the near-fault (NF) and the far-fault (FF) ground motions in combination with the effect of the soil deformability, on the peak seismic response are also examined and presented.

In particular, the peak interstorey drifts and the peak absolute floor accelerations, which represent the potential damage on the structural and non-structural elements due to deformations and the effect of excess accelerations on the occupants and contents of the building, are considered. Regarding the investigation of the effect of soil deformability, three cases for each loading combination (as stated in Chapter 4.8) are created and used, one for each different soil profile, as shown in Table 5.1.

***Table 5.1: Loading Combinations for each soil profile***

| Soil profile | Loading Combinations |
|---|---|
| Rock | G + 0.3 Q + Ex + 0.3 Ey |
| Sand | G + 0.3 Q + Ex + 0.3 Ey |
| Soft clay | G + 0.3 Q + Ex + 0.3 Ey |

The values of the structures' peak seismic responses for the first and the second storeys, are extracted by the corresponding corner nodes at each floor, as presented in Figure 5.1. Taking into account that all the nodes of each floor are constrained by a rigid diaphragm and that the structural models are symmetric without any eccentricities, monitoring the peak seismic responses of a corner node at each story is sufficient in this case.

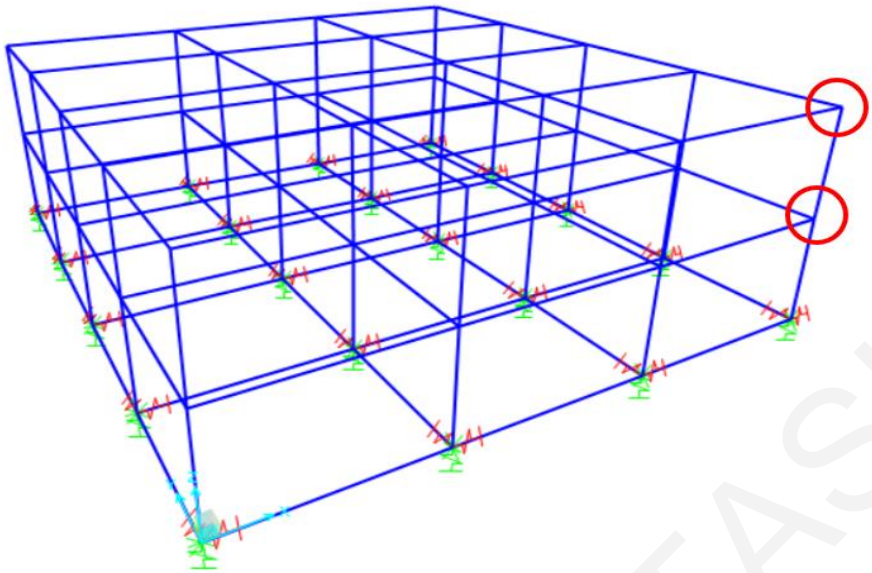

***Figure 5.1: Nodes of the examined model that used for the extraction of results***

## 5.2 Soil deformability effects

In order to investigate the soil deformability effects to the response of a typical conventionally supported structure, the building is subjected to the Cape Medocino seismic excitation, using different soil conditions. Specifically, the excitation that is used is the one that had been recorded at Eureka-Myrtle and West, during the 7.01 Mw Cape Medocino Earthquake, which happened in California (USA) in 1992. The fault-normal (FN) and the fault-parallel (FP) components of the excitation are illustrated in Figure 5.2, while Figure 5.3 shows the response spectra of the Cape's Medocino time-history records. The peak ground acceleration (PGA) is equal to 0.15g for the FN component and 0.18g for the FP component. The ground acceleration records are considered to act simultaneously in the two horizontal directions, the Fault-Normal (FN) and Fault-Parallel (FP) for each ground motion. The above data has been obtained through the Pacific Earthquake Engineering Research Center (PEER) ground motion database. It is worth to mention that the response of the building founded on rock, represents satisfactory the structure that is fixed-supported to an infinitely rigid base.

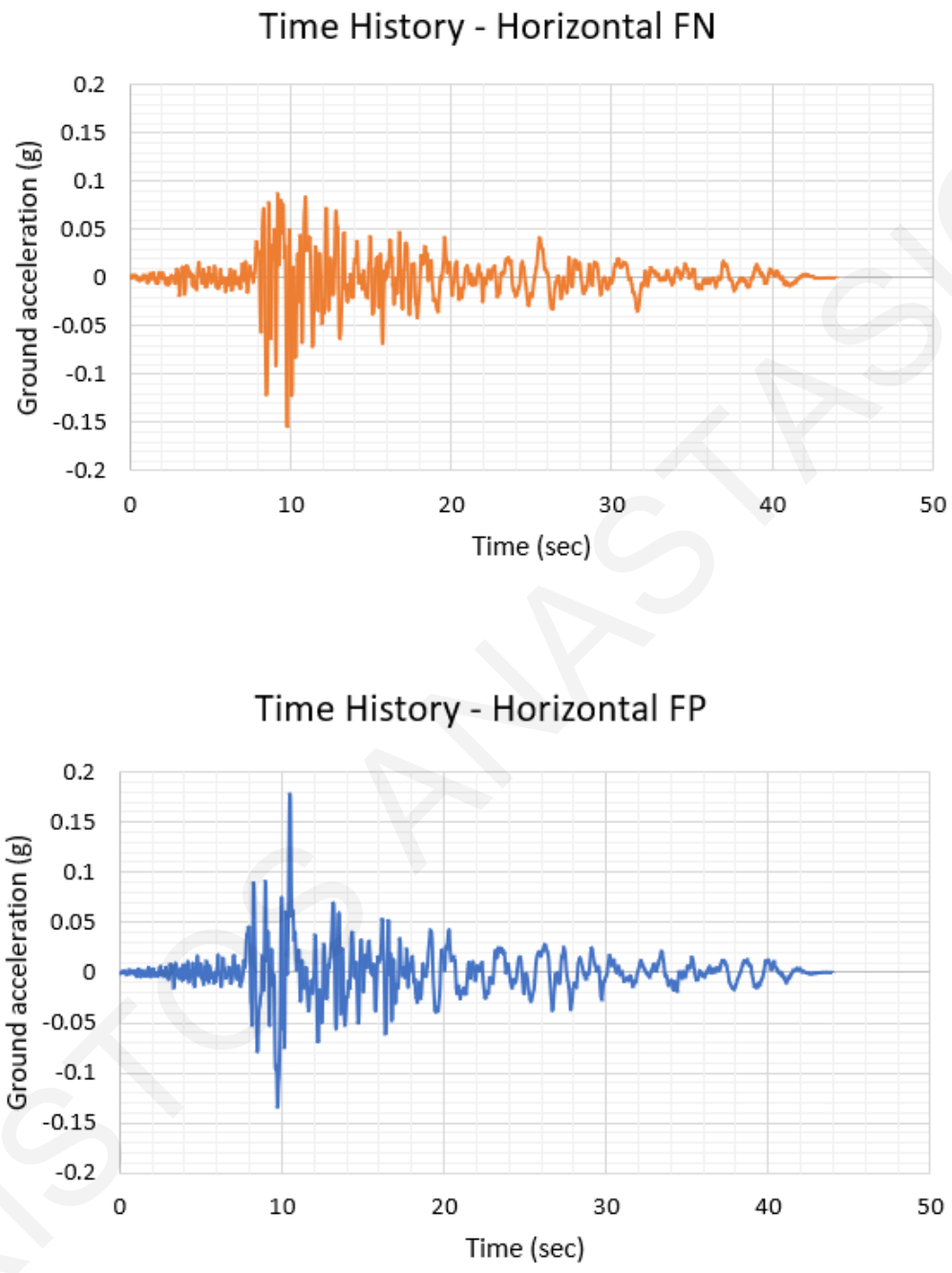


***Figure 5.2: Time histories of the FN and FP components of the Cape Medocino Earthquake***

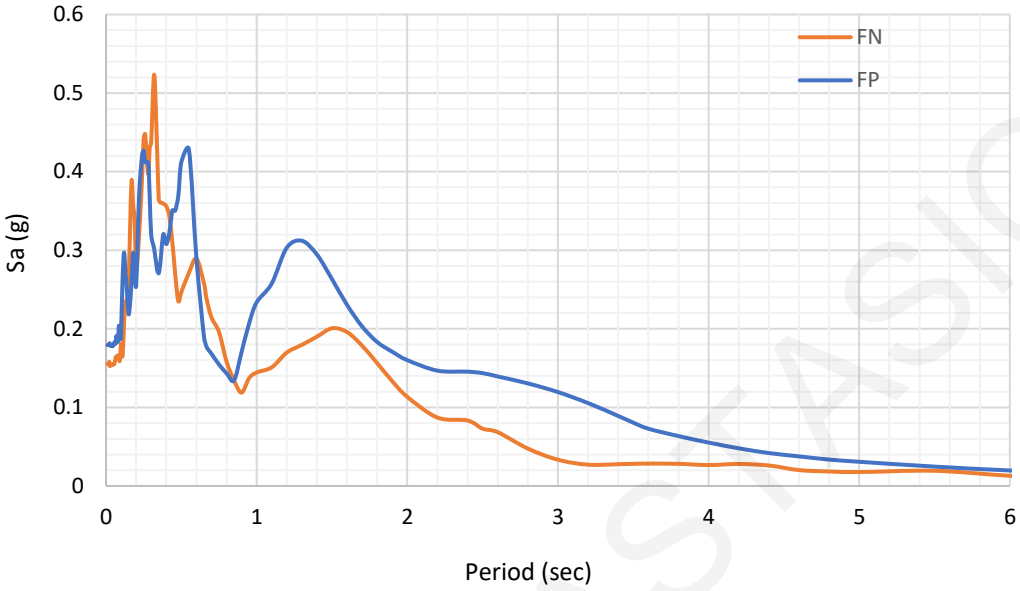


***Figure 5.3: Pseudoaccelerations response spectra for Cape's Medocino ground motion records***

### 5.2.1 Peak interstorey drifts

<u>Loading Combination G + 0.3Q + Ex + 0.3Ey</u>

The comparison of the maximum interstorey drifts of the conventional building for the three, under consideration, soil types: rock, sand and soft clay are used to assess the influence of the soil deformability. In particular, the peak, in absolute values, interstorey drifts in the two orthogonal horizontal directions of the conventionally supported building on rock, sand and soft clay, under the loading combination G+0.3Q+Ex+0.3Ey, are summarized in Table 5.2. Additionally, schematic illustrations of the above for the orthogonal horizontal directions X and Y are provided in Figure 5.4 and Figure 5.5, respectively.

***Table 5.2: Maximum, in absolute values, interstorey drifts in the two orthogonal horizontal directions of the conventionally supported building under the loading combination G+0.3Q+Ex+0.3Ey for all three soil types***

| Floor level | Maximum Interstorey Drifts | | | | | |
|---|---|---|---|---|---|---|
| | **Rock** | | **Sand** | | **Soft clay** | |
| | $\Delta U_x$ (mm) | $\Delta U_y$ (mm) | $\Delta U_x$ (mm) | $\Delta U_y$ (mm) | $\Delta U_x$ (mm) | $\Delta U_y$ (mm) |
| 2nd floor | 13 | 3.0 | 13 | 6.0 | 4.0 | 4.0 |
| 1st floor | 14 | 4.0 | 31 | 15 | 34 | 13 |

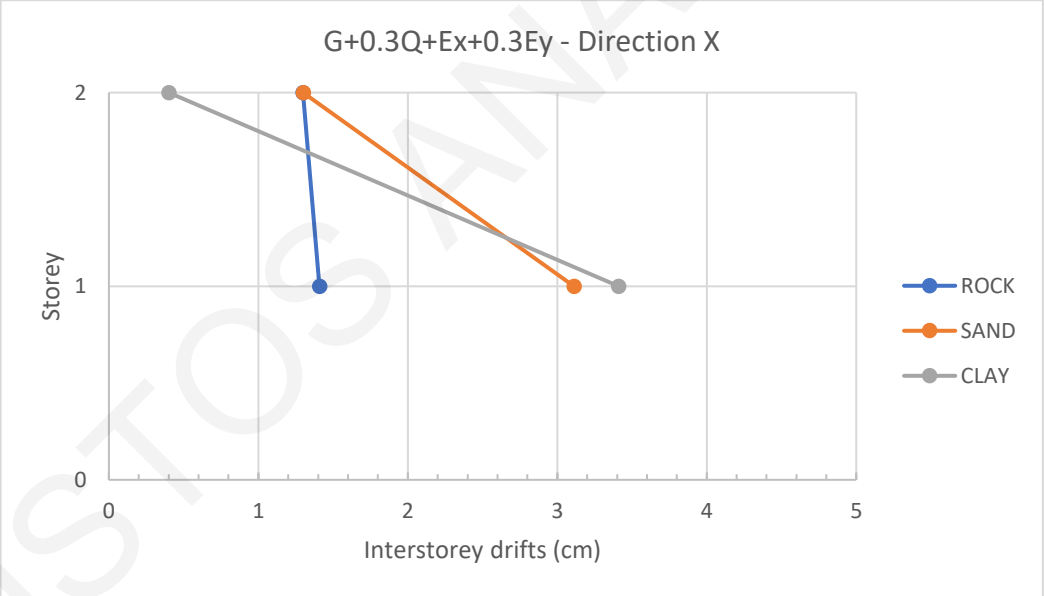


***Figure 5.4: Maximum, in absolute values, interstorey drifts in the X direction of the conventionally supported building, under the loading combination G+0.3Q+Ex+0.3Ey, on rock, sand and soft clay.***

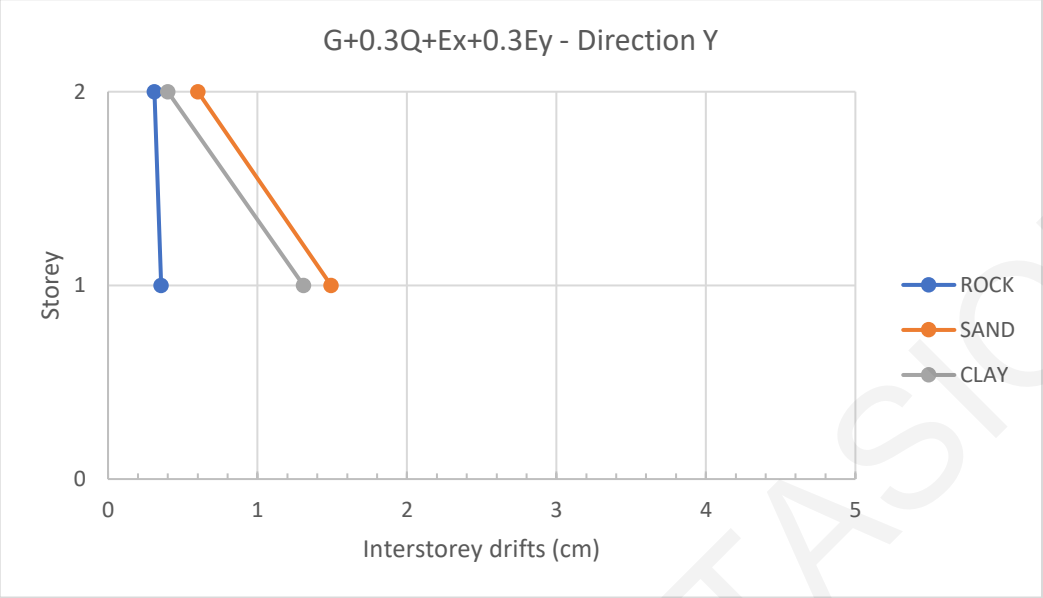


***Figure 5.5: Maximum, in absolute values, interstorey drifts in the Y direction of the conventionally supported building, under the loading combination G+0.3Q+Ex+0.3Ey, on rock, sand and soft clay.***

As it can be observed from the Figure 5.4, the maximum interstorey drifts for the building founded on rock and sand in the X direction are identical regarding the second floor, while the maximum interstorey drift in the first-floor level for the structure founded on sand, is more than double than the corresponding value of rock. In the case of soft clay, the maximum interstorey drift at the second-floor level is quite smaller than the rock's and sand's, whereas in the first floor level it has the highest value.

Specifically, the maximum interstorey drifts for the model founded on rock are 13 mm for the second-floor level and 14 mm for the first-floor level. In the case of sand, the maximum value at the second-floor level remains the same, while at the first-floor level an increase of about 121% is observed. Moreover, the value of the maximum interstorey drift for the structure supported on soft clay in comparison with the structure supported on rock, shows a reduction of approximately 69% in the first-floor level and an increase of about 134% for the second-floor level. Also, comparing the maximum interstorey drifts of the structure founded on sand with that on soft clay, it can be noticed that the former's value at the second-floor level is more than 3 times bigger than the latter, while in the first-floor level is 10% smaller.

On the other hand, as can be seen from Figure 5.5, the maximum interstorey drifts in the Y direction for the building founded on sand are increased compared to the corresponding values for the structure founded on rock. In addition, the maximum interstorey drift values for the structure founded on soft clay, of the first and second floor are bigger than the rock's values, but smaller that the corresponding values for sand. More precisely, the interstorey drifts in the Y direction for the case of rock are 3.0 mm for the second-floor level and 4.0 mm for the first-floor level. For the structure founded on sand, the corresponding values are increased to 6.0 mm and 15 mm. Regarding the soft clay's interstorey drift values, it can be noted that they are bigger about 25% and 225% respectively, compared to the rock's values. Nevertheless, soft clay's interstorey drifts are smaller than the corresponding interstorey drifts of the structure founded on sand. Thus, in the Y direction the largest interstorey drift values are developed in the case of sand. In conclusion, the soil deformability influences are likely more significant at the first-floor level than the second-floor level.

Loading Combination G + 0.3Q + 0.3Ex + Ey

Furthermore, the maximum, in absolute values, interstorey drifts in the two orthogonal horizontal directions X and Y of the typical conventionally supported building for rock, sand and soft clay, under the loading combination G+0.3Q+0.3Ex+Ey, are provided in Table 5.3. Moreover, schematic demonstrations are presented by Figures 5.6 and 5.7, respectively.

***Table 5.3: Maximum interstorey drifts, in absolute values, in the two orthogonal horizontal directions of the conventionally supported building under the loading combination G+0.3Q+0.3Ex+Ey for all soil types***

| Floor level | Maximum Interstorey Drifts | | | | | |
|---|---|---|---|---|---|---|
| | **Rock** | | **Sand** | | **Soft clay** | |
| | $\Delta U_x$ (mm) | $\Delta U_y$ (mm) | $\Delta U_x$ (mm) | $\Delta U_y$ (mm) | $\Delta U_x$ (mm) | $\Delta U_y$ (mm) |
| 2nd floor | 4.0 | 10 | 4.0 | 20 | 2.0 | 15 |
| 1st floor | 4.0 | 11 | 9.0 | 50 | 10 | 42 |

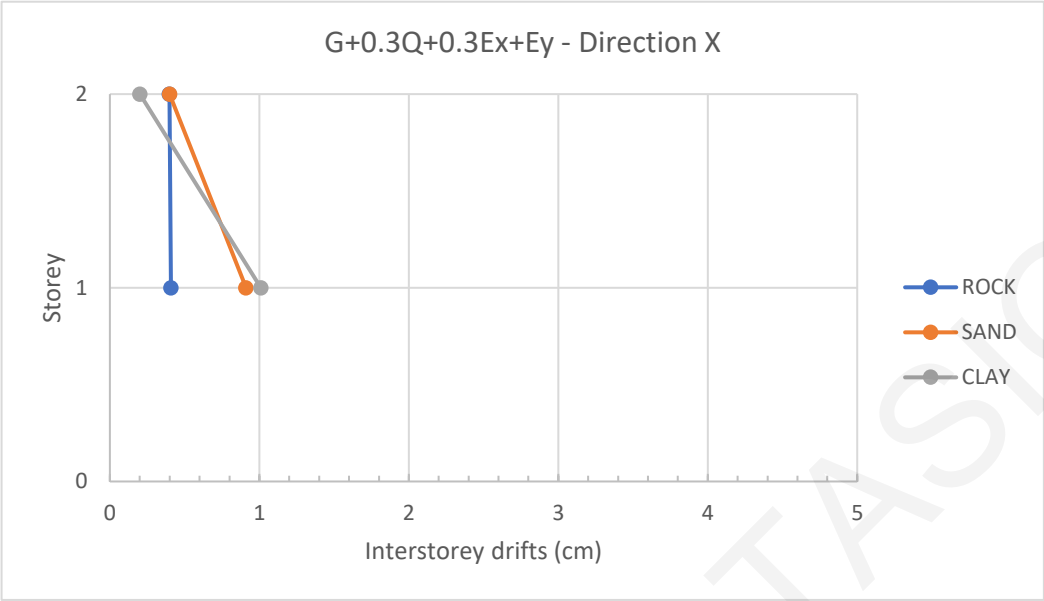


***Figure 5.6: Absolute values of the maximum interstorey drifts in the X direction of the conventionally supported building, under the loading combination G+0.3Q+Ex+0.3Ey, on rock, sand and soft clay.***

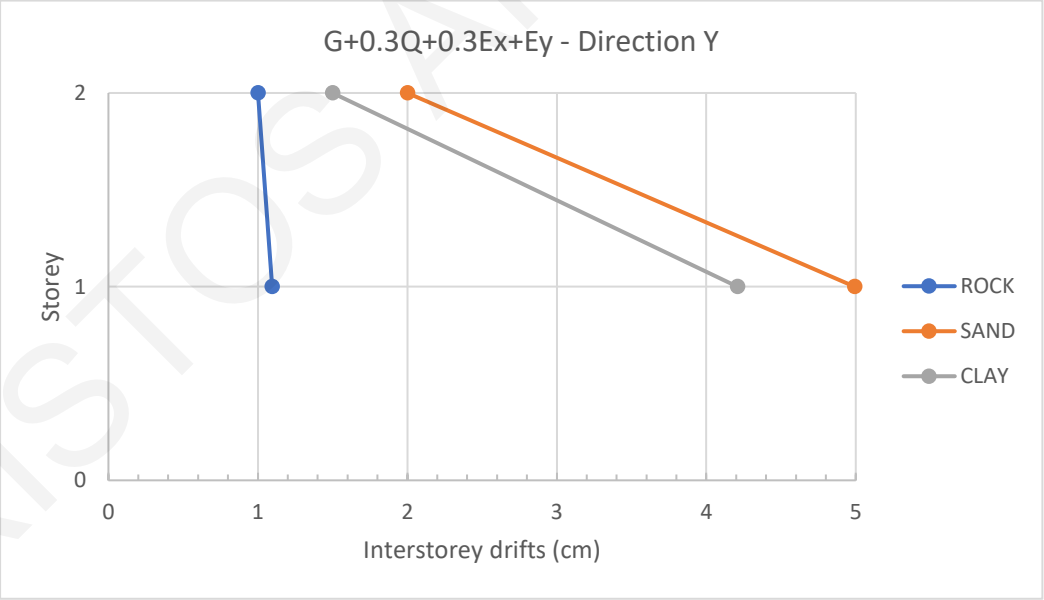


***Figure 5.7: Maximum interstorey drifts, in absolute values, in the Y direction of the conventionally supported building, under the loading combination G+0.3Q+Ex+0.3Ey, on rock, sand and soft clay.***

In general, it can be noticed from the above figures that, the results indicate similar trends and observations to the results under the load combination G+0.3Q+Ex+0.3Ey. Basically, for both X and Y directions the highest interstorey drift values arise when the building is founded on sand and soft clay. Hence, it can be clearly observed that ignoring the soil deformability could be unconservative regarding the assessment of the peak seismic response of a structure, in terms of the interstorey drifts, especially for the first-floor level.

### 5.2.2 Peak absolute floor accelerations

The peak total floor accelerations that would occur to the superstructure, while the conventionally supported structure is subjected to a strong seismic excitation, may cause damage to any sensitive equipment or contents of the building. Additionally, high absolute floor accelerations cause panic and discomfort to the occupants. The comparative study of the peak total accelerations at the floor levels, is considered important for the examination of soil's deformability impact to the building and its contents.

Loading Combination G + 0.3Q + Ex + 0.3Ey

The maximum total floor accelerations in both X and Y direction of the conventionally supported building founded on rock, sand and soft clay, under the loading combination G+0.3Q+Ex+0.3Ey, are shown in Figures 5.8 and 5.9, respectively. Moreover, their exact values are provided in Table 5.4.

***Table 5.4: Absolute values of the maximum total floor accelerations in the two orthogonal horizontal directions of the conventionally supported building under the loading combination G+0.3Q+Ex+0.3Ey for all soil types***

| Floor level | Maximum Floor Accelerations | | | | | |
|---|---|---|---|---|---|---|
| | **Rock** | | **Sand** | | **Soft clay** | |
| | $\ddot{u}_x$ (m/s$^2$) | $\ddot{u}_y$ (m/s$^2$) | $\ddot{u}_x$ (m/s$^2$) | $\ddot{u}_y$ (m/s$^2$) | $\ddot{u}_x$ (m/s$^2$) | $\ddot{u}_y$ (m/s$^2$) |
| 2$^{nd}$ floor | 11.70 | 3.09 | 6.34 | 3.11 | 2.05 | 0.85 |
| 1$^{st}$ floor | 6.30 | 1.59 | 4.59 | 2.31 | 2.55 | 0.58 |

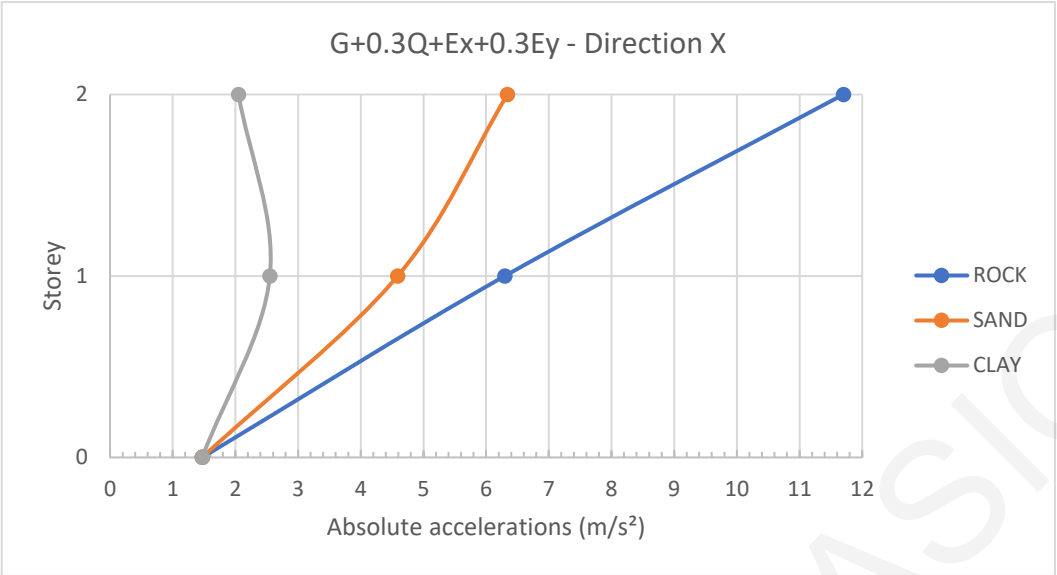


***Figure 5.8: Absolute values of the total floor accelerations in the X direction of the conventionally supported building under the loading combination G+0.3Q+Ex+0.3Ey on rock, sand and soft clay***

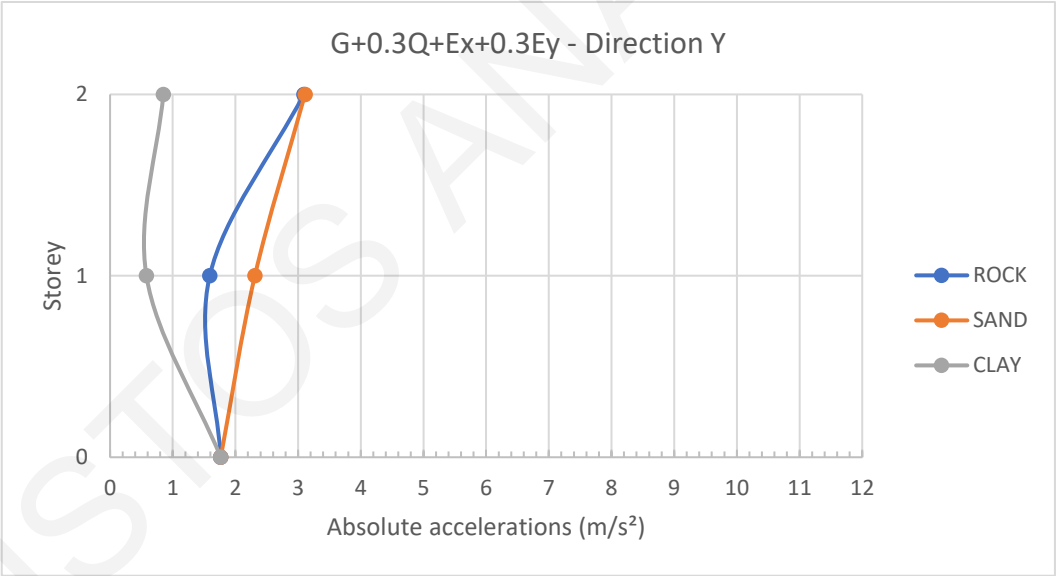


***Figure 5.9: Absolute values of the total floor accelerations in the Y direction of the conventionally supported building under the loading combination G+0.3Q+Ex+0.3Ey on rock, sand and soft clay***

First of all, it is evident that the maximum total accelerations are the highest when the building is founded on rock, in the X direction. More specifically, the maximum floor acceleration values are 11.70 m/s$^2$ for the second floor and 6.30m/s$^2$ for the first floor, which are about 8 and 4 times larger than the peak ground acceleration (PGA), respectively. The second highest absolute floor acceleration values can be observed in the case of sand, where there is a reduction in the values of about 46% and 37% for the second and first floor, respectively, in relation to the corresponding values of rock. Finally, the building founded on soft clay has develops the smallest total accelerations in direction X.

Contrarily, for the Y direction, the model founded on sand develops the largest total accelerations with 3.11 m/s$^2$ at the second floor and 2.31 m/s$^2$ at the first floor. In relation to the peak ground acceleration, the above values are about 53% and 36% higher. In the case of rock, the peak absolute floor acceleration value at the second floor has a minor reduction, but the peak total acceleration at the first floor decreases by about 31% compared to the corresponding sand's values. Furthermore, the structure founded on soft clay develops the smallest values of absolute floor accelerations, with both values being less than the PGA.

It can be noticed that by taking into consideration the soil deformability, the peak absolute floor accelerations of the conventionally supported structure are affected positively in the X direction. Whereas in the Y direction, the soil deformability amplifies the peak absolute floor accelerations.

Loading Combination G + 0.3Q + 0.3Ex + Ey

Furthermore, the peak absolute floor accelerations for the load combination G+0.3Q+0.3Ex+Ey in both X and Y direction of the conventional building founded on rock, sand and soft clay are illustrated in Figures 5.10 and 5.11, respectively, while the numerical values of the peak total floor accelerations, in absolute values, are provided in Table 5.5.

***Table 5.5: Absolute values of the maximum total floor accelerations in the two orthogonal horizontal directions of the conventionally supported building under the loading combination G+0.3Q+0.3Ex+Ey supported on all the three soil types***

| Floor level | Maximum Floor Accelerations | | | | | |
|---|---|---|---|---|---|---|
| | **Rock** | | **Sand** | | **Soft clay** | |
| | $\ddot{u}_x$ (m/s$^2$) | $\ddot{u}_y$ (m/s$^2$) | $\ddot{u}_x$ (m/s$^2$) | $\ddot{u}_y$ (m/s$^2$) | $\ddot{u}_x$ (m/s$^2$) | $\ddot{u}_y$ (m/s$^2$) |
| 2$^{nd}$ floor | 3.56 | 9.80 | 1.91 | 10.53 | 0.62 | 2.84 |
| 1$^{st}$ floor | 1.88 | 5.39 | 1.34 | 7.82 | 0.77 | 1.94 |

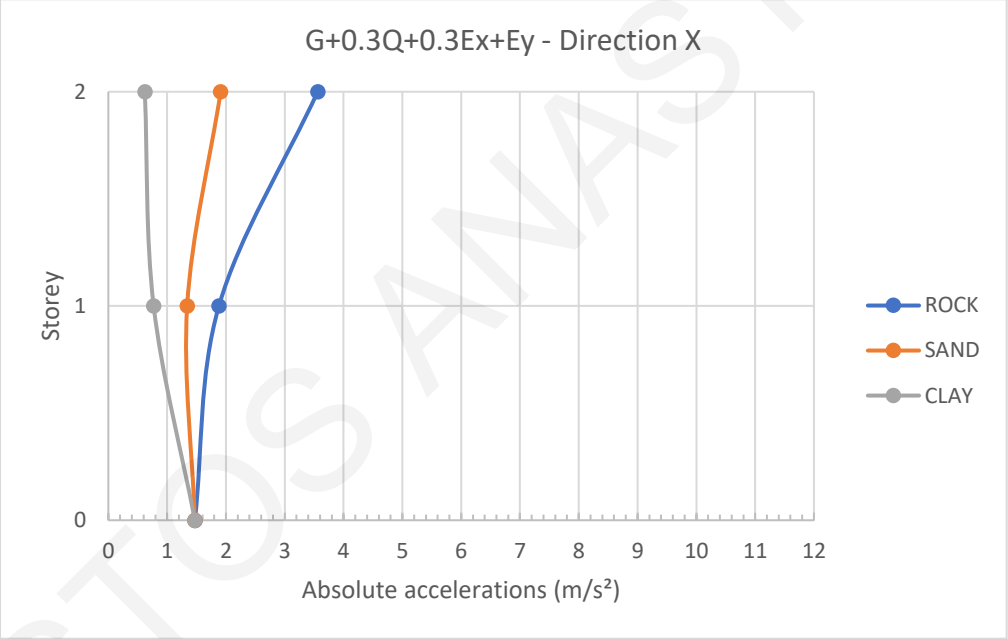


***Figure 5.10: Absolute values of the maximum total floor accelerations in X direction of the conventionally supported building under the loading combination G+0.3Q+0.3Ex+Ey supported on rock, sand and soft clay***

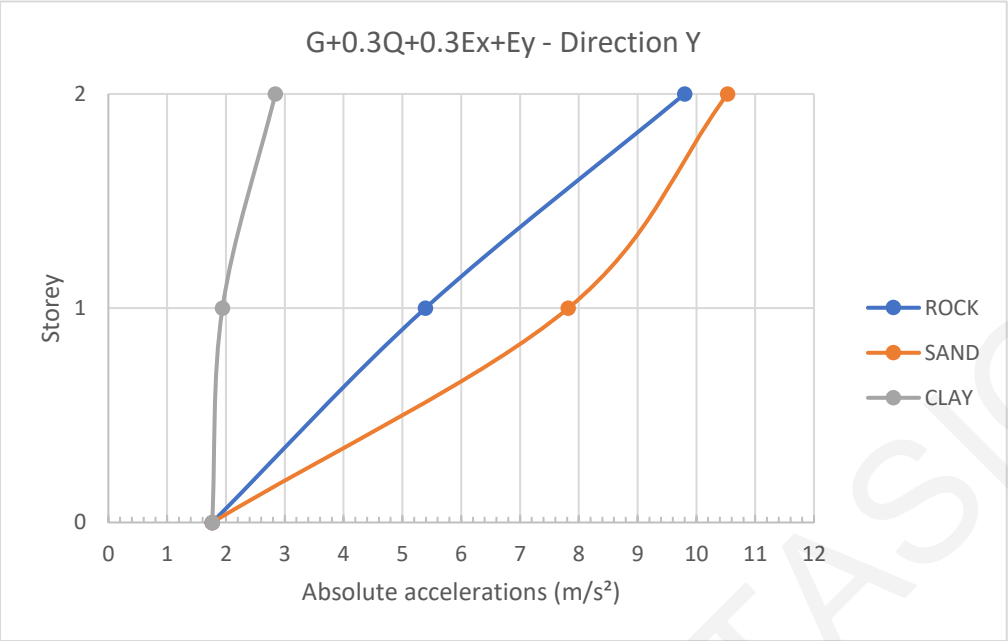


***Figure 5.11: Absolute values of the maximum total floor accelerations in Y direction of the conventionally supported building under the loading combination G+0.3Q+0.3Ex+Ey supported on rock, sand and soft clay***

As shown in Figure 5.10, soil deformability does not seem to negatively affect the absolute floor accelerations of the structure in the X direction, since the highest values of peak absolute floor accelerations are developed in the case of rock.

However, in the Y direction the soil deformability negatively influences the peak absolute floor accelerations. More precisely, the structure founded on sand reaches the highest peak total floor accelerations with values of 10.53 m/s$^2$ for the second floor and 7.82 m/s$^2$ for the first floor. These values are about 6 and 4 times higher than the peak ground acceleration, respectively. Furthermore, peak floor accelerations of the building founded on soft clay are reduced about 73% and 75% compared to the corresponding values for the building founded on sand, which has the minimum floor acceleration values. In brief, the computed results indicate that soil deformability should be taken into account to obtain more realistic and reliable results of the peak seismic response, since neglecting it might not always be conservative.

### 5.2.3 Conclusions

First of all, it is worth to highlight that these conclusions concern the computed results of the examined typical conventionally supported structure under the specific examined seismic excitation, the Cape's Medocino earthquake excitation, as mentioned above.

Specifically, the fundamental eigenperiod of the models for rock, sand and soft clay is 0.30 s, 0.53 s and 0.91 s, respectively. The rise on the fundamental eigenperiod indicates indirectly the significant influences of soil deformability to the peak seismic response of the simulated building, as confirmed by the changes in the peak responses when the soil deformability is taken into account.

Figure 5.12 and Figure 5.13 provide the spectral-displacements and spectral accelerations, respectively, for the seismic excitations that have been used for the time-history analyses. Furthermore, in both response spectra, the fundamental eigenperiods for the models founded on rock, sand and soft clay are also indicated with vertical lines.

Considering the response spectra ventures the findings of the conducted time-history analyses regarding the effects of the soil deformability. The consideration of soil deformability increases the fundamental eigenperiods compared to the rigid-base assumption. As a consequence, for the current time-history record, the increase of the fundamental eigenperiods due to soil deformability, results in higher values of the maximum interstorey drifts and the peak floor accelerations in most of the cases. In summary, these results indicate that soil deformability is not always beneficial, and thus, it has to be taken into consideration in the seismic design of structures.

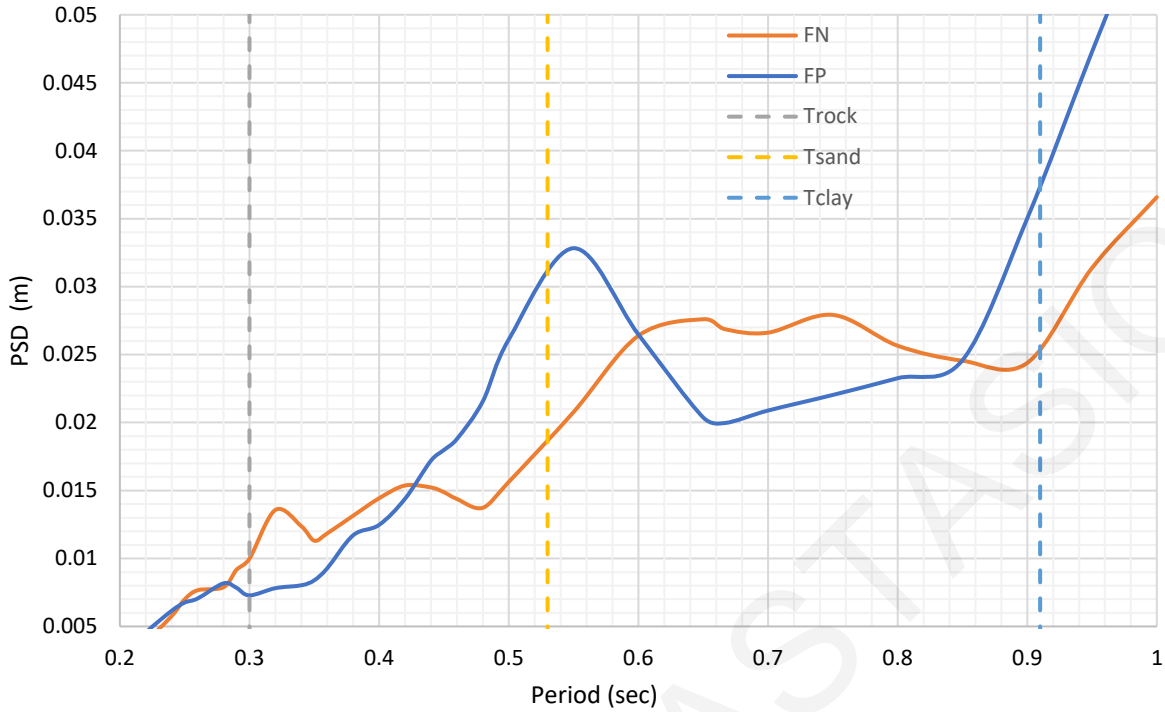


***Figure 5.12: Spectral-displacements response spectra for Cape's Medocino excitation record, (scaled to a pga=0.25g) with the fundamental eigenperiods of the buildings founded on rock, sand and soft clay, noted.***

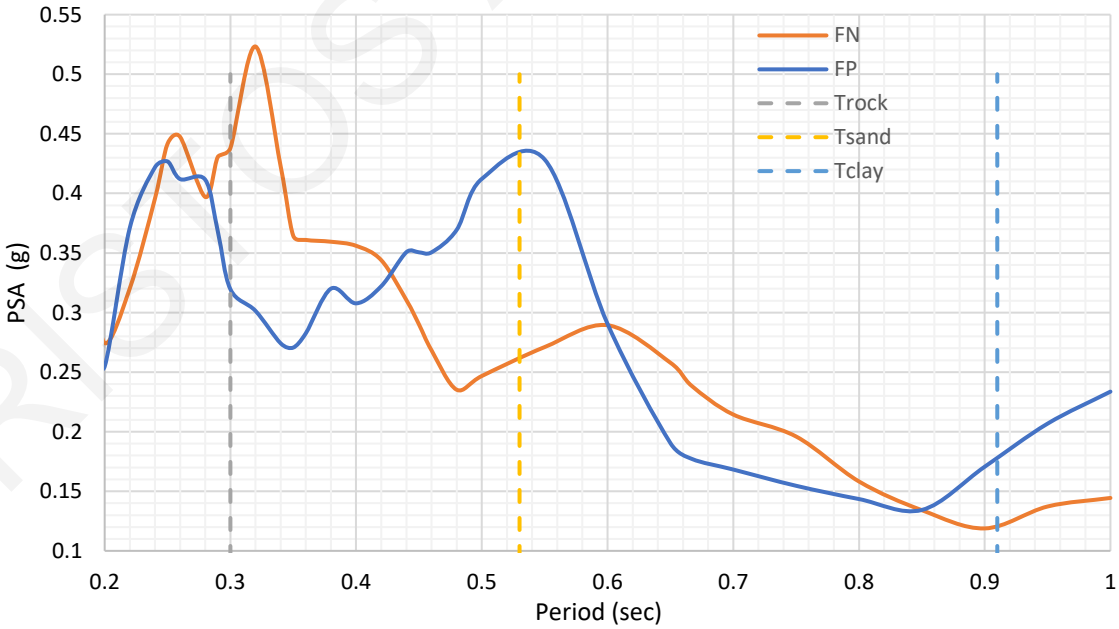


***Figure 5.13: Spectral-accelerations response spectra for Cape's Medocino excitation record, (scaled to a pga=0.25g) with the fundamental eigenperiods of the building founded on rock, sand and soft clay, noted.***

Lastly, the time-history analyses show that the maximum values of the interstorey drifts are developed in the models with the soil deformability taken into account. In regards to the maximum total floor accelerations, it is observed that it is not always conservative to ignore the soil deformability.

Conclusively, the soil deformability is a dominant factor in the peak seismic response of buildings, as shown by the computed time-history analyses' results under the Cape's Medocino time-history record. Therefore, it should be indispensably taken into consideration for the earthquake design of structures, to more accurately and reliably compute the peak seismic responses.

## 5.3 Soil deformability effects under NF *vs.* FF seismic excitations

The seismic activity of the region where the structure is constructed is a significant factor for its seismic response. In addition, the seismic response depends on the intensity and the characteristics of the expected earthquake excitations. Thus, the seismic response of the conventionally supported building is examined under pairs of both NF and FF seismic excitations, considering the soil deformability as well.

In order to investigate the effect of NF seismic ground motions combined with soil deformability, 5 sets of NF and 5 sets of FF accelerograms, which have been obtained from the Pacific Earthquake Engineering Research Center Database, are used. Specifically, the peak seismic response of the conventional building founded on rock, sand and soft clay is computed by linear elastic time-history analyses. As already stated in previous studies (Somerville, 2005), to achieve more accuracy, two acceleration records are considered to act simultaneously in the two horizontal directions, the Fault-Normal (FN) and Fault-Parallel (FP), for each ground motion.

The selection of the NF ground motion records is based on specific criteria, as stated by Mavronicola (2016). Specifically, the earthquake magnitude is equal or higher than 6.0 ($w \geq 6.0$) and the distance to the fault rupture less than fifteen kilometres ($Rrup$<15 $km$). The FF accelerograms are selected from the same seismic event, but at a further distance from the fault rupture, $Rrup$>40 $km$. Relevant information is provided in Table 5.6, for the NF accelerograms, and in Table 5.7 for the FF accelerograms.

***Table 5.6: Description of the selected horizontal near-fault (NF) ground motions***

| EQ No. | NGA seq. No. | Event | Year | Station | $M_w$ | FN PGA (g) | FP PGA (g) | $R_{rup}$ (km) | $Vs_{30}$ (m/sec) |
|---|---|---|---|---|---|---|---|---|---|
| 1 | 171 | Imperial Valley-06 | 1979 | El Centro - Meloland Geot. Array | 6.53 | 0.32 | 0.30 | 0.07 | 264.57 |
| 2 | 723 | Superstition Hills-02 | 1987 | Parachute Test Site | 6.54 | 0.43 | 0.38 | 0.95 | 348.69 |
| 3 | 1489 | Chi Chi - Taiwan | 1999 | CHY057 | 7.62 | 0.28 | 0.24 | 3.80 | 487.30 |
| 4 | 1176 | Kocaeli - Turkey | 1999 | Cekmece | 7.50 | 0.23 | 0.32 | 4.80 | 297.00 |
| 5 | 292 | Irpinia Italy - 01 | 1980 | Arienzo | 6.90 | 0.23 | 0.32 | 10.80 | 1000.00 |

***Table 5.7: Description of the selected horizontal far-fault (FF) ground motions***

| EQ No. | NGA seq. No. | Event | Year | Station | $M_w$ | FN | FP | $R_{rup}$ (km) | $Vs_{30}$ (m/sec) |
|---|---|---|---|---|---|---|---|---|---|
| | | | | | | PGA (g) | PGA (g) | | |
| 6 | 826 | Cape Mendocino | 1992 | Centerville Beach_Naval | 7.01 | 0.15 | 0.18 | 41.91 | 337.46 |
| 7 | 946 | Northridge - 01 | 1994 | Pico Canyon Rd | 6.69 | 0.05 | 0.07 | 46.91 | 572.57 |
| 8 | 283 | Irpinia Italy - 01 | 1980 | Sturno | 6.90 | 0.03 | 0.03 | 52.94 | 612.78 |
| 9 | 799 | Loma Prieta | 1989 | Saratoga - Aloha Ave | 6.93 | 0.24 | 0.33 | 58.65 | 190.14 |
| 10 | 751 | Loma Prieta | 1989 | Gilroy - Historic Bldg | 6.93 | 0.07 | 0.12 | 78.41 | 512.27 |

In order to have compatible response results, all near-fault and far-fault ground motion records are scaled to have their peak ground accelerations (PGA) equal to $0.3g$. Figures 5.14 and 5.15 illustrate the ground acceleration time-histories for the fault-normal (FN) and fault-parallel (FP) components of the selected near-fault and far-fault ground motions, respectively.

Moreover, Figure 5.16 provides the corresponding response spectra of each seismic record that is used. As it can be observed, intense pulses with large durations is a typical phenomenon in acceleration time-histories of the NF excitations records, while in the FF ground motion records less such variations are observed.

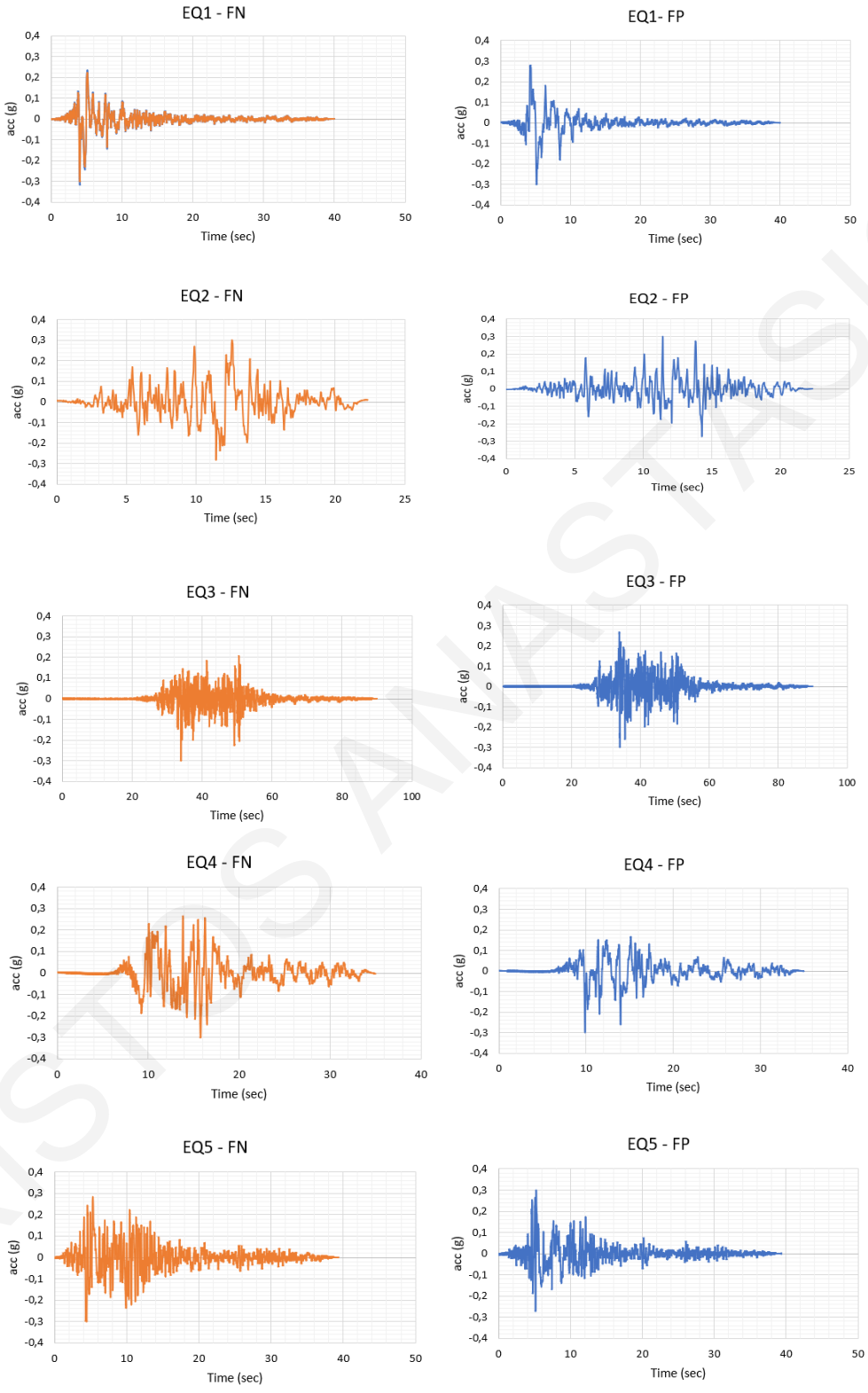


***Figure 5.14: Scaled (PGA=0.3g) time-history records for FN and FP components of the selected NF ground motions***

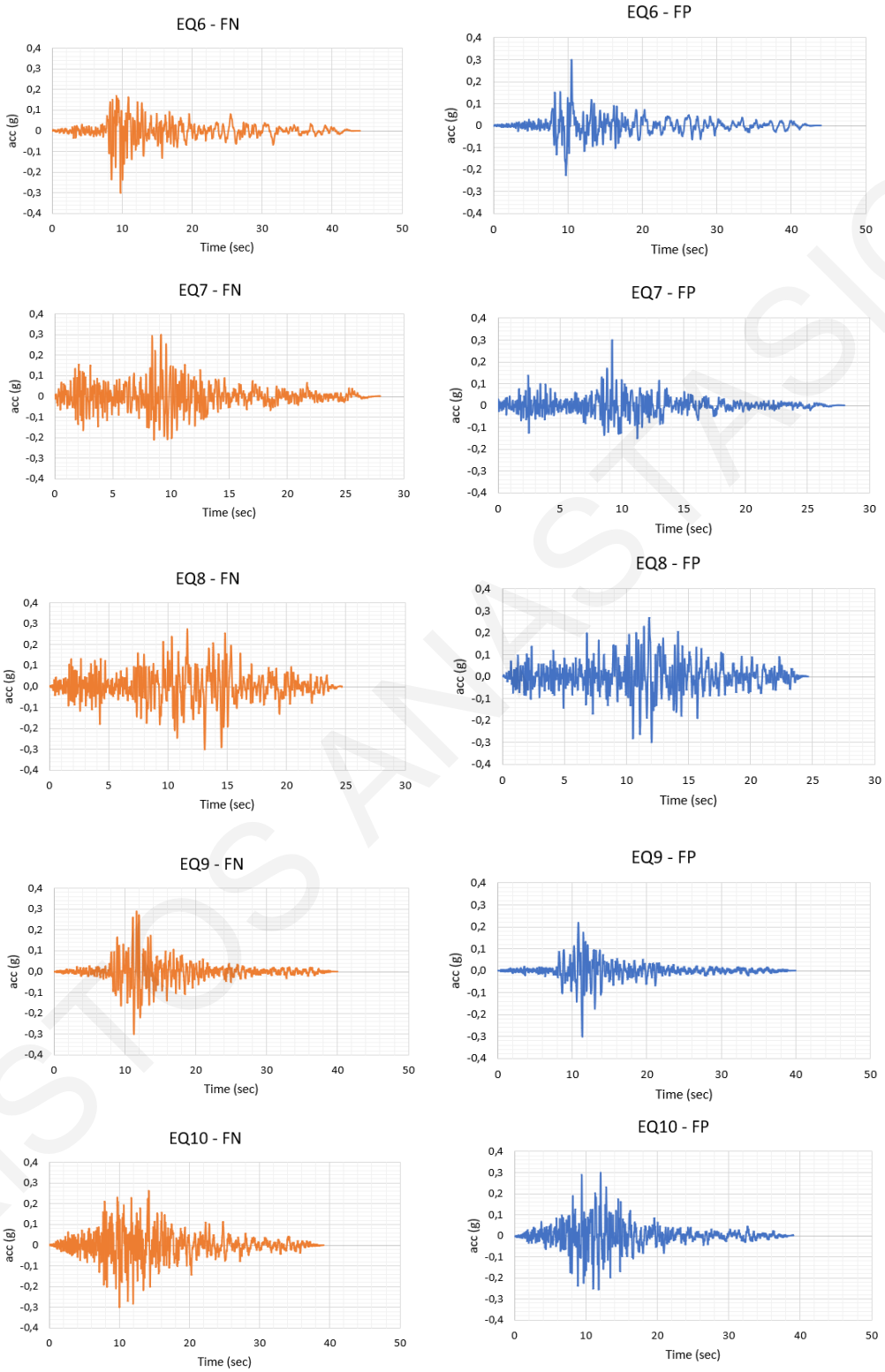


***Figure 5.15: Scaled (PGA=0.3g) time-history records for FN and FP components of the selected FF ground motions***

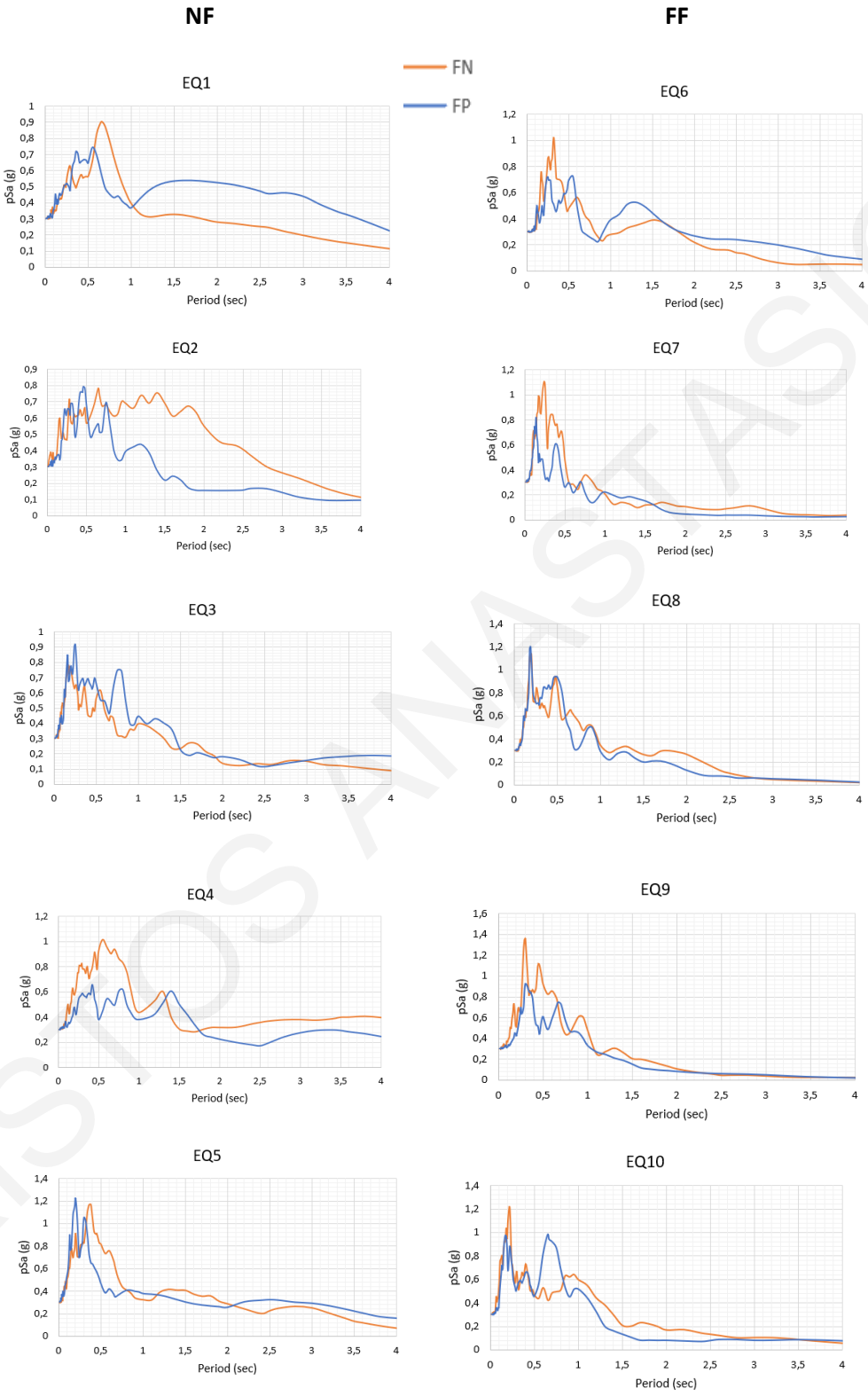


***Figure 5.16: Spectral acceleration response spectra of the selected NF and FF ground motions in the FN and FP directions***

From the execution of the time-history analyses, only the peak interstorey drifts are going to be discussed with a brief mention to the absolute floor accelerations. It is noted that the buildings are examined only under the loading combination G+0.3Q+Ex+0.3Ey in the orthogonal horizontal direction X.

### 5.3.1 Peak interstorey drifts

Figures 5.17 and Figure 5.18 demonstrate the maximum interstorey drifts (in absolute values) in the X direction for the selected NF and FF ground motions of the structures founded on rock, sand and soft clay, respectively, under the loading combination G+0.3Q+Ex+0.3Ey. It is worth to note that when referring to NF1 it represents the EQ No.1, which is a NF earthquake ground motion record, and FF6 represents the EQ No.6, which is an FF earthquake ground motion record. The same applies for the rest of the earthquake ground motion records, as well.

It is evident from the figures below that the influence of the soil deformability is very important in the peak seismic response of the building, in terms of interstorey drifts. More specifically, from all of the NF ground motion records, the structure founded on soft clay develops the largest interstorey drift values at both the second and the first-floor levels. Also, the same occurs for the FF ground motion records. Furthermore, by comparing the structure founded on sand and rock, it can be observed that the maximum interstorey drifts are higher when the building is supported on sand. This fact confirms the importance of soil deformability to the structure's response.

Additionally, the peak seismic responses show that for the models with the soil deformability taken into account, lead to increased maximum interstorey drifts than when the soil deformability is ignored. The above observations prove that the soil deformability is a very important factor that has to be taken into consideration, in the earthquake design of structures. Lastly, the effects of the NF and the FF ground motion records are related to the soil characteristics that the structure is founded on, which is another case that confirms the significance of considering the soil deformability.

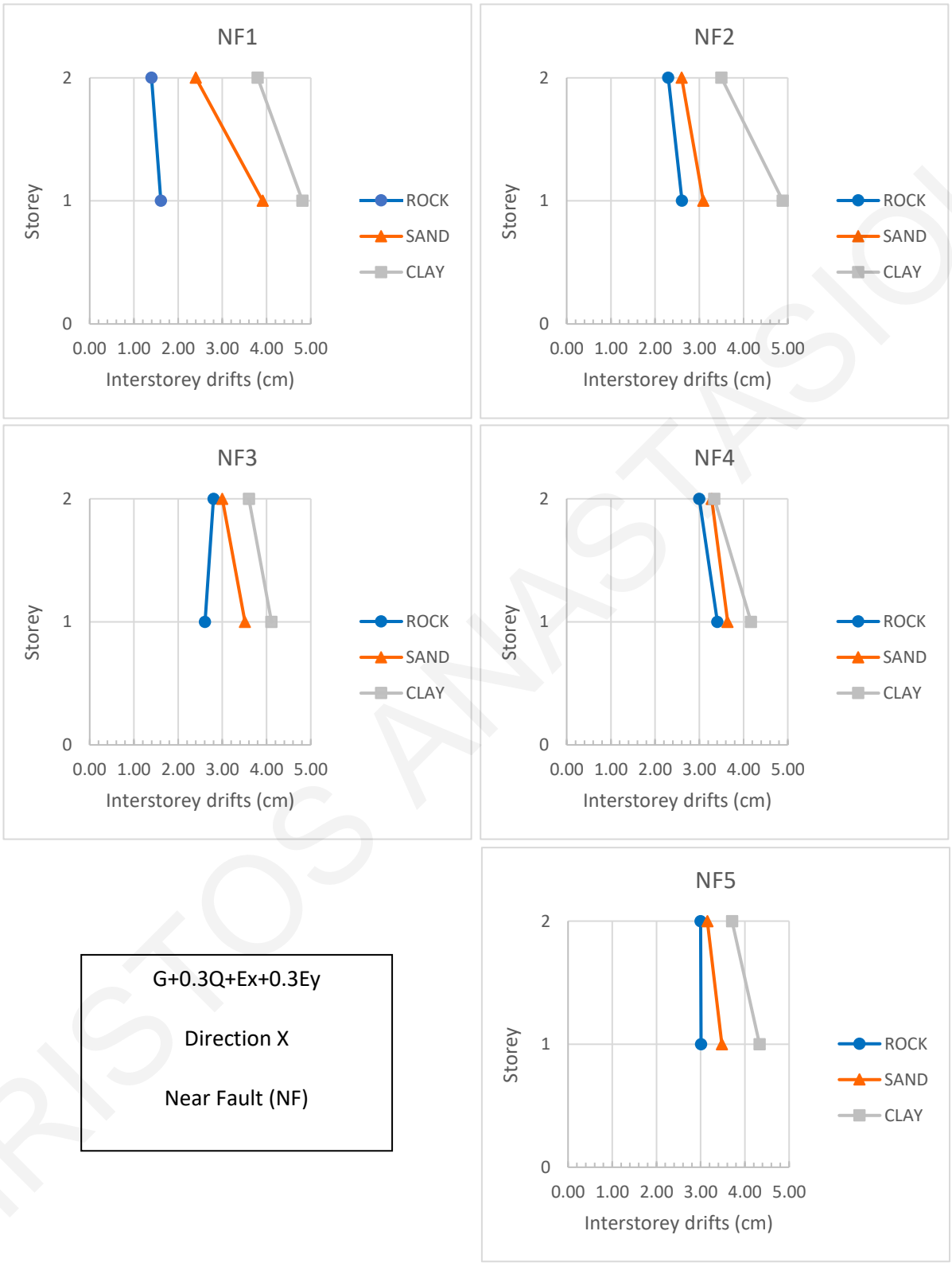


***Figure 5.17: Maximum interstorey drifts in absolute values in the X direction for the selected NF ground motions of the building founded on rock, sand and soft clay***

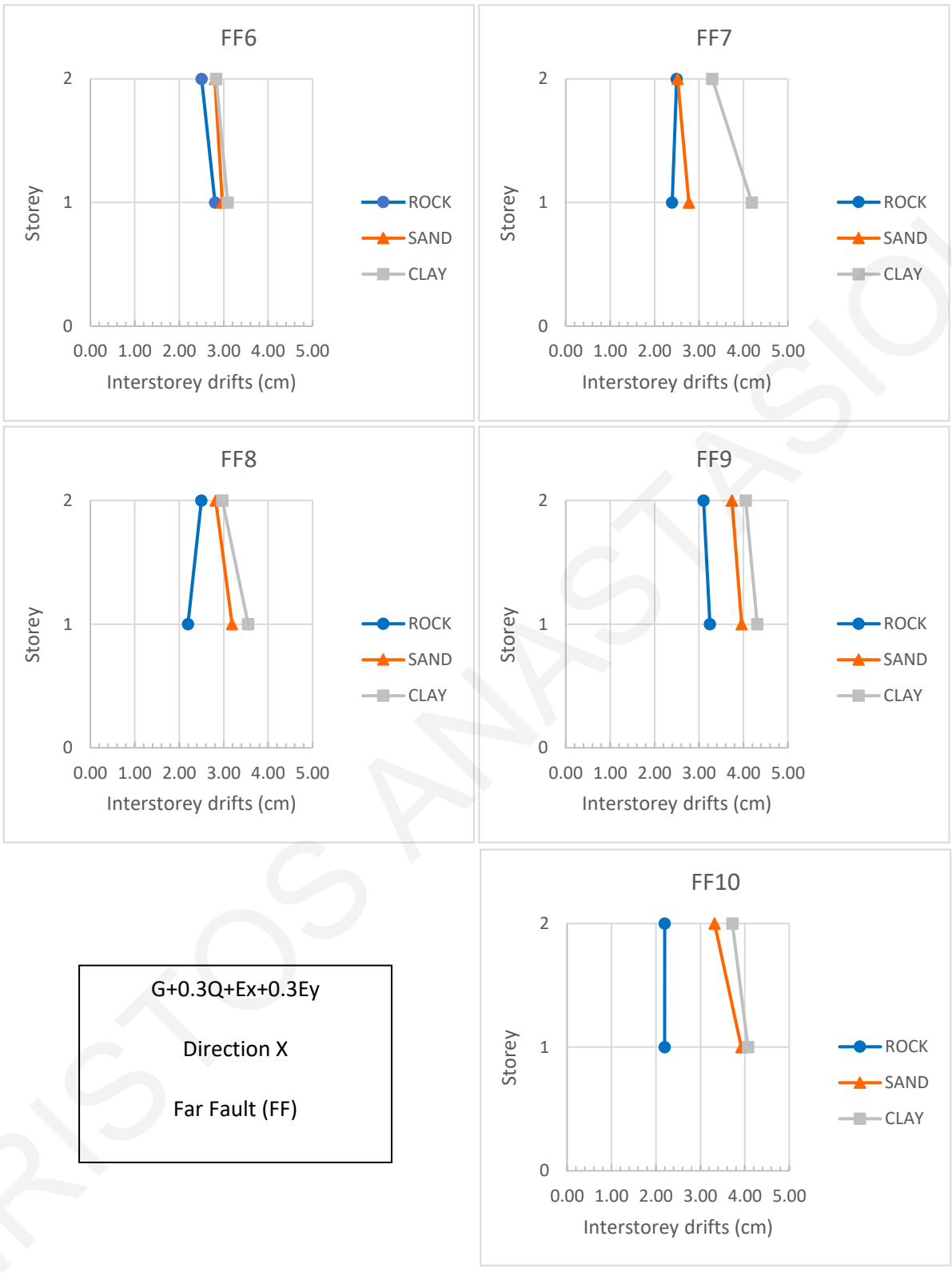


***Figure 5.18: Maximum interstorey drifts in absolute values in the X direction for the selected FF ground motions of the building founded on rock, sand and soft clay***

### 5.3.2 Peak absolute floor accelerations

Figures 5.19 and Figure 5.20 provide the peak total floor accelerations (in absolute values) in the X direction for the selected NF and FF ground motions of the buildings founded on rock, sand and soft clay, respectively, under the loading combination G+0.3Q+Ex+0.3Ey.

It is pointed out that, the maximum absolute floor acceleration results are higher when the building is founded on rock, in all cases. Specifically, the consideration of the soil deformability leads to smaller absolute floor accelerations, which in brief, means that the effect of the accelerations felt by the occupants and the building's contents, are lower.

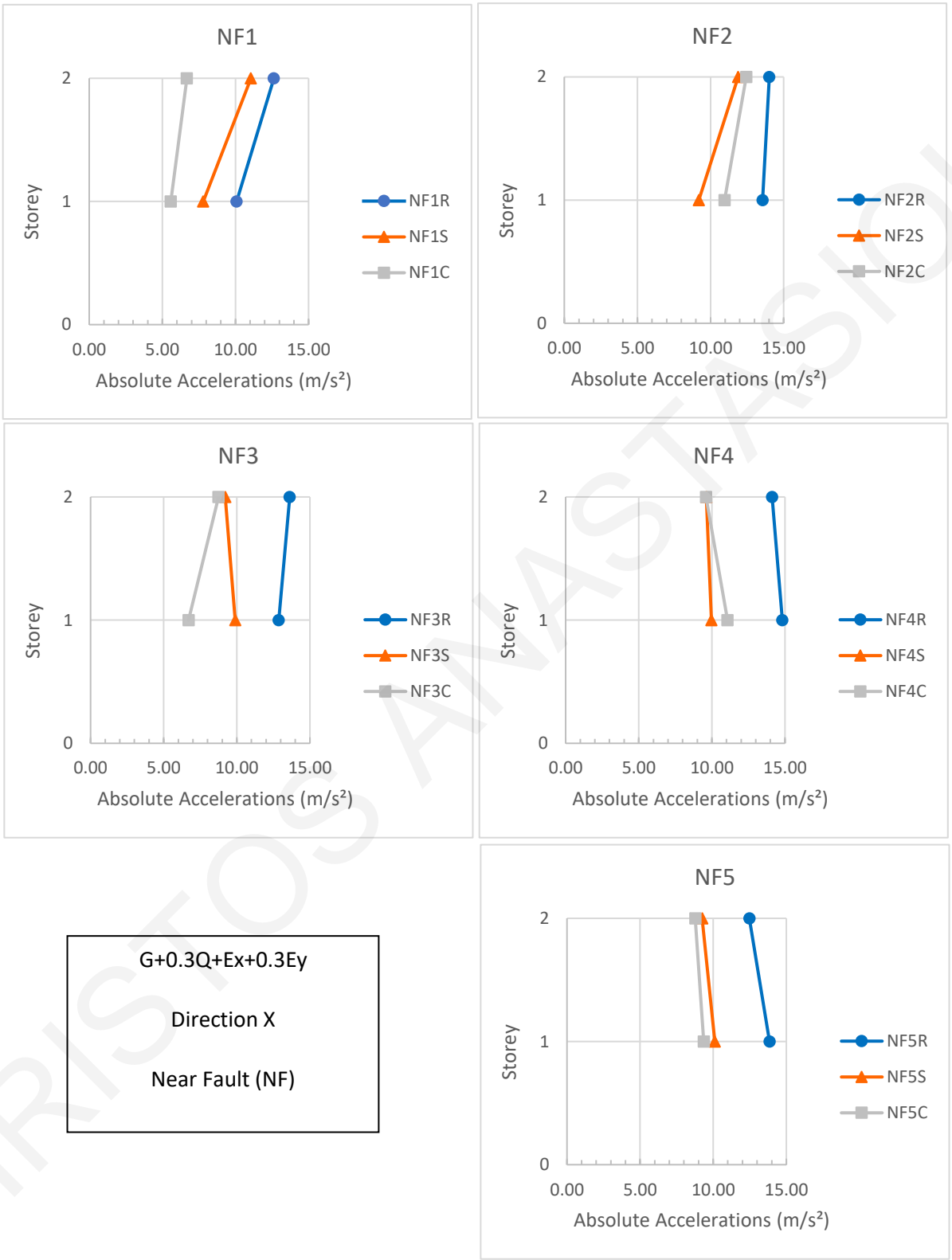


***Figure 5.19: Peak total floor accelerations (in absolute values) in the X direction for the selected NF ground motions of the building founded on rock, sand and soft clay***

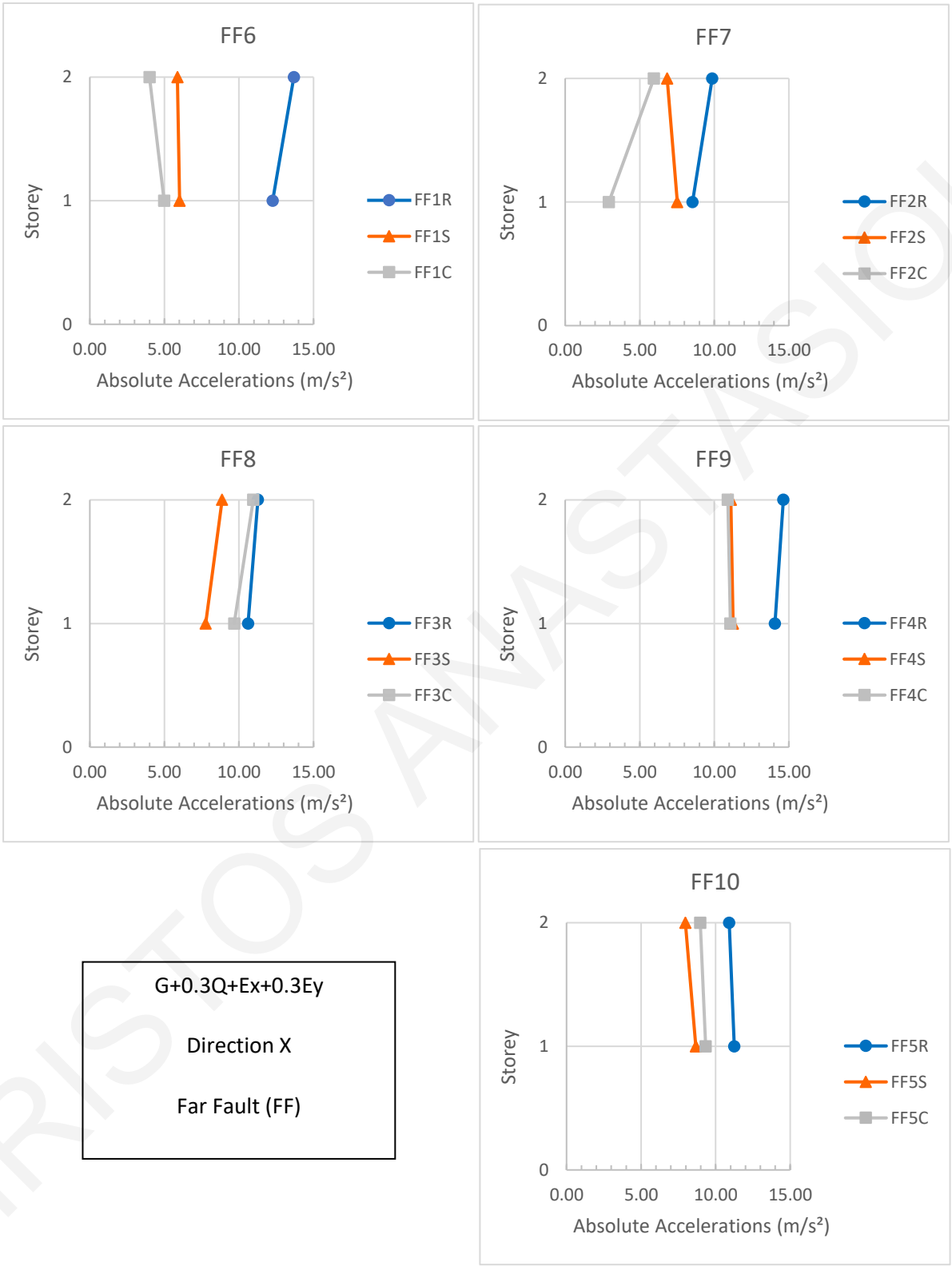


***Figure 5.20: Peak total floor accelerations (in absolute values) in the X direction for the selected FF ground motions of the building founded on rock, sand and soft clay***

# Chapter 6 – UTILIZATION OF SEISMIC ISOLATION

## 6.1 Introduction

Numerous earthquakes occur every year worldwide, which they can cause significant damage to structures and ruin thousands of human lives, too. In high seismicity areas, the most critical external action on structures are strong earthquake excitations. In addition, severe earthquakes remain at the top of the list of the most destructive phenomena of nature. They can pose a serious threat to humanity, especially in countries with buildings not satisfying any earthquake resistant design requirements. Advances in structural engineering and earthquake resistant design, have remarkably reduced both human damage and casualties, during strong earthquakes.

The fundamental eigenperiods of low- to medium-rise fixed-supported buildings happen to coincide with the predominant frequencies of common earthquakes. During strong seismic excitations, the induced seismic forces to the buildings, due to resonance, can be excessively high that, inelastic deformations are developed. Due to the extremely high induced seismic forces, which are caused by the resonance of the fundamental eigenfrequencies of relatively low-rise stiff buildings with the common predominant earthquake frequencies, buildings cannot be designed to respond elastically during strong earthquakes. That would be not economically affordable and is aesthetically unattractive. Hence, conventional earthquake-resistant design philosophy is focused on the protection of human lives, while, sufficient ductility provided by earthquake-resistant designed buildings, avoid brittle structural collapses, which are the main reason for human deaths, during severe earthquakes.

The limitation of the conventional earthquake resistance design to prevent damage has forced the utilisation of innovate passive and active control approaches, such as the seismic isolation. Basically, seismic isolation can be utilized to reduce the induced seismic loads of the superstructure by avoiding resonance of the fundamental eigenfrequency of the building with the predominant frequencies of seismic excitations. In order to avoid resonance, the dynamic characteristics of the building have to be modified. Specifically, flexibility must be inserted to the structure, by installing seismic isolators in the horizontal directions, typically at the base of the building. By avoiding resonance, the interstorey drifts

and the floor accelerations can be significantly reduced. In addition, damage of the structural and non-structural components, as well as equipment that might be hosted in a seismically isolated building, can be avoided and the superstructure can remain linear elastic during a seismic excitation, moving almost as a rigid body without deformations (see Figure 6.1).

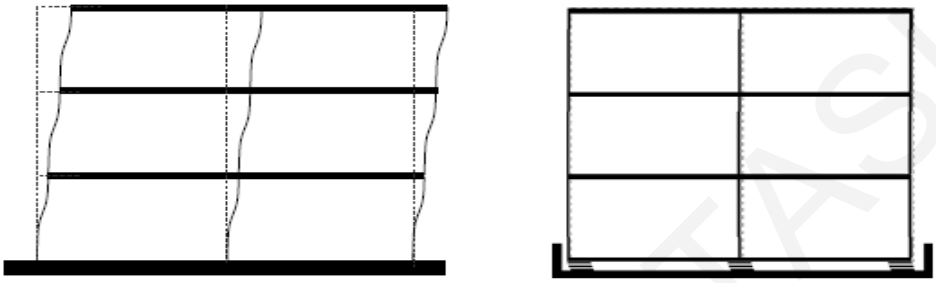


***Figure 6.1: Schematic response during an earthquake excitation of a (a) fixed supported building and a (b) base isolated building (Mavronicola, 2009)***

Seismic isolators mainly operate in the horizontal directions and not in the vertical direction, in which most structures are already overdesigned with sufficient strength to safely carry the vertical loads with significant safe factors. Commonly the structures in the vertical direction are designed properly to handle large vertical loads due to significant gravity loads. Besides, the effect of seismic loads in the vertical direction is usually not as significant as in the horizontal directions. Furthermore, the respective values of maximum ground accelerations in the vertical direction are usually lower than the peak ground accelerations in the horizontal directions.

The two major categories of seismic isolation systems that are widely used are the elastomeric bearings and the sliding systems. In general, a seismic isolation system has to provide a mechanism for the decrease of the induced seismic loads, to levels that cannot cause damage, by lengthening the fundamental eigenperiod of the structure, in order to avoid resonance. Moreover, it should provide an adequate initial horizontal stiffness and sufficient stiffness in the vertical direction to avoid oscillations under other minor horizontal loads and excessive vertical oscillations, respectively. Furthermore, an energy dissipation mechanism is required to reduce the expected large relative displacements at

the isolation level. In addition, a seismic isolation system must provide a mechanism to restore the seismically isolated structure to its initial position, after the end of a strong seismic excitation, in order to avoid any permanent displacements.

## 6.2 Elastomeric isolation systems

Common elastomeric bearings have already been extensively used in bridges in order to provide the ability to the decks to move over piers and abutments, during thermal expansion and contraction with circular or rectangular shapes. Elastomeric bearings that are used for seismic isolation, consist of bonded thin rubber layers 8 to 20 mm thick, with steel sheets 2 to 3 mm thick (see Figure 6.2). The elastomer is essentially rubber that is either natural or synthetic, for example neoprene, with low inherent damping, typically corresponding to 2% to 3% of the critical viscous damping. Specifically, the rubber layers provide the required horizontal flexibility for achieving the lengthening of the fundamental eigenperiod of the structure, to avoid resonance. Moreover, the desired restoring force of the structure after the end of the seismic excitation, is supplied by the elastic properties of the rubber, which deforms. In contrast, the steel sheets of the elastomeric bearings provide the indispensable stiffness in the vertical direction, which prevents bulging of the rubber layers and excessive vertical vibrations (Naeim and Kelly, 1999).

***Figure 6.2: Circular elastomeric bearing produced by the company FIP INDUSTRIALE (Italy) (Varnava, 2012)***

In addition, as it can be observed from Figure 6.2, thick steel plates are applied at the top and bottom of each bearing to attach it to the superstructure and the foundation, respectively. To protect the bearings from environmental effects, each bearing is wrapped in a rubber cover. The selection of proper elastomeric bearings should be done according to the characteristics of the building and the expected seismic excitation, too. The utilization of elastomeric bearings has shown that their life span exceeds the 50 years of operation, regarding their resistance to time effects.

### 6.2.1 Natural Rubber Bearings (NRBs)

NRBs are made of successive elastomeric layers of natural rubber or neoprene, and steel sheets, which are vulcanized or glued together. The elastomeric layers provide the desired horizontal flexibility and the elastic restoring force, to the seismic isolation system. Moreover, the steel plates reinforce the bearings by providing vertical load capacity and prevent any lateral bulge. Thus, the bearings are very stiff vertically, yet flexible for horizontal movements. However, they do not provide a significant amount of damping and they can be too flexible under wind or other minor horizontal loads and actions. Consequently, the NRBs are typically used in conjunction with supplementary damping devices or other types of seismic isolators.

Nowadays, the manufacturing of natural elastomeric bearings is an easy process, since vulcanization is a typical industrial process. Hence, the simplicity of manufacturing has contributed to the increase of the NRBs' production and their wider usage. NRBs are effective on lessening the accelerations of the floors (Kelly 2001) and their mechanical behaviour is unaffected by creep, fatigue and aging and remains unaltered by temperature changes and past charging (Naeim & Kelly 1999). Lastly, NRBs' mechanical characteristics and especially their elastic behaviour simplifies their design.

The main disadvantage of the natural rubber bearings is the inherently low damping ratio of the elastomeric material. This fact, motivated to the development of high damping rubber bearings, which are described next. The amount of structures that have been exclusively isolated with NRBs, is limited. Therefore, when NRBs are used for seismic isolation, they are combined either with other types of bearings that provide higher damping or with auxiliary dampers. Furthermore, using solely NRBs as a seismic isolation

system, large relative displacements can be developed in the structure under strong seismic loads. As a consequence, an increase of the required seismic gap arises. Thus, their usage without combining them with other types of seismic isolators is not recommended especially, in places with limited spatial availability for the seismic gap.

### 6.2.2 High Damping Rubber Bearings (HDRBs)

HDRBs are manufactured similarly with NRBs. Specifically, they consist of consecutive thin layers of high-damping rubber and steel plates. The lateral stiffness of the bearing is controlled by the low shear modulus of the elastomer, while the high vertical stiffness of the HDRBs is provided by the steel plates, which also prevent the bulging of the rubber. By adding extra-fine carbon blocks, oils, resins, and other proprietary fillers, the inherent damping of the damper is remarkably increased. The deformation of the high damping rubber dissipates energy, due to the generated heat when shear forces and deformations are imposed to the bearing. The effective viscous damping ratio of HDRBs typically corresponds to about 15-20% equivalent viscous damping ratio.

Kelly (2001) stated that by adding fillers to the natural rubber of a HDRB, the damping of the bearing increases as it exhibits a hysteretic behavior. In addition, according to Asta and Ragni (2008), those fillers are responsible for the nonlinear behavior of HDRBs. However, the hysteretic behavior of HDRBs can be satisfactory simulated by an equivalent linear elastic model with equivalent (effective) elastic stiffness and equivalent (effective) viscous damping ratio of the bearing.

The HDRBs' main advantage is that they can be used as autonomous seismic isolation systems without the need of additional damping devices. In addition, according to Kelly (2001), HDRBs are more effective than the natural elastomeric bearings, since they provide the desired flexibility to the building to avoid resonance and to effectively reduce the accelerations of the superstructure, too, while they provide an energy dissipation mechanism.

According to Pan et al. (2005), the mechanical and damping properties of HDRBs strongly depends on the temperature changes. Thus, they change during repeated load cycling. Furthermore, they are prone to aging effects, which may decrease the stiffness and the energy absorption capacity. By adding fillers to the natural rubber, the response of

a HDRB becomes strain history-dependent and causes a transient behavior in which stiffness and damping change significantly. In comparison with the NRBs, the HDRBs are more expensive. Additionally, the simulation and the analysis of HDRBs are more difficult, as they are characterized by nonlinear inelastic behavior.

### 6.2.3 Lead Rubber Bearings (LRBs)

Lead Rubber Bearings are manufactured in a similar way with the NRBs. The main difference between LRBs and NRBs is that the LRBs includes one or more, cylindrical lead cores. The inserted lead cores provide a very effective hysteretic energy dissipation mechanism. A typical LRB cylindrical section is shown in Figure 6.3.

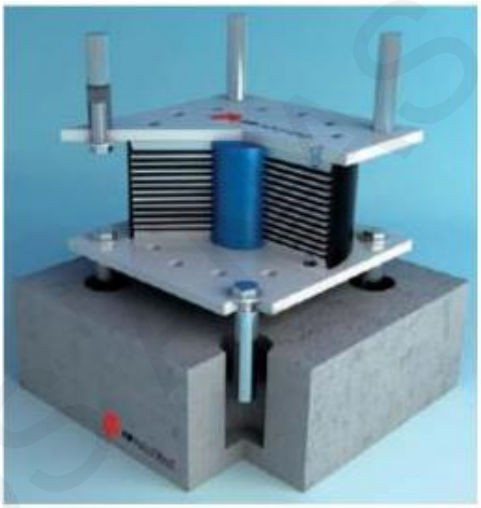

***Figure 6.3: Lead Rubber Bearing produced by the company FIP INDUSTRIALE (Italy) (Pavlidou, 2019)***

Firstly, the lead cores provide rigidity against wind loads and minor-seismic ground motions. Furthermore, they provide a hysteretic energy dissipation mechanism, with which large amounts of energy are dissipated, as it yields and recrystallizes during a strong earthquake excitation. Secondly, the elastomeric layers of an LRB provide the desired horizontal flexibility to significantly lengthen the fundamental eigenperiod of the structure in order to avoid resonance and substantially decrease the induced seismic loads. In addition, they provide the required restoring force that the building needs to return to its initial position, after the end of the seismic excitation. Thirdly, the steel sheets of this type

of seismic isolation are providing the vertical stiffness to support the superstructure's weight without excessive vertical vibrations.

LRBs exhibit a hysteretic behavior and a non-linear relation between the imposed shear forces and the displacements of the seismic isolation system. This can be approximately simulated with a bilinear force-displacement model at least for a preliminary design stage. The stiffness changes during yielding can cause an increase of the accelerations and the contribution of the higher eigenmodes to the seismic response, which does not correspond to the actual behavior of the LRBs.

The inelastic behavior of the LRBs can be approximately simulated, in a more simplified way, using the equivalent linearized model. Specifically, the effective stiffness $K_{eff}$ and also the effective damping coefficient $\xi_{eff}$, are required to be assessed, for the selected maximum horizontal displacement at the isolation level. The stiffness of the isolator prior and post yielding, $K_{elastic}$=$K_r$+$K_{lead}$ and $K_r$, respectively, are shown in Figure 6.4. Hysteretic loops are generated by repeated force-displacement cycles, leading to considerable energy dissipation. The equivalent viscous damping ratio of an LRB produced by its hysteretic behavior ranges from 15 to 35% (Kelly, 2001).

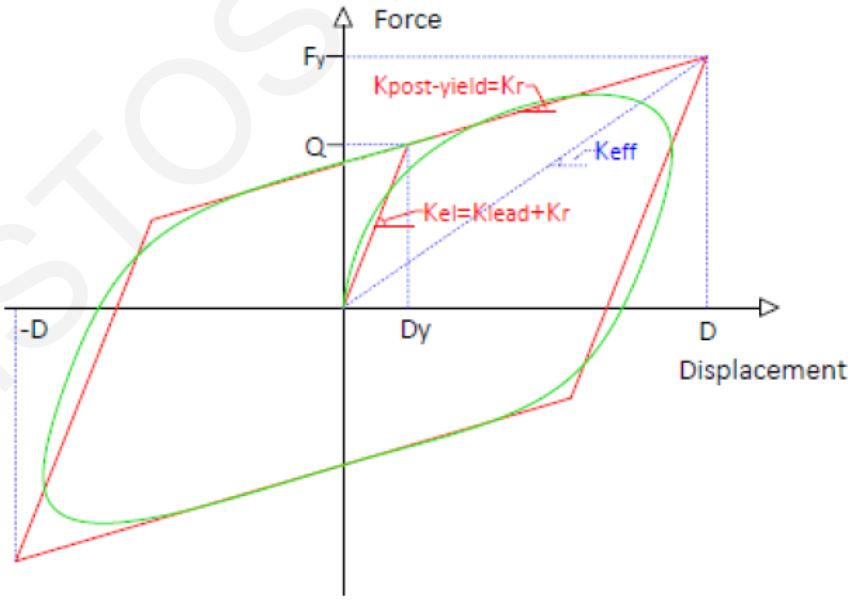


***Figure 6.4: Equivalent linear properties from an idealized bilinear hysteresis loop (Pavlidou, 2019)***

The area of the hysteretic loops represents the hysteretic energy dissipation under repeated inelastic cycles. The energy production during loading that is not fully recovered during unloading and transformed from kinetic into thermal energy, is the energy that is dissipated. Despite the fact that, the nonlinear behaviour of the lead core provides significant damping rates, it can probably cause more intense stimulation of higher eigenmodes, due to the successive and sudden changes in stiffness, which may increase the peak floor accelerations.

Kelly (2001) underlined the flexibility that is provided by this type of seismic isolator, in the design of an isolation system. The cross section of the lead core is the main characteristic for achieving the target stiffness and damping of the isolation, which depends on the desired behavior of the examined structure.

The cost of an LRB exceeds the cost of an NRB. However, it is an autonomous device that provides sufficient stiffness for the vertical loads, horizontal flexibility to avoid resonance, and hysteretic damping due to the plastic deformations of the lead core. Therefore, the employment of an LRB system eliminates the need for using dampers, which increases the construction cost (Robinson, 1982).

The change of the LRBs' mechanical characteristics during cycles of deformation, requires the usage of appropriate hysteretic models, in order to properly simulate the structural behavior (Kelly, 2001). When an equivalent linear elastic model is employed with effective stiffness and effective viscous damping ratio, it is important to assess the maximum relative displacements and the corresponding effective damping at the isolation level. The reason is that the effective stiffness and the effective viscous damping ratio of an LRB depend on the maximum relative displacement occurring at the isolation level (Naeim and Kelly, 1999).

## 6.3 Sliding isolation systems

The operation of the sliding bearings is based on friction. Specifically, the shear force is transmitted from the the superstructure to the foundation, up to a certain limit. Beyond that limit, the resistive friction force cannot be exceeded and therefore the slip begins. Due to the slip, the transmission of seismic forces beyond a certain magnitude, is prevented. The design of the seismic isolation with sliding bearings, mainly focuses on the

determination of the sliding surfaces' friction coefficient. In particular, the limitation of the friction coefficient limits the magnitude of the transmitted shear forces. The above property of the sliding bearings, remains of particular importance, since the forces transmitted to the superstructure are independent of the seismic intensity and they depend solely on the friction coefficient and the vertical loads. Hence, the sliding bearings are remarkably effective in mitigating the response of structures, even under strong seismic excitations.

The construction materials of sliding bearings are usually polytetrafluoroethylene (PTFE or Teflon) and stainless steel (Naeim and Kelly, 1999). The characteristics of a sliding system depend on the temperature, the speed at the slip interface, the degree of decay and the purity of the slip surfaces. The affordable supply costs of sliding bearings, turn them to be preferable than the elastomeric bearings in some cases. In addition, their compact volume makes them suitable for use in interventions and upgrades of existing structures.

The continuous research activity has contributed to the improvement of sliding bearings. Their initially flat original shape turned them to be inefficient due to the absence of a restoring mechanism, after the end of a seismic action. Therefore, the newer sliding systems have curved surfaces based on the philosophy of the pendulum, such the friction pendulum systems.

### 6.3.1 Friction Pendulum Systems (FPS)

A Friction Pendulum System consists of an upper and a lower spherical plate and a friction slider (Figure 6.5). The spherical surface of an FPS is the part of the system that provides the desired restoring force, as well as the required friction for the energy dissipation (Zayas et al., 1987). The slider is faced with the bearing material that, when it is in contact with the spherical concave, leads to a sliding friction coefficient that ranges from about 0.1 at high sliding velocities to approximately 0.5 for very low sliding velocities.

During a seismic action the structure, which is isolated with FPS, slides on the bearings whenever the sliding force is exceeded. Due to the bearings' curved surface, the building moves in the horizontal directions, while it rises in the vertical direction. The sliding mechanism limits the lateral seismic forces, which could otherwise cause excessive deformations and damage to the building. In addition, the movement in the vertical

direction lifts the building and thus, the restoring force is provided in the form of gravity force. The restoring force is inversely proportional to the curvature of the spherical plate and directly proportional to the displacement of the system. Furthermore, by modifying the bearing's curved surface radius, the fundamental eigenperiod of the building can be properly adjusted. Finally, the FPS tend to be more attractive due to its easy installation and its simple mechanism of restoring force by the utilization of the gravity loads.

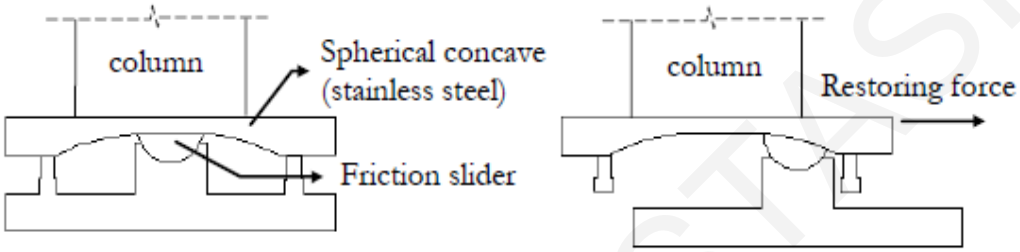


***Figure 6.5: Friction Pendulum System (FPS) seismic isolation (Mavronicola, 2009)***

Since the FPS provides an inherent damping mechanism, it can be used autonomously without the need of using additional damping devices. This contributes to a reduction of the construction cost of a seismically isolated structure. In addition, it provides satisfactory resistance to the vertical imposed loads and minor horizontal loads, such as wind loads and weak seismic actions. Furthermore, the relatively short height of the bearing makes it ideal for the seismic isolation of existing structures, as well as for new structures, for ensuring the maximum possible effective height.

A disadvantage of friction pendulum systems is the fact that the friction coefficient, which determines the forces that can be transmitted to the superstructure, is not constant. Taylor and Igusa (2004) reported that, the coefficient of friction depends on a variety of factors, where the most important are the composition of the sliding surfaces, the bearing pressure and the sliding speed. Therefore, the transmitted seismic forces to the superstructure may be greater than the design shear forces, which can have a devastating effect on the superstructure.

## 6.4 Hybrid seismic isolation system

Generally, some seismic isolated structures are equipped with only one type of bearing. However, each type of bearing is characterized by some disadvantages. Kelly (2001) highlighted that no one seismic isolation is perfect. The selection of the suitable isolation system depends on the specific characteristics of each structure. Therefore, the trend to isolate structures with more than one type of isolation system, has been developed in order to secure the advantages of different types of seismic isolatiors and to mitigate their potential vulnerabilities. More specifically, where one type of isolation system lacks, a second type is used in combination with the other, to cover the shortcomings of the first.

The most common combination of seismic isolation system is the utilisation of elastomeric bearings with friction bearings (Braga et al., 2005). Kelly (2001) stated that friction bearings, provide a remarkable energy damping mechanism and they are efficient to handle large vertical loads. However, they allow the structure to be slightly lifted, to ensure a restoring force by gravity. Therefore, by using the friction bearings in combination with the elastomeric bearings, which have an inherent restoring mechanism due to the properties of the elastomeric material, the inabilities of the friction bearings are minimized. The philosophy of this combination is based on the restoring mechanism and the control of the torsional response of the structure, which is provided by the elastomeric bearings and on the satisfactory damping which is provided by the friction bearings (Naeim and Kelly, 1999).

An effective isolation system should better combine two damping mechanisms, one viscous and one hysteretic. Firstly, the viscous damping due to the elastomer, leads to a lasting damping mechanism, which is more effective for minor seismic excitations and less effective for stronger ones. Secondly, the hysteretic damping, which is provided by the development of friction by the sliding bearing, is quite effective under strong earthquakes. In addition, it offers the desired initial stiffness. Furthermore, the friction damping is more effective than viscous damping in minimizing the displacement increase, which occurs in structures with a lengthen eigenperiod of isolation under long-term pulse seismic excitations (Chang et al., 2002).

Obviously, by combining the two aforementioned types of seismic isolation bearings, the desired energy dissipation mechanism for each structure can be achieved. Moreover, the combination of seismic isolation systems is an effective solution for optimizing the performance of an isolation system. Additionally, the design and manufacture of the isolation system becomes cheaper and more affordable.

## 6.5 Design and configuration of the seismic isolation system

The design of the base isolation system that is used in the presented research work has been done by Varnava (2012). First of all, the type of isolation that has been chosen for this study is the hybrid isolation system. Specifically, it consists of NRBs and LRBs, with the latter being necessary to provide the desired energy dissipation mechanism.

Moreover, it is highlighted that the dynamic time-history analyses of the seismically isolated buildings are conducted using the SAP2000 OAPI, as explained in Chapter 3. The modelling of the NRBs and the LRBs is done by using the "Rubber Isolator" type link element. According to the user manual of SAP2000, *"CSI Analysis Reference Manual for SAP2000"*, the "Rubber Isolator" element provides the ability to the user to define both linear and nonlinear properties for the two horizontal shear degrees of freedom. In addition, hysterical behavior is considered, which is based on the plasticity model of Wen and Park (1976), and Wen and Ang (1986).

The main difference between the NRB and the LRB is that the first has linear properties in the two horizontal shear degrees of freedom, while the latter has nonlinear properties. For the determination of the nonlinear properties of the two horizontal translational degrees of freedom of the "*Rubber Isolator*" type link element in SAP200 software, the elastic stiffness, the yield strength and the post yield stiffness ratio should be defined. Furthermore, the LRBs exhibit a hysteretic behavior, according to the Bouc-Wen model, and therefore, no viscous damping ratio is defined. The software considers directly and precisely the energy dissipation, according to the Bouc-Wen hysteretic model during the nonlinear time-history analyses.

The arrangement of the NRBs and LRBs, for the current research study is illustrated in Figure 6.6. Additionally, the mechanical characteristics of the two types of isolators, as calculated taking into account the procedure of Varnava (2012), are provided in Table 6.1.

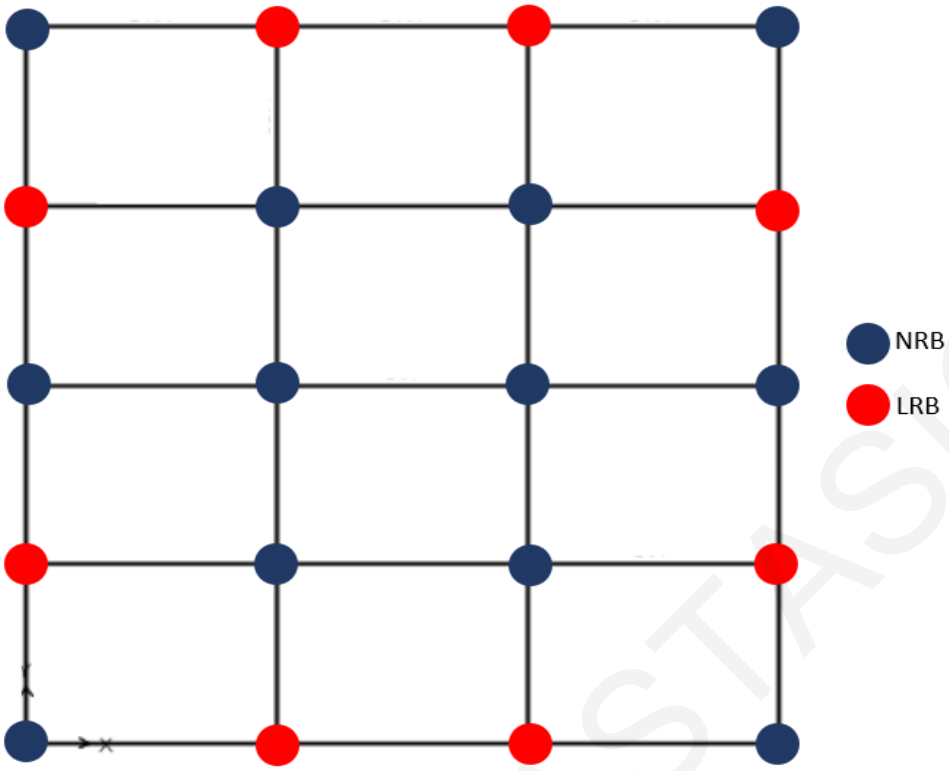


***Figure 6.6: Layout of the NRBs and the LRBs for the current study***

***Table 6.1: Characteristics of the NRBs and the LRBs that are used***

| | NRB | LRB |
|---|---|---|
| Number of bearings | 12 | 8 |
| Mass (kg) | 118 | 119 |
| Weight (kN) | 1.158 | 1.167 |
| Rotational Inertia (kN/m²) | 0.032 | 0.032 |
| Design Displacement (mm) | 52.71 | 52.71 |
| Total design displacement (mm) | 59.80 | 59.80 |
| Vertical Effective stiffness (kN/m) | 1273048 | 897048 |
| Translational Effective stiffness (kN/m) | 1239 | 2288 |
| Rotational Effective stiffness (kN/m) | 21.58 | 21.56 |
| Elastic stiffness (kN/m) | 1239 | 32961 |
| Yield Displacement (mm) | - | 1.504 |
| Yield strength (kN) | - | 49.59 |
| Post yield stiffness ratio | - | 0.036 |

## 6.6 Modal Analysis

The first three eigenmodes of the base-isolated building for each soil type: rock, sand and soft clay are provided in Figures 6.7, 6.8 and 6.9, respectively. It can be observed that in all cases, the first eigenmode is translational in the horizontal X direction, while the second eigenmode is translational in the horizontal Y direction. The third eigenmode in all three cases is torsional around the vertical axis Z.

Furthermore, it can be noticed that the maximum deformations are developed at the base-isolation level, while the superstructure moves almost like a rigid body, since the maximum interstorey drifts are substantially reduced in the superstructure, above the seismic isolation level.

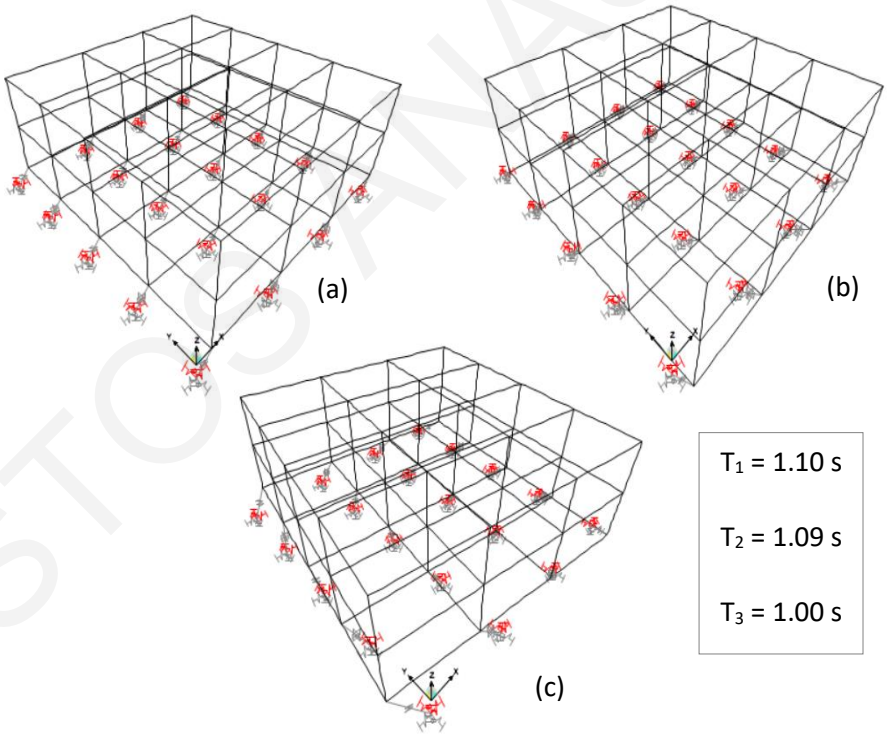


***Figure 6.7: (a) 1st, (b) 2nd and (c) 3rd eigenmodes of the base isolated building founded on rock***

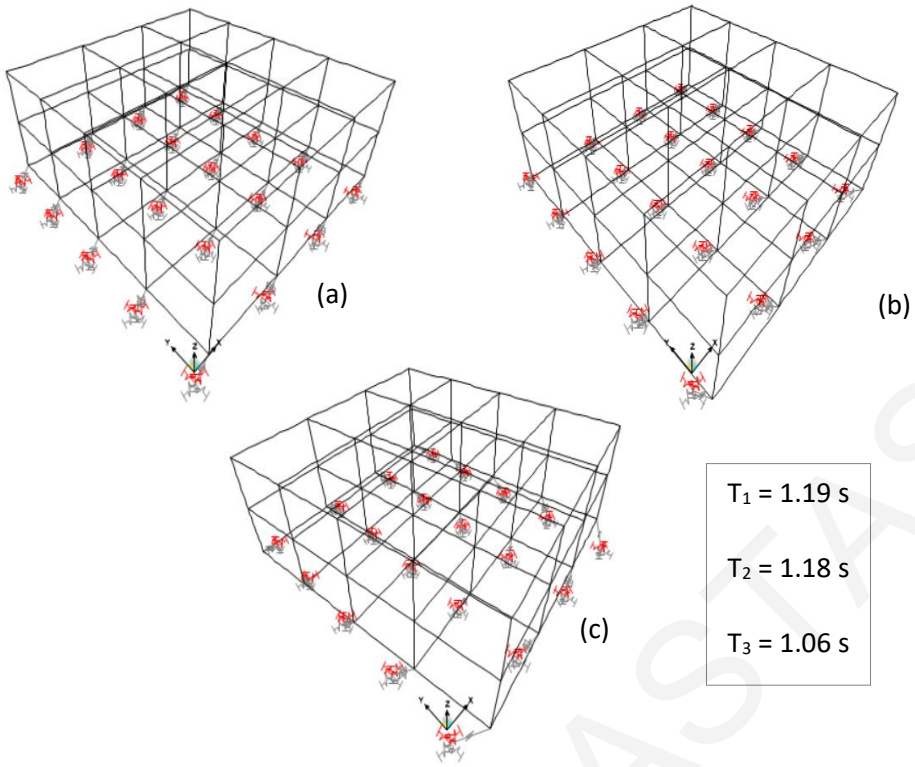


***Figure 6.8: (a) 1st, (b) 2nd and (c) 3rd eigenmodes of the base isolated building founded on sand***

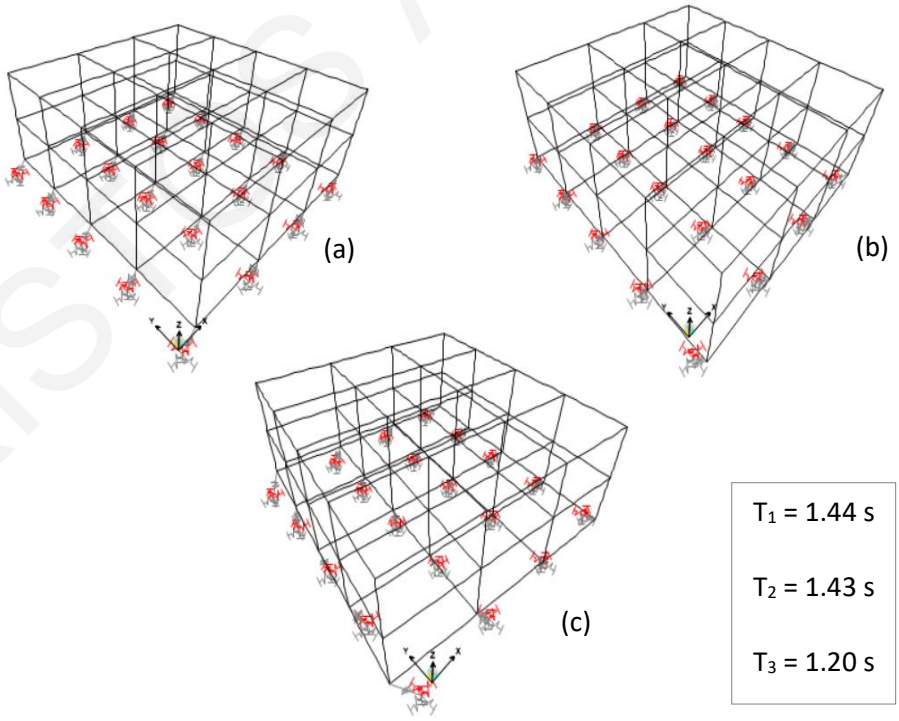


***Figure 6.9: (a) 1st, (b) 2nd and (c) 3rd eigenmodes of the base isolated building founded on soft clay***

Table 6.2 provides the fundamental eigenperiods of the base-isolated building founded on each different soil type. It is clear that the insertion of the seismic isolation system provides, as expected, significant flexibility at the base of the structure, which leads to a significant lengthening of the fundamental eigenperiod of the structure compared to that of the corresponding conventionally supported structure. Therefore, the combination of seismic isolation with soil deformability leads to a further increased lengthening of the fundamental eigenperiod of the building, in comparison with the fundamental eigenperiod of the corresponding conventionally supported building.

***Table 6.2: 1st, 2nd and 3rd eigenperiods (T1, T2 and T3) and eigenmodes (Φ1, Φ2 and Φ3) of the base-isolated building for rock, sand and soft clay***

| Soil Type | $T_1$ (s) | $\Phi_1$ | $T_2$ (s) | $\Phi_2$ | $T_3$ (s) | $\Phi_3$ |
|---|---|---|---|---|---|---|
| Rock | 1.10 | Translational in (horizontal) X direction | 1.09 | Translational in (horizontal) Y direction | 1.00 | Torsional around Z (vertical) axis |
| Sand | 1.19 | | 1.18 | | 1.06 | |
| Soft clay | 1.44 | | 1.43 | | 1.20 | |

# Chapter 7 - PEAK SEISMIC RESPONSE OF BASE ISOLATED BUILDING

The seismic isolation system is usually installed at the base of the structure, between the foundation and a diaphragm that should be ensured above the isolation level. In the conducted parametric study, the structure is assumed to be founded on rock, sand and soft clay soil types, in order to assess the effect of the soil deformability on the peak seismic response of the base-isolated building. Moreover, the effects of the NF and FF ground motions for the base-isolated structure founded on rock, sand and soft clay, are also investigated. In order to examine the above, a large number of nonlinear time-history analyses are conducted, using the SAP2000 structural analysis program through the OAPI, as explained in previous chapters.

## 7.1 Influence of soil deformability

The dynamic time-history analysis of the base-isolated structure founded on three different soil types: rock, sand and soft clay, is indicatively conducted using the Cape's Medocino seismic excitation. More information concerning the utilized seismic record, is provided in Chapter 5.1. In order to examine the soil deformability effects on the base-isolated structure, the peak interstorey drifts and the peak absolute floor accelerations, which represent the potential damage on the structural and non-structural elements due to deformations and the effect of excess accelerations on the occupants and contents of the building, are presented next.

### 7.1.1 Peak interstorey drifts

The peak (in absolute values) interstorey drifts in the two orthogonal horizontal directions of the base-isolated structure for rock, sand and soft clay, under the loading combination G+0.3Q+Ex+0.3Ey, for the aforementioned earthquake excitation (Cape Medocino), are provided in Table 7.1 and Figures 7.1 and 7.2.

***Table 7.1: Maximum interstorey drifts in the two orthogonal horizontal directions of the base-isolated building under the loading combination G+0.3Q+Ex+0.3Ey for the three soil types***

| Floor level | Maximum Interstorey Drifts | | | | | |
|---|---|---|---|---|---|---|
| | **Rock** | | **Sand** | | **Soft clay** | |
| | $\Delta U_x$ (mm) | $\Delta U_y$ (mm) | $\Delta U_x$ (mm) | $\Delta U_y$ (mm) | $\Delta U_x$ (mm) | $\Delta U_y$ (mm) |
| 2nd floor | 2.0 | 1.0 | 3.0 | 1.0 | 12 | 5.0 |
| 1st floor | 5.0 | 2.0 | 6.0 | 2.0 | 14 | 6.0 |

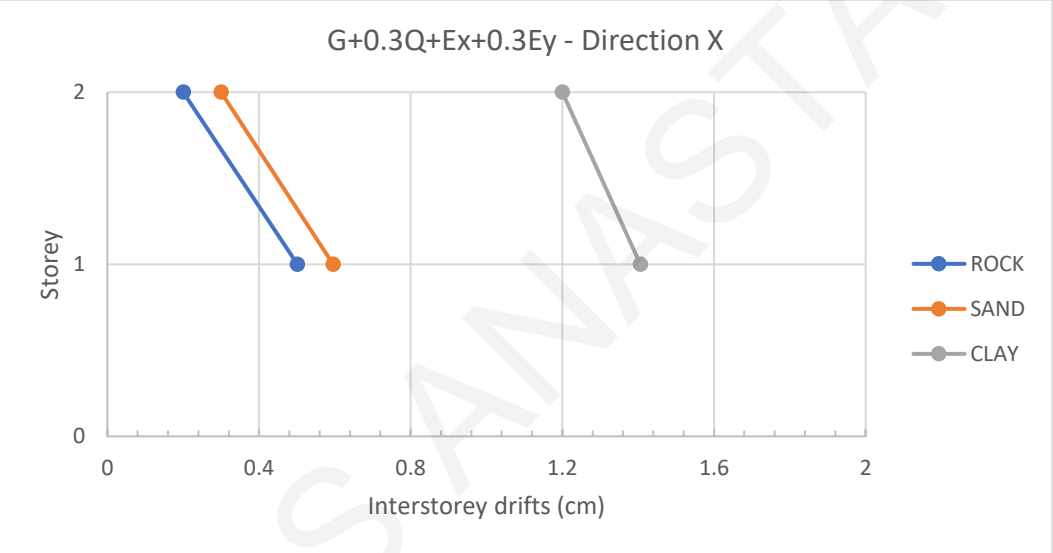


***Figure 7.1: Peak interstorey drifts in the X horizontal direction of the base-isolated building under the loading combination G+0.3Q+Ex+0.3Ey for rock, sand and soft clay***

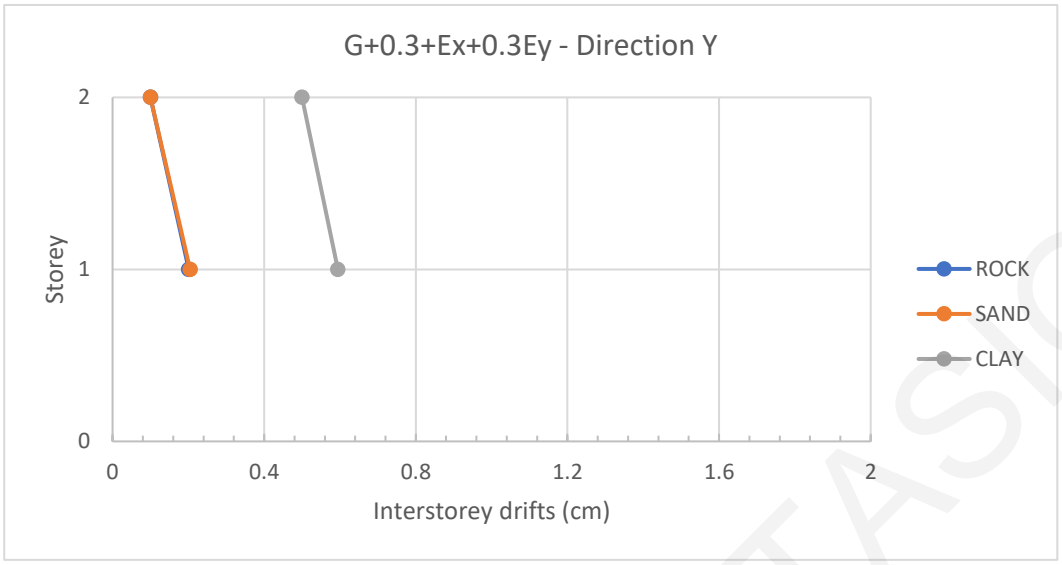


***Figure 7.2: Peak interstorey drifts in the Y horizontal direction of the base-isolated building under the loading combination G+0.3Q+Ex+0.3Ey for rock, sand and soft clay***

As shown in Figure 7.1, the soil deformability has a significant influence on the developed interstorey drifts of the base-isolated structure, since the building founded on soft clay has the highest values. Specifically, the values of the interstorey drifts for the structure founded on rock are 2.0 mm for the second-floor level and 5.0 mm for the first-floor level. Furthermore, a slight increase in the values can be noticed for the structure founded on sand, compared to the rock's values. However, the values for the structure founded on soft clay soil type shows a remarkable increase of the peak interstorey drifts. At the second-floor level the interstorey drift are risen by six and four times than the corresponding values of rock and sand, respectively, while at the first-floor level there is an increase of about 64% and 57% in comparison to the rock and sand values, respectively.

Similar behavior is exhibited in the Figure 7.2, which provides the peak interstorey drifts for the base-isolated structure in the Y direction. Specifically, the building founded on soft clay develops the highest interstorey drifts, while the building founded on rock and sand has almost identical interstorey drift values.

The peak (in absolute values) interstorey drifts in the orthogonal horizontal X direction of both the conventionally supported building and the base-isolated structure for

rock, sand and soft clay, under the loading combination G+0.3Q+Ex+0.3Ey are shown in Figure 7.3.

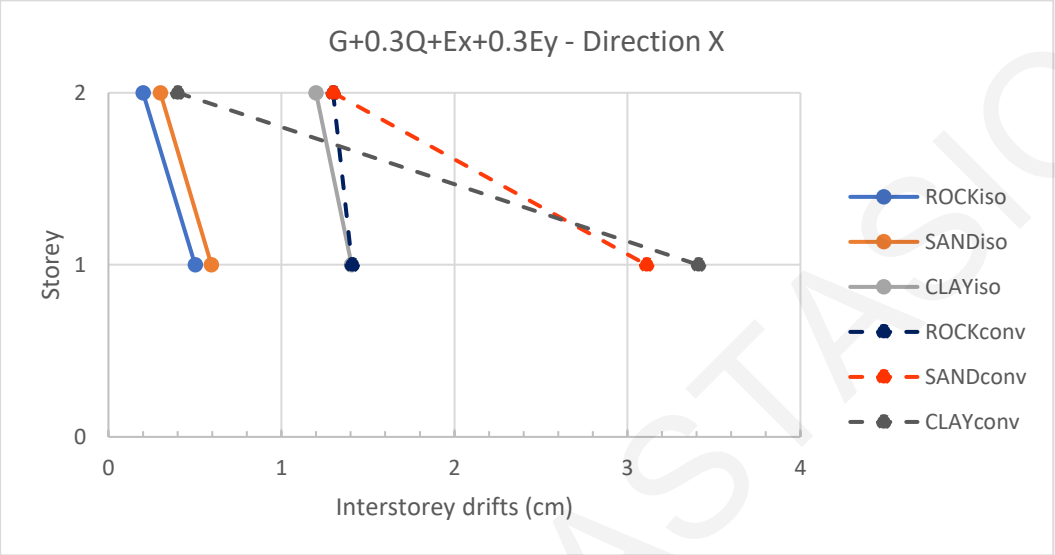


***Figure 7.3: Peak interstorey drifts in the X horizontal direction of both conventionally supported building and base-isolated building under the loading combination G+0.3Q+Ex+0.3Ey for rock, sand and soft clay***

The developed interstorey drifts of the base-isolated structure are quite smaller compared to the corresponding values of the conventionally supported building for all three soil types, excluding the second-floor level of the structure founded on soft clay. This fact confirms the efficiency of the seismic isolation, since the superstructure moves almost like a rigid body.

### 7.1.2 Peak absolute floor accelerations

The maximum total floor accelerations (in absolute values) in the two orthogonal horizontal directions of the base-isolated structure for rock, sand and soft clay, under the loading combination G+0.3Q+Ex+0.3Ey, are presented in Table 7.2 and Figures 7.4 and 7.5.

***Table 7.2:Peak absolute floor accelerations in the two orthogonal horizontal directions of the base-isolated building under the loading combination G+0.3Q+Ex+0.3Ey, for all soil types***

| Floor level | Maximum Floor Accelerations | | | | | |
|---|---|---|---|---|---|---|
| | **Rock** | | **Sand** | | **Soft clay** | |
| | $\ddot{u}_x$ (m/s$^2$) | $\ddot{u}_y$ (m/s$^2$) | $\ddot{u}_x$ (m/s$^2$) | $\ddot{u}_y$ (m/s$^2$) | $\ddot{u}_x$ (m/s$^2$) | $\ddot{u}_y$ (m/s$^2$) |
| 2$^{nd}$ floor | 1.89 | 0.78 | 1.88 | 0.78 | 2.00 | 0.77 |
| 1$^{st}$ floor | 1.69 | 0.67 | 1.38 | 0.70 | 1.84 | 0.54 |

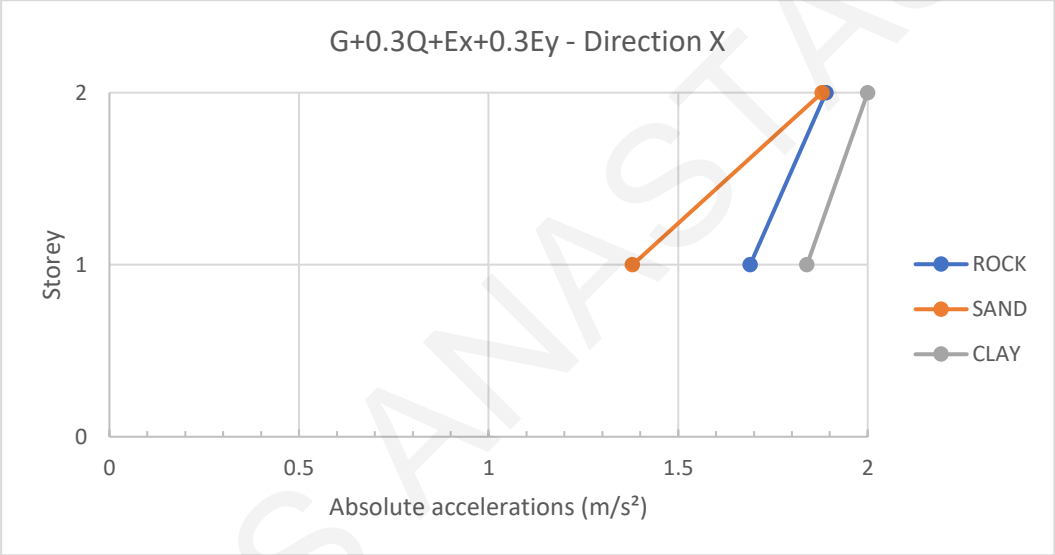


***Figure 7.4: Peak absolute floor accelerations in the X direction of the base-isolated building under the loading combination G+0.3Q+Ex+0.3Ey for rock, sand, and soft clay***

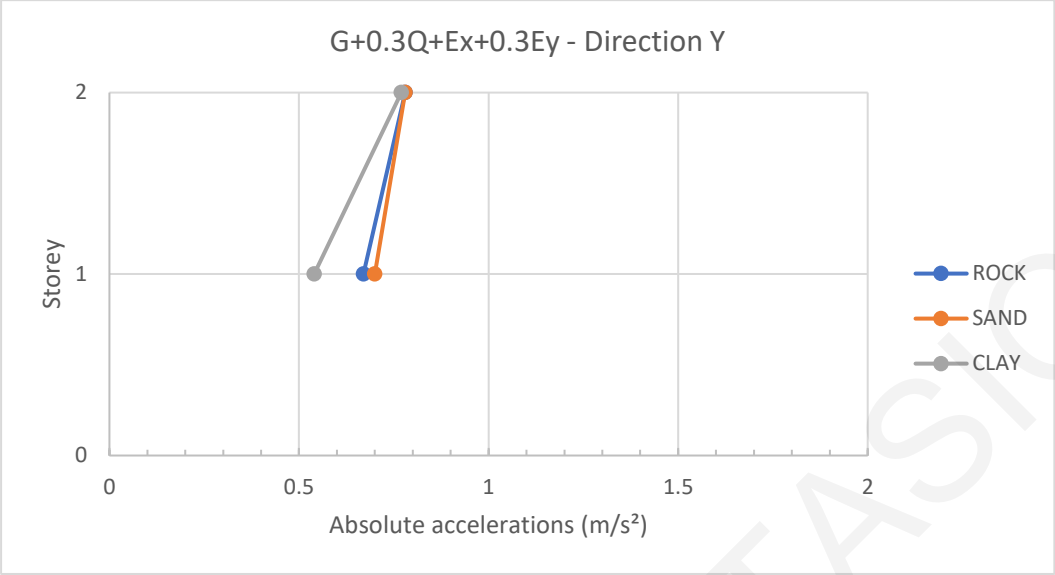


***Figure 7.5: Peak absolute floor accelerations in the Y direction of the base-isolated building under the loading combination G+0.3Q+Ex+0.3Ey for rock, sand and soft clay***

The highest values of the maximum absolute floor accelerations at both floor levels reach their highest values when the structure is founded on soft clay. Whereas the smallest values of the maximum absolute floor accelerations are developed for the structure founded on sand. Therefore, the soil deformability has an important effect on the values of the maximum absolute floor accelerations, which either beneficial or detrimental.

Regarding the Y direction, the maximum absolute floor accelerations in each storey are almost identical for all the soil types, with the structure founded on sand having slightly higher values than the corresponding values of rock and soft clay. Hence, the soil deformability has minor influence on the maximum absolute floor accelerations in the Y direction. The impact of the soil deformability for the maximum absolute floor accelerations, is more significant along the primary axis, in the case under examination.

The maximum absolute floor accelerations in the orthogonal horizontal X direction of both the conventionally supported building and the base-isolated structure for rock, sand and soft clay, under the loading combination G+0.3Q+Ex+0.3Ey are shown in Figure 7.6.

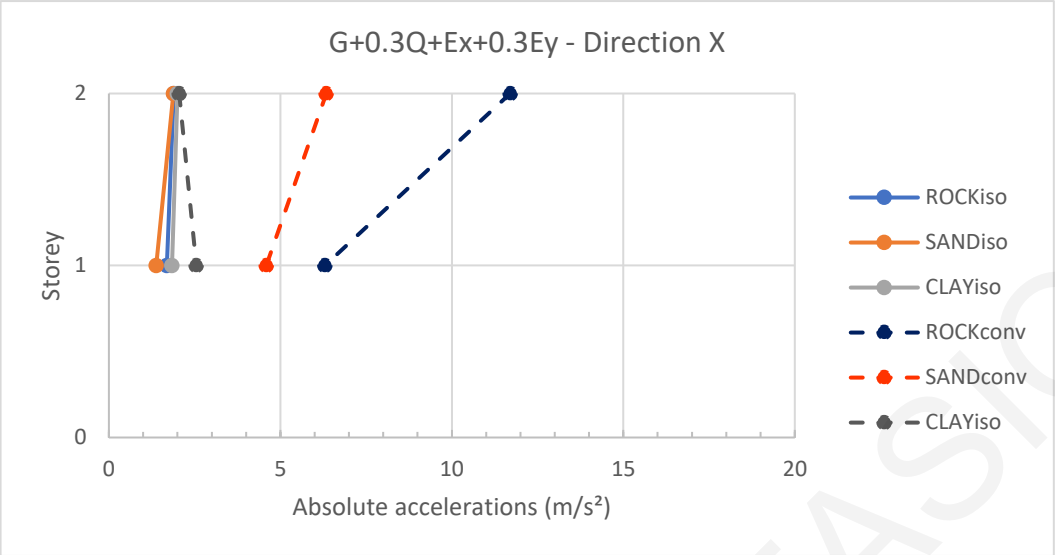


***Figure 7.6: Peak absolute floor accelerations in the orthogonal horizontal X direction of both conventionally supported building and base-isolated building under the loading combination G+0.3Q+Ex+0.3Ey for rock, sand and soft clay***

The developed maximum absolute floor accelerations of the base-isolated structure are quite smaller compared to the corresponding values of the conventionally supported building for all the three soil types, excluding the second-floor level of the structure founded on soft clay. This fact confirms the efficiency of the seismic isolation.

## 7.2 Soil deformability and NF *vs.* FF excitation effects

The assessment of the influence of soil deformability on the examined base-isolated structure, combined with the effect of NF and FF ground motions, is important to be investigated. Therefore, the peak seismic response of the base-isolated structure under the excitation of 10 different ground motions, 5 NF and 5 FF, all calibrated to have a PGA equal to 0.3g, is parametrically studied in order to better understand the soil deformability effects in combination with the characteristics of the seismic excitation. The emphasis will be put on the interstorey drifts and the maximum absolute floor accelerations, as they are the major measures for potential damage. The selection of the near-fault and far-fault ground motion records, has already been discussed in Section 5.2.

### 7.2.1 Peak interstorey drifts

The peak interstorey drifts in absolute values in the X horizontal direction for the loading combination G+0.3Q+Ex+0.3Ey, of the base-isolated structure founded on rock, sand and soft clay, under the excitation of the selected NF and FF ground motions, are displayed in Figure 7.7 and Figure 7.8, respectively.

The soil deformability, as it can be noticed from the aforementioned figures, plays a significant role in the peak seismic response of the base-isolated building. The fact that in all examined seismic ground motion records, the highest values of the peak interstorey drifts are developed in the cases where the soil deformability has taken into account, confirms its significance.

More specifically, the maximum value of the interstorey drifts at both the second- and the first-floor level for the NF and FF ground motions, occur during the EQ2 (NF2) and the EQ6 (FF6) ground motions, respectively, for all soil types. In addition, the building founded on soft clay, which develops the highest interstorey drifts compared to the buildings founded on rock and sand in both NF and FF cases, is affected more negatively under the excitation of the NF ground motions than by the corresponding FF ground motions.

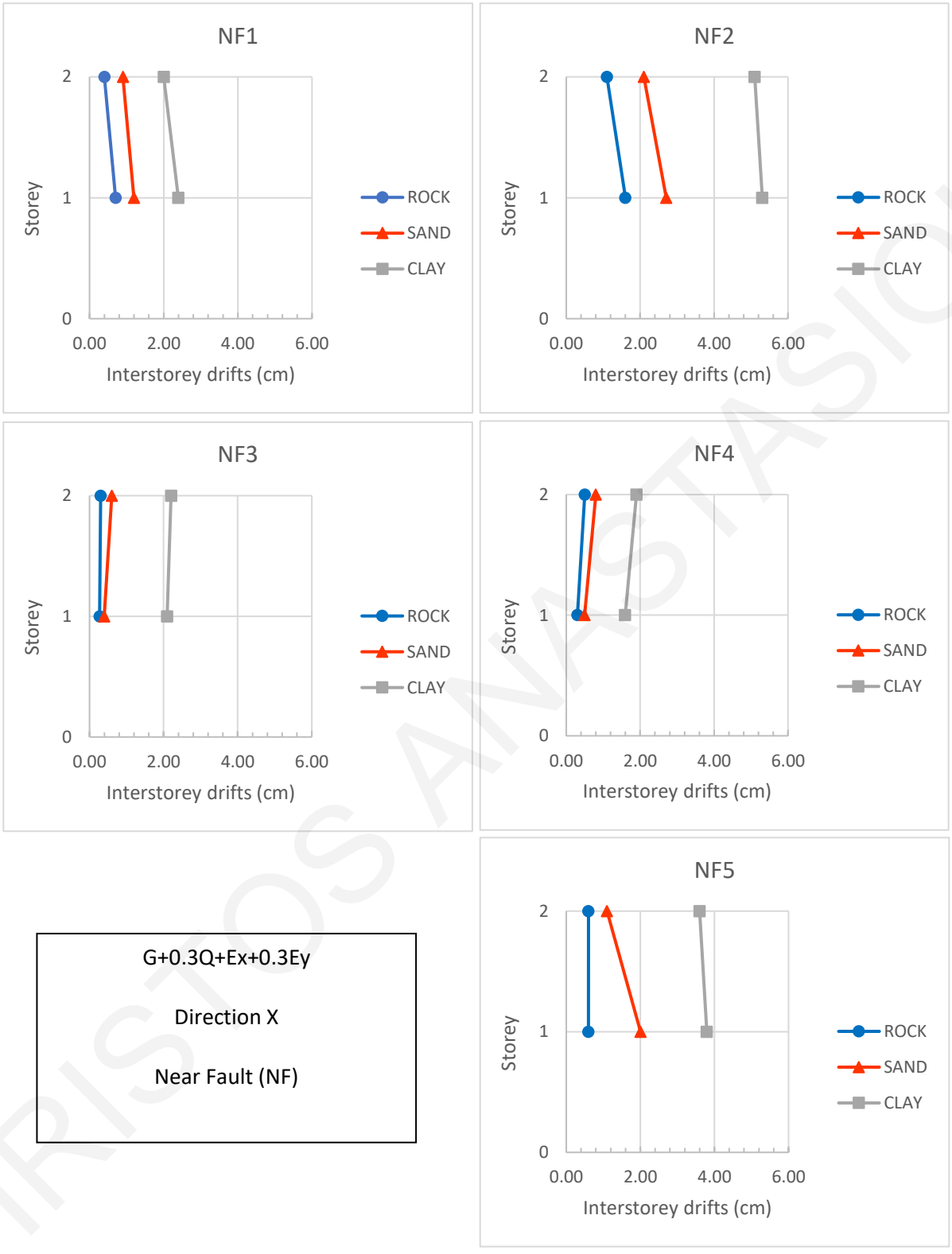


***Figure 7.7: Peak interstorey drifts (in absolute values) in direction X for the selected NF ground motions of the base-isolated building founded on rock, sand and soft clay***

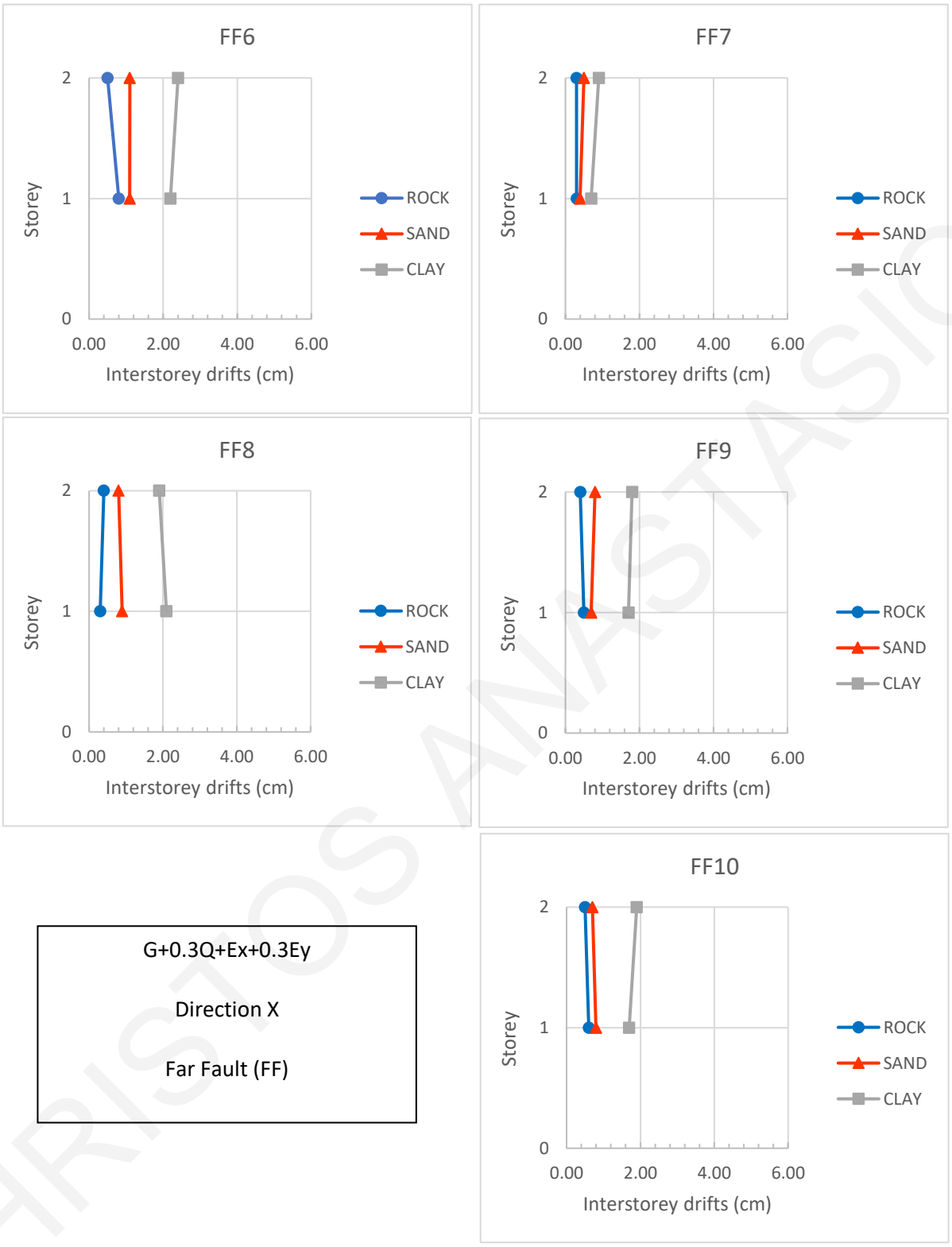


***Figure 7.8: Peak interstorey drifts (in absolute values) in direction X for the selected FF ground motions of the base-isolated building founded on rock, sand and soft clay***

The peak interstorey drifts in absolute values in the Y horizontal direction for the loading combination G+0.3Q+Ex+0.3Ey, of the base-isolated structure founded on rock, sand and soft clay, under the excitation of the selected NF and FF ground motions, are provided in Figure 7.9 and Figure 7.10, respectively.

The results of the Y direction indicate similar trend to X direction. Specifically, soil deformability plays a significant role in the peak seismic response of the base-isolated building. The fact that in all examined seismic ground motion records, the highest values of the peak interstorey drifts are developed in the cases where the soil deformability has taken into account, confirms its significance.

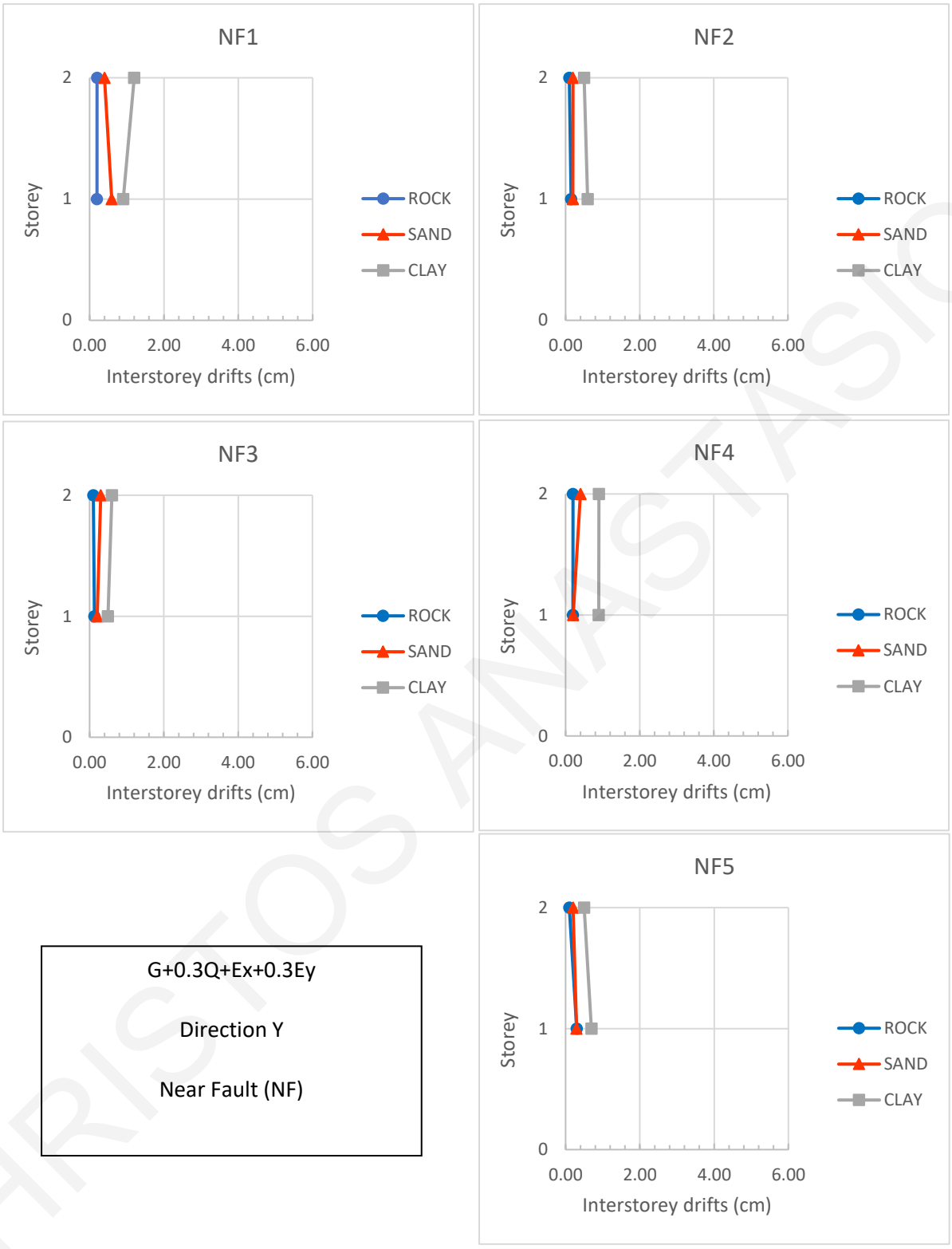


***Figure 7.9: Peak interstorey drifts (in absolute values) in direction Y for the selected NF ground motions of the base-isolated building founded on rock, sand and soft clay***

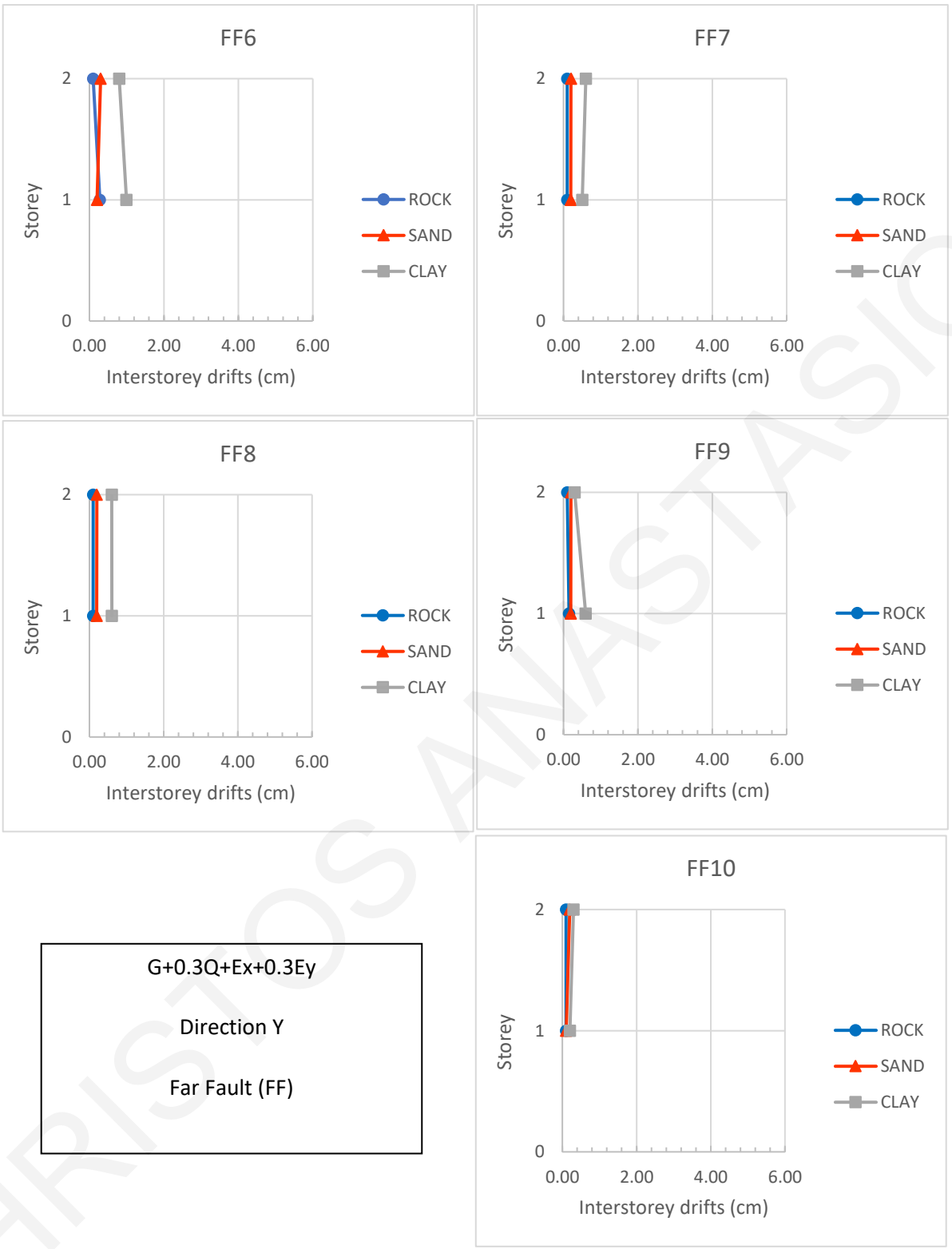


***Figure 7.10: Peak interstorey drifts (in absolute values) in direction Y for the selected FF ground motions of the base-isolated building founded on rock, sand and soft clay***

### 7.2.2 Peak absolute floor accelerations

Figures 7.11 and 7.12 provide the maximum (in absolute values) total floor accelerations in the X direction on all three soil types under both NF and FF seismic excitations, respectively.

As it can be clearly seen from the figures below (see Figure 7.11 and Figure 7.12), the highest absolute floor acceleration values correspond to the second NF seismic ground motion record (NF2), among all seismic excitations that are used. In addition, the worst FF ground motion record in terms of absolute floor accelerations, is the EQ No. 6-FF6 (see Table 5.7 – Chapter 5). These concerns all the examined soil types, and especially the structure founded on sand, which has the maximum floor acceleration values for the two above mentioned ground motion records (except for FF6 in the first-floor level, which has the rock's value slightly higher than the sand's).

Furthermore, nearly for all the FF ground motion records, the soil deformability leads to slightly smaller peak absolute floor accelerations, except of the FF6. Whereas, among the NF ground motions the soil deformability increases the peak seismic response, regarding the peak absolute floor accelerations.

Overall, it is very important to take into consideration the soil deformability, in order to limit the effect of excess accelerations on the occupants and the contents of the building.

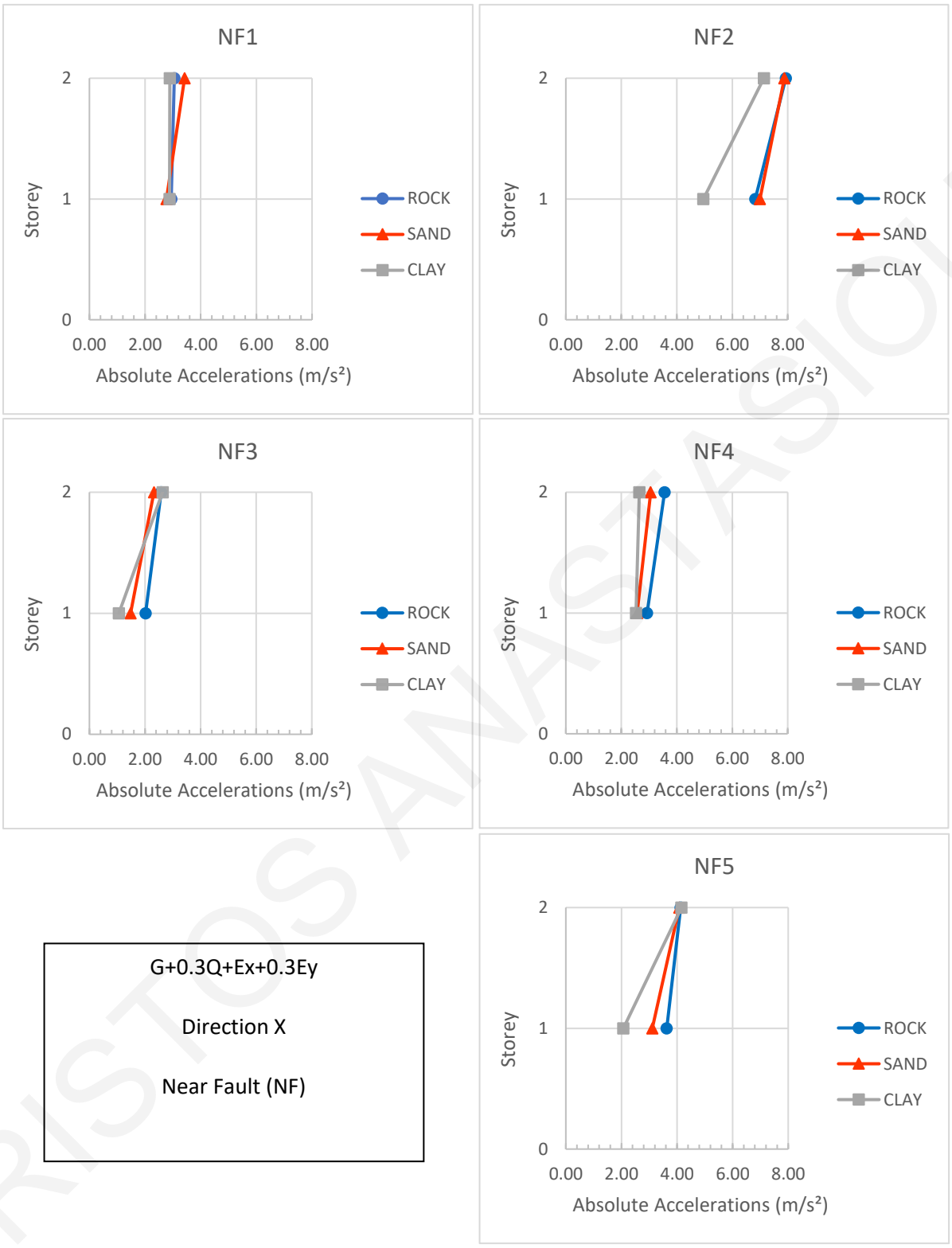


***Figure 7.11: Maximum absolute floor accelerations in X direction for the selected NF ground motions of the base-isolated building founded on rock, sand and soft clay***

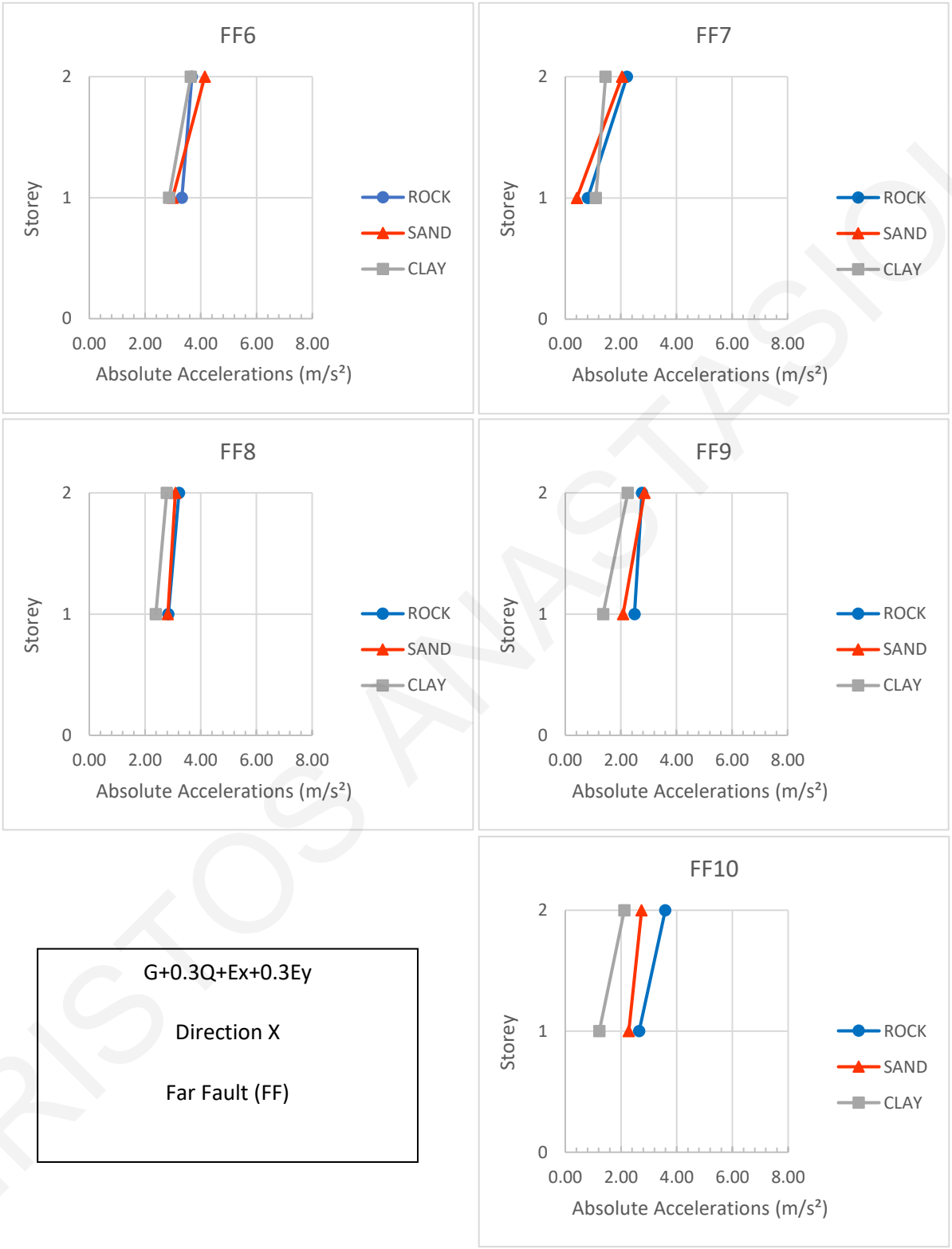


***Figure 7.12: Maximum absolute floor accelerations in X direction for the selected FF ground motions of the base-isolated building founded on rock, sand and soft clay***

## 7.3 Peak relative displacements at the isolation level

The main limitation in the utilization of a seismic isolation system is the provision of sufficient clearance, as a seismic gap, perimetrically of a seismically isolated structure, in order to facilitate the expected large relative displacements at the isolation level and avoid potential pounding with the perimeter wall or adjacent structures. Such collisions could be destructive, not only for the structural and non-structural elements of the building, but also for the contents of the structure due to excessive large accelerations that can be developed in case of a collision. Additionally, a possible collision will result in much higher seismic loads and shear forces, and to the excitation of the non-fundamental eigenmodes, with detrimental effects on the structure and its contents.

Nevertheless, ensuring a sufficiently wide seismic gap is not always possible, principally in densely populated areas, due to the spatial constraints and the urban planning regulations.

Therefore, the examination of the influence of soil deformability on the maximum relative displacements at the base isolation level, which determines the size of the required seismic gap, is of very high importance. Figure 7.13 provides the maximum relative displacements at the base isolation level for the base-isolated structure founded on rock, sand, and soft clay, in the horizontal X direction for the load combination G + 0.3Q + Ex + 0.3Ey for the selected NF ground motion records. Moreover, the values of the maximum (in absolute values) relative displacements at the isolation level for each soil type are provided in Table 7.3.

***Table 7.3: Absolute values of the maximum relative displacements at the isolation level in the X direction for the selected NF ground motions for the base-isolated building founded on rock, sand, and soft clay***

| Maximum relative displacements (cm) | | | | | |
|---|---|---|---|---|---|
| | **NF1** | **NF2** | **NF3** | **NF4** | **NF5** |
| Rock | 15.5 | 42.8 | 11.8 | 17.7 | 20.9 |
| Sand | 17.1 | 46.1 | 9.90 | 16.9 | 22.8 |
| Soft clay | 21.5 | 44.1 | 15.1 | 19.0 | 24.9 |

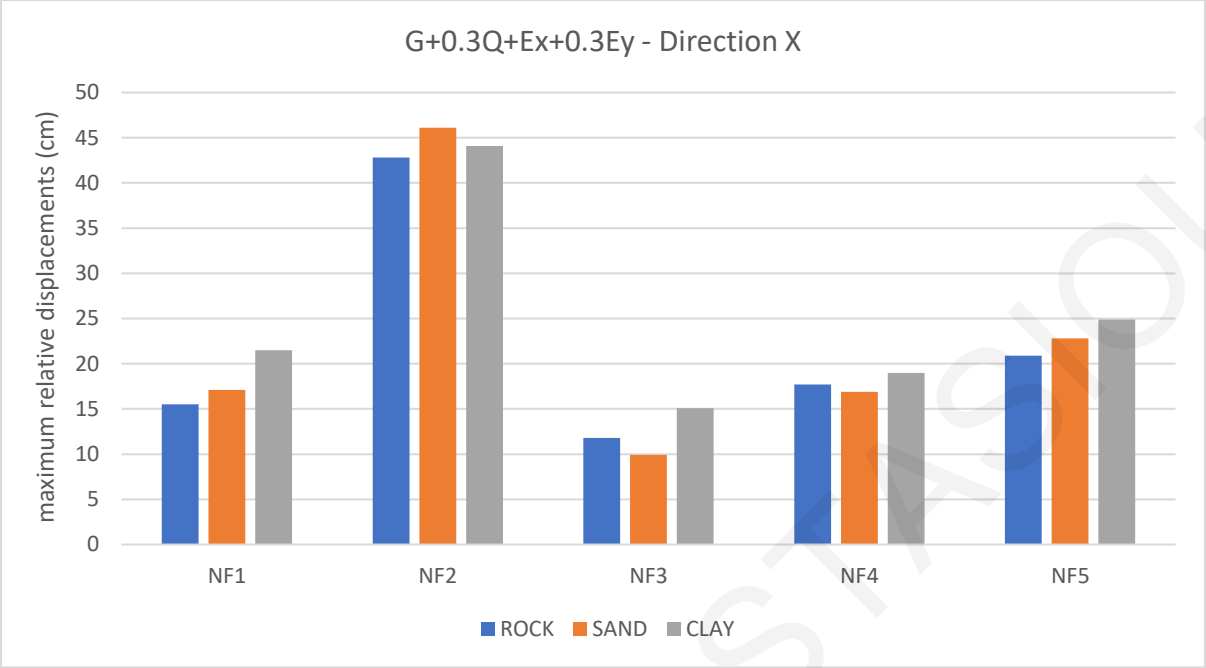


***Figure 7.13: Maximum relative displacements (in absolute values) at the isolation level in the X direction for the base-isolated building founded on rock, sand and soft clay for the selected NF ground motions***

First of all, it is noted that the structure founded on rock, essentially corresponds to the typical assumption of a rigid ground, whereas the structure founded on sand and soft clay are the cases where the soil deformability is taken into consideration. The results of the dynamic time-history analyses (see Table 7.3) show that the required seismic gap that is needed for the base-isolation, to operate without limitations for the structure founded on a rigid ground, is 15.5 cm, 42.8 cm, 11.8 cm, 17.7 cm and 20.9 cm under the excitations of NF1, NF2, NF3, NF4 and NF5, respectively.

According to the computed peak relative displacements at the isolation level, the consideration of soil deformability has remarkably influenced the width of the seismic gap. Specifically, in all cases, the width of the required clearance is significantly higher for the structures founded on sand and soft clay compared to the structure founded on rock. More specifically, for the NF1 there is a rise of about 10% of the maximum relative displacement at the isolation level in the case of sand and an increase of about 39% in the case of soft clay, in comparison to the rock's value. Moreover, the results of the NF5 ground motion are similar to the NF1, with a growth of 9% and 19%, respectively, compared to the

corresponding values on rock. However, the required clearance in the case of sand, under the excitation of NF3, is nearly 2 cm smaller than the corresponding of rock, but soft clay's required gap is larger by more than 3 cm and 5 cm, compared to the first and the latter. The same trend happens under the NF4, too. The only difference is observed in the case of NF2, where the peak relative displacement at the isolation level for the base-isolated structure founded on sand, is the highest among the three cases, while the rock's value is still the smallest.

Overall, it is clear that the required width of the seismic gap that is demanded for a base-isolated structure in order to avoid structural pounding with adjacent structures or the surrounding moat wall due to the expected large relative displacements at the isolation level, is, in general, increasing with the soil deformability. Therefore, the consideration of soil deformability is crucial in the design of a base-isolated structure, for the proper estimation of the required width of the seismic gap at the isolation level, which is something very critical in the design of a base-isolated building.

Figure 7.14 provides the maximum relative displacements at the isolation level for the base-isolated structure founded on rock, sand and soft clay, in the X horizontal direction for the load combination G + 0.3Q + Ex + 0.3Ey for the selected FF ground motion records. The values of the maximum relative displacements for each soil type are provided in Table 7.4.

***Table 7.4: Maximum relative displacements (in absolute values) at the isolation level in the X direction for the selected FF ground motions for the base-isolated building founded on rock, sand and soft clay***

| Maximum relative displacements (cm) | | | | | |
|---|---|---|---|---|---|
| | **FF6** | **FF7** | **FF8** | **FF9** | **FF10** |
| Rock | 18.6 | 6.2 | 15.9 | 13.3 | 15.8 |
| Sand | 21.3 | 6.1 | 16.5 | 13.5 | 13.8 |
| Soft clay | 23.1 | 7.4 | 17.4 | 11.5 | 12.7 |

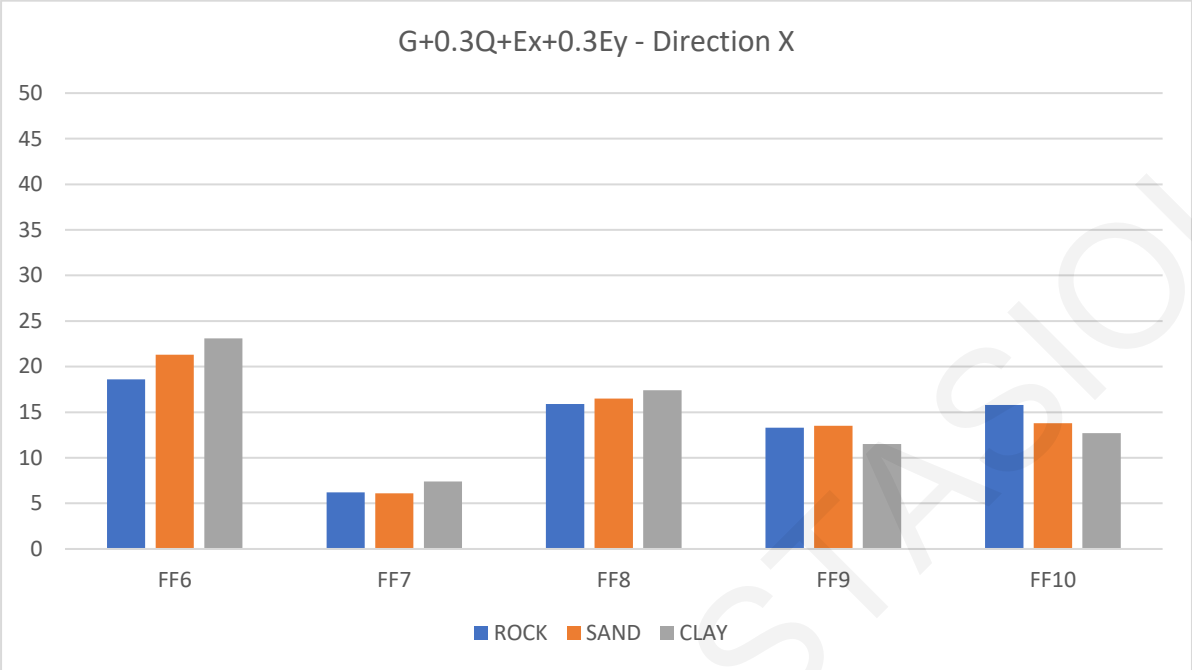


***Figure 7.14: Maximum relative displacements (in absolute values) at the isolation level in the X direction for the base-isolated building founded on rock, sand and soft clay for the selected FF ground motions***

In general, the peak seismic responses, regarding the maximum relative displacements at the isolation level, show that the consideration of the soil deformability increases the demand for the required width of the seismic gap in the case of the FF ground motions, too. Specifically, for the ground motions FF6, FF7 and FF8, the building founded on soft clay develops the highest values of the maximum relative displacement at the isolation level. Moreover, under the FF9 the building founded on sand require the widest seismic gap. However, under the excitation of the FF10, the maximum relative displacement at the isolation level occurs in the case of rock soil type, which is the only case that the soil deformability leads to smaller relative displacements at the isolation level and potentially decreased required width of the seismic gap.

Overall, according to the conducted dynamic analyses, the soil deformability increases the demand of the required width of the seismic gap under the excitation of all the selected NF ground motion records. In contrast, under the excitation of the selected FF ground motions, the required width of the seismic gap is not always bigger when the soil deformability is taken into account.

Furthermore, the maximum relative displacements at the isolation level under the NF ground motion records are much higher than the corresponding peak seismic responses under the corresponding FF ground motion records. Specifically, the NF ground motion records tend to slightly increase the required seismic gap at the isolation level, since the highest maximum relative displacements at the isolation level, among all, are developed under the excitation of NF ground motion records. The only exception is the case of the FF6 excitation, under which the developed maximum relative displacements at the isolation level is the third highest value.

## 7.4 Conclusions

First of all, it is worth to mention that these conclusions concern the computed peak seismic response of the examined base-isolated building under the aforementioned seismic excitations.

The present chapter demonstrates the importance of considering the soil deformability to the peak seismic response of a base-isolated structure. First of all, the analysis results have revealed that the soil deformability has a significant influence on the peak seismic response of a base-isolated structure. Specifically for the excitations that have been considered, the values of the peak interstorey drifts and the maximum floor accelerations are higher for the base-isolated building founded on sand and soft clay, than for the corresponding building founded on rock. Furthermore, the analysis results of the structures under the excitation of the selected NF seismic excitations, show that the soil deformability increases the peak seismic responses. Additionally, the soil deformability under the selected FF ground motion records leads to higher interstorey drifts. However, it is not always negatively affecting the peak seismic response of the building, in terms of absolute floor accelerations.

More importantly, it is worth to underline the significant influence of soil deformability to the proper estimation of the expected maximum relative displacements at the seismic isolation level, which is directly related to the width of the seismic gap that is required to be secured at the perimeter of a base-isolated structure, in order to avoid structural collisions to any adjacent structures. The analysis results show that the relative displacements at the isolation level remarkably increase when the building is founded on

sand and soft clay. Hence, the estimation of the required width of the seismic gap is most likely underestimated when the soil deformability is neglected. Furthermore, the computed maximum relative displacements at the isolation level indicate the importance of using NF seismic excitations to estimate the desired clearance around a base-isolated building.

In conclusion, the consideration of the soil deformability is extremely important, in order to achieve a safer and a more accurate design of a seismically isolated structure and should not be neglected, especially for the estimation of the required width of the seismic gap.

# Chapter 8 - CONCLUDING REMARKS

The dynamic analysis of a building under an earthquake excitation is almost always performed under the assumption that the structure is fixed-supported to an infinitely rigid ground. Hence, the deformability of the supporting soil is customarily neglected, as a conservative simplification. This assumption is based on the expectation that soil deformability can only be beneficial. The soil deformability can alter remarkably the peak seismic response of a structure. Therefore, by neglecting the soil deformability a lower estimation of the peak seismic response might result. Thus, in this thesis the potential influence of the soil deformability on the peak seismic response of a typical conventionally supported and the corresponding base-isolated building, has been assessed.

## 8.1 Summary of the thesis

First of all, in order to examine the potential effect of the soil deformability on the structure's peak seismic response, three different soil types have been considered: rock, sand and soft clay. It is noted that very soft clay is considered deliberately, in order to examine the soil deformability effects in a relatively extreme case. Rock soil type essentially corresponds to the infinitely rigid ground, whereas considering sand and soft clay soil types introduces the relevant soil deformability. It is worth to mention that the whole procedure of configuring and analysing the structure has been implemented through a large number of parametric analyses, using the Python programming language and the Open Application Programming Interface (OAPI) of the SAP2000 structural analysis and design software, as explained in detail in Chapter 3.

More precisely, the soil deformability has been indirectly taken into account with the use of three translational and three rotational springs at each support joint. It has been assumed that the springs behave linearly. Moreover, the springs' coefficients, which represent the stiffness of each spring, depend on the dimensions of the structure's foundation and the mechanical properties of the supporting soil. The calculation of the springs' stiffnesses has been based on Gazetas (1991) expressions, as described in Chapter 4. The structure that has been under examination is a typical two-storey building founded on rock, sand or soft clay.

Specifically, in Chapter 5, the effects of the soil deformability for the examined typical two-storey conventionally supported building have been assessed based on the

computed peak seismic responses, under the selected seismic excitations. In particular, the peak interstorey drifts and the peak absolute floor accelerations, which represent the potential damage on the structural and non-structural elements due to deformations and the effect of excess accelerations on the occupants and contents of the building, have been considered. Furthermore, the soil deformability has been examined in combination with the structure's excitation, under 5 pairs of near-fault (NF) and 5 pairs of far-fault (FF) seismic ground motions. In brief, the results by the executed dynamic time-history analyses have indicated that, the soil deformability can have detrimental effects. Therefore, it might be important to be taken into consideration for the earthquake design of typical conventionally supported structures, to eliminate the possibility of failure due to soil deformability effects.

Moreover, the study of the potential effects of soil deformability on the examined typical base-isolated building has been provided in Chapters 6 and 7. Specifically, the seismically isolated building's superstructure is identical with the conventionally supported structure, while its seismic isolation system consists of a combination of NRBs and LRBs. Through the peak seismic response, it has been shown that the soil deformability can be unfavorable for a base-isolated building and affects remarkably the dynamic response of a base-isolated structure. Lastly, but more importantly, the effect of soil deformability on the maximum relative displacements at the isolation level have been considered. This is very crucial since the maximum relative displacements at the isolation level determine the required width of the seismic gap that is provided perimetrically to a seismic isolated structure, in order to avoid collisions with the moat wall or adjacent structures due to the expected large relative displacements at the isolation level. The computed maximum relative displacements indicate that in all considered cases, the width of the seismic gap that is required has significantly increased for the base-isolated building founded on sand and soft clay compared to the same building founded on rock. Hence, neglecting the soil deformability might lead to an underestimation of the required width of the seismic gap, which can be extremely detrimental for the anticipated operation of the seismic isolation and the adequate protection of the building.

## 8.2 Research outcomes

In general, the results of the conducted parametric studies and dynamic analyses conducted in this research work, agree with most conclusions of the other researchers that

are provided in the scientific literature. The seismic behavior of the examined building founded on different media and subjected to various seismic excitations illustrates that soil deformability, can dramatically affect its peak seismic responses.

First of all, the computed peak seismic responses of the examined typical conventionally supported building is negatively affected by soil deformability, in most of the considered cases. Therefore, the soil deformability should be taken into account in order to obtain more realistic and reliable results of the peak seismic response. Particularly, the computed maximum interstorey drifts values are in most cases higher when the building is founded on sand and soft clay. However, the conducted parametric analyses showed that the influence of soil deformability on the seismic response of the second-floor level can be less intense compared to the first-floor level. Ignoring the soil deformability can lead to an underestimation of the peak seismic response of the structure in terms of the interstorey drifts, especially for the first-floor level. Therefore, the soil deformability can be an important factor for the accurate assessment of peak seismic response of the typical conventionally supported buildings and consequently, it should be taken into consideration in the design of such structures.

More importantly, this thesis indicates that the examined seismically isolated building can be affected even more, by the soil deformability. The isolation system that has been applied at the base level of the examined building consists of 8 LRBs and 12 NRBs, symmetrically distributed. The results of the peak seismic response have shown the strong impact of the soil deformability to the peak seismic behavior of the examined base-isolated building, since the building founded on soft clay develops the highest values for both interstorey drifts and maximum absolute floor accelerations. Furthermore, the soil deformability combined with the effects of the NF and FF seismic ground motion records has illustrated that in all the examined seismic ground motion records, the largest values of the peak interstorey drifts have emerged in the cases where the soil deformability is taken into account. Hence, the soil deformability plays a significant role in the response of the base-isolated structures and should be taken into account.

Furthermore, in this thesis the examination of the potential influence of soil deformability to the maximum relative displacements at the seismic isolation level, which determines the width of the clearance that is demanded for the examined base-isolated building to operate seamlessly and to avoid potential collisions with the surrounding moat

wall and adjacent structures due to the expected large relative displacements at the seismic isolation level, has been considered very important. Hence, the performed dynamic time-history analyses have demonstrated that the base relative displacement at the seismic isolation level is increasing when the soil deformability is taken into account. Consequently, the omission of the effect of the soil deformability can detrimentally lead to an underestimation of the required seismic gap at the isolation level and potential pounding with adjacent structures in case of a very strong earthquake excitation.

Last but not least, the use of the SAP2000 Open Application Programming Interface (OAPI) in combination with the Python programming language has provided the capability of conducting numerous parametric analyses. Specifically, in this thesis 138 parametric analyses have been executed to obtain the desired results. The parametric analyses have been executed in a limited time while changing some values of the developed software in the Python programming language, for each parametric analysis. In comparison with the standard point-and-click procedure, which would have need very long time for the configuration of the model and the extraction of the results, this procedure has saved precious time. Therefore, with this approach parametric analyses have been easily conducted with great flexibility and efficiency. Moreover, the computed results have been efficiently and effectively postprocessed through the OAPI interactions, for their comparison through the parametric studies.

## 8.3 Potential research extensions

This research work aimed to investigate the potential influences of the soil deformability to a typical conventionally supported building, as well the corresponding base-isolated building. The performed dynamic time-history analyses, which have been executed with the utilization of SAP2000 OAPI through software developed in the Python programming language, demonstrated that the peak seismic response can be remarkably affected by the soil deformability. Basically, in order to simulate the soil deformability, a typical R/C building has been founded on sand and soft clay soil types in addition to the typical assumption that the structure is founded on infinitely rigid ground or rock soil type. The mechanical characteristics of rock, sand and soft clay, which have been used in the current thesis, have been chosen through the scientific literature (Bowles, 1997; Fjaer *et al.*, 2008).

The fact that the mechanical characteristics of the utilized soil types are directly related to the peak seismic response of the building, further research can be conducted, using more than a range of values for the definition of each soil type, in order to obtain more comparative results.

Furthermore, in this thesis the building that has been examined is a typical symmetrical two-storey reinforced concrete building. Hence, to expand the investigation of the potential soil deformability effects to other structural systems, different types of buildings such as steel buildings and composite buildings, would have led to more generalized results. Additionally, the examination of taller buildings and/or buildings with larger masses would have achieved a clearer overview of the soil deformability effects and it would have been probably investigated if these factors intensify or not, the soil deformability influences to the structures. Moreover, the assessment of the accidental mass eccentricities of a non-symmetrical structure, in combination with the consideration of the soil deformability would have been of high interest.

Concerning the examined base-isolated structure, the applied isolation system consists of LRBs and NRBs. Due to the lack of similar studies on base isolated structures, an additional study that would have investigated the eventual soil deformability effects by the use of various isolation systems, would be helpful to discover the importance and the magnitude of soil deformability influences on different cases of seismically isolated buildings with different types of seismic isolation system. Finally, it is worth to highlight that further research on how the seismic gap that is demanded at the isolation level is changing, when the soil deformability is taken into account, is essential in order to obtain more comparative results and to extract more general conclusions.

Lastly, the study of the potential effects of the soil deformability on the peak seismic response of a conventionally supported building and a base-isolated building, considering different types of foundations such as strip footings or mat foundation, would have been essential. However, in that case the computational cost of the dynamic time-history analyses would have increased significantly.

# REFERENCES


Aden, M. A. et al. (2019) 'Effects of soil-structure interaction on base-isolated structures', IOP Conference Series: Earth and Environmental Science, 357(1). doi: 10.1088/1755-1315/357/1/012031.

Alavi, B. and Krawinkler, H. (2004) 'Behavior of moment-resisting frame structures subjected to near-fault ground motions', 706(September 2003), pp. 687–706. doi: 10.1002/eqe.369.

Baaren, E. (2021). 'What is Python: the major features and what it's used for'. [online] Available at: https://python.land/python-tutorial/what-is-python [Accessed 01 Feb. 2021].

Bhattacharya, K., Dutta, S. C. and Dasgupta, S. (2004) 'Effect of soil-flexibility on dynamic behaviour of building frames on raft foundation', Journal of Sound and Vibration, 274(1–2), pp. 111–135. doi: 10.1016/S0022-460X(03)00652-7.

Bowles, J. E. (1997) Foundation analysis and design. Fifth Edit. Singapore: The McGraw-Hill Companies, Inc.

Bray, J. D. and Rodriguez-Marek, A. (2004) 'Characterization of forward-directivity ground motions in the near-fault region', 24, pp. 815–828. doi: 10.1016/j.soildyn.2004.05.001.

(2020). 'Comparison of Python with Other Programming Languages'. [online] Available at: https://www.geeksforgeeks.org/comparison-of-python-with-other-programming-languages/ [Accessed 21 Jan. 2021]

'Comparing Python to Other Languages'.[online] Available at: https://www.python.org/doc/essays/comparisons/ [Accessed 21 Jan. 2021]

(2021). 'Difference between Python and C++'. [online] Available at: https://www.geeksforgeeks.org/difference-between-python-and-c/?ref=lbp [Accessed 22 Jan. 2021]

Fajfar, P., Marusic, D. and Perus, I. (2005) 'Torsional effects in the pushover-based seismic analysis of buildings', pp. 37–41. doi: 10.1080/13632460509350568.

Forcellini, D. (2018) 'Seismic assessment of a benchmark based isolated ordinary building with soil structure interaction', Bulletin of Earthquake Engineering, 16(5), pp. 2021–2042. doi: 10.1007/s10518-017-0268-6.

Gazetas, G. (1991) 'Formulas and charts for impedances of surface and embedded foundations'.

Gazetas, G. and Dobry, R. (1984) 'Horizontal response of piles in layered soils', Journal of Geotechnical Engineering, 110(1), pp. 20–40. doi: 10.1061/(ASCE)0733-9410(1984)110:1(20).

Gowda, R., Narayana, G. and Narandra, B. (2015) 'Soil Flexibility Effect on Dynamic Behaviour of Asymmetric 3d Building Frames with Strip Footing by Continuum Model', International Journal of Engineering Research and, V4(06), pp. 892–898. doi: 10.17577/ijertv4is060891.

Hassan, A. and Pal, S. (2018) 'Effect of soil condition on seismic response of isolated base buildings', International Journal of Advanced Structural Engineering, 10(3), pp. 249–261. doi: 10.1007/s40091-018-0195-z.

Karabork, T., Deneme, I. O. and Bilgehan, R. P. (2014) 'A comparison of the effect of SSI on base isolation systems and fixed-base structures for soft soil', Geomechanics and Engineering, 7(1), pp. 87–103. doi: 10.12989/gae.2014.7.1.087.

Kavvadas, M. and Gazetas, G. (1993) 'Kinematic seismic response and bending of free-head piles in layered soil', Geotechnique, 43(2), pp. 207–222. doi: 10.1680/geot.1993.43.2.207.

Krishnamoorthy, A. and Anita, S. (2016) 'Soil-structure interaction analysis of a FPS-isolated structure using finite element model', Structures, 5, pp. 44–57. doi: 10.1016/j.istruc.2015.08.003.

Kunde, M. C. and Jangid, R. S. (2006) 'Effects of Pier and Deck Flexibility on the Seismic Response of Isolated Bridges', Journal of Bridge Engineering, 11(1), pp. 109–121. doi: 10.1061/(asce)1084-0702(2006)11:1(109).

Liao, W., Loh, C. and Wan, S. (2001) 'Earthquake responses of rc moment frames subjected to near-fault ground motions', 229(January 2001), pp. 219–229. doi: 10.1002/tal.178.

Mahmoud, S., Austrell, P. E. and Jankowski, R. (2012) 'Simulation of the response of base-isolated buildings under earthquake excitations considering soil flexibility', Earthquake Engineering and Engineering Vibration, 11(3), pp. 359–374. doi: 10.1007/s11803-012-0127-z.

Malik, U. (2019). 'Advantages and Disadvantages of the Python Programming Language'. [online] Available at: https://learnpython.com/blog/python-programming-advantages-disadvantages/ [Accessed 01 Feb. 2021]

Manos, G. C., Naxakis, D. and Soulis, V. (2015) 'The dynamic and earthquake response of a two story old R/C building with masonry infills in Lixouri-Kefalonia, Greece including soil-foundation deformability', COMPDYN 2015 - 5th ECCOMAS Thematic Conference on Computational Methods in Structural Dynamics and Earthquake Engineering, (January 2015), pp. 435–459. doi: 10.7712/120115.3407.787.

Mavroeidis, G. P., Dong, G. and Papageorgiou, A. S. (2004) 'Near-fault ground motions, and the response of elastic and inelastic single-degree-of-freedom (SDOF) systems', Earthquake Engineering and Structural Dynamics, 33(9), pp. 1023–1049. doi: 10.1002/eqe.391.

Mavronicola, E. (2009). 'Assessing the suitability of equivalent linear elastic analysis of seismically isolated multi-story buildings'. MSc Thesis. University of Cyprus.

Mazza, F. and Vulcano, A. (2011) 'Effects of near-fault ground motions on the nonlinear dynamic response of base-isolated r . c . framed buildings', (May 2011), pp. 211–232. doi: 10.1002/eqe.

Miura, K. et al. (1997) 'NII-Electronic Library Service', Chemical Pharmaceutical Bulletin, 57(534), pp. 364–370. Available at: http://www.mendeley.com/research/geology-volcanic-history-eruptive-style-yakedake-volcano-group-central-japan/.

Mylonakis, G. and Gazetas, G. (2000) 'Seismic soil-structure interaction: Beneficial or detrimental?', Journal of Earthquake Engineering, 4(3), pp. 277–301. doi: 10.1080/13632460009350372.

Narayana, G., Sharada Bai, H. and Manish, A. (2010) 'Effect of Soil Flexibility on Dynamic Behavior of Building Frames Resting on Strip Foundation', Asce, (204), pp. 34–41.

Nikolaou, S. et al. (2001) 'Kinematic pile bending during earthquakes: analysis and field measurements'.

Patel, C., Sharma, K. and Patel, H. S. (2011) 'Modeling of Soil-Structure Interaction as Finite Element Using Using SAP2000'.

Pavlidou, C. (2019). 'Peak seismic response of base-isolated buildings: under near vs. far fault excitations and varying incidence angle'. MSc Thesis. University of Cyprus.

'Python Advantages and Disadvantages – Step in the right direction'. [online] Available at: https://techvidvan.com/tutorials/python-advantages-and-disadvantages/ [Accessed 01 Feb. 2021]

(2021). 'Python vs Java: key differences and code examples'. [online] Available at: https://www.imaginarycloud.com/blog/python-vs-java/ [Accessed 21 Jan. 2021]

(2020). 'Python vs Java: What's The Difference?'. [online] Available at: https://www.bmc.com/blogs/python-vs-java/ [Accessed 21 Jan. 2021]

(2020). 'Python vs. Other Programming Languages'. [online] Available at: https://www.geeksforgeeks.org/python-vs-other-programming-languages/ [Accessed 21 Jan. 2021]

'Python vs. Other Programming Languages'. [online] Available at: https://www.stxnext.com/python-vs-other-programming-languages/ [Accessed 21 Jan. 2021]

(2021). 'Python vs PHP'. [online] Available at: https://www.geeksforgeeks.org/python-vs-php/ [Accessed 22 Jan. 2021]

Somerville, P. G. et al. (1997) 'Modification of Empirical Strong Ground Motion Attenuation Relations to Include the Amplitude and Duration Effects of Rupture Directivity', 68(1).

Somerville, P. G. (2005) 'Engineering characterization of near fault ground motions', (1), pp. 1–8.

Soneji, B. B. and Jangid, R. S. (2008) 'Influence of soil-structure interaction on the response of seismically isolated cable-stayed bridge', Soil Dynamics and Earthquake Engineering, 28(4), pp. 245–257. doi: 10.1016/j.soildyn.2007.06.005.

Spyrakos, C. C., Koutromanos, I. A. and Maniatakis, C. A. (2009) 'Seismic response of base-isolated buildings including soil-structure interaction', Soil Dynamics and Earthquake Engineering, 29(4), pp. 658–668. doi: 10.1016/j.soildyn.2008.07.002.

Stehmeyer, E. H. and Rizos, D. C. (2008) 'Considering dynamic soil structure interaction (SSI) effects on seismic isolation retrofit efficiency and the importance of natural frequency ratio', Soil Dynamics and Earthquake Engineering, 28(6), pp. 468–479. doi: 10.1016/j.soildyn.2007.07.008.

Tongaonkar, N. P. and Jangid, R. S. (2003) 'Seismic response of isolated bridges with soil-structure interaction', Soil Dynamics and Earthquake Engineering, 23(4), pp. 287–302. doi: 10.1016/S0267-7261(03)00020-4.

Vlassis, A. G. and Spyrakos, C. C. (2001) 'Seismically isolated bridge piers on shallow soil stratum with soil-structure interaction', Computers and Structures, 79(32), pp. 2847–2861. doi: 10.1016/S0045-7949(01)00105-5.

'What is an API? (Application Programming Interface)'. [online] Available at: https://www.mulesoft.com/resources/api/what-is-an-api [Accessed 01 Feb. 2021]

(2021). 'What Is an API? Introduction to Basics and Examples of APIs for 2022'. [online] Available at: https://www.upwork.com/resources/what-is-an-api [Accessed 01 Feb. 2021]

Wolf, J. P. and Somaini, D. R. (1986) 'Approximate dynamic model of embedded foundation in time domain', Earthquake Engineering & Structural Dynamics, 14(5), pp. 683–703. doi: 10.1002/eqe.4290140502.

Wu, W. H. and Chen, C. Y. (2001) 'Simple lumped-parameter models of foundation using mass-spring-dashpot oscillators', Journal of the Chinese Institute of Engineers, Transactions of the Chinese Institute of Engineers,Series A/Chung-kuo Kung Ch'eng Hsuch K'an, 24(6), pp. 681–697. doi: 10.1080/02533839.2001.9670665.

Zhang, S. and Wang, G. (2013) 'Effects of near-fault and far-fault ground motions on nonlinear dynamic response and seismic damage of concrete gravity dams', Soil Dynamics and Earthquake Engineering, 53, pp. 217–229. doi: 10.1016/j.soildyn.2013.07.014.

(2018). '8 advantages of APIs for developers'. [online] Available at: https://www.bbvaapimarket.com/en/api-world/8-advantages-apis-developers/ [Accessed 13 Jul. 2021]

**Greek Literature**

Βαρνάβα, Β. (2012). 'Προσομοίωση, ανάλυση και σχεδιασμός σεισμικά μονωμένου μεταλλικού κτιρίου'. Έρευνα Διατριβής. Πανεπιστήμιο Κύπρου.

ΚΩΣΤΟΠΟΥΛΟΥ Δ. ΑΙΚΑΤΕΡΙΝΗ (2016) Ι. Ν. Ψυχάρης. Διπλωματική Εργασία. ΕΘΝΙΚΟ ΜΕΤΣΟΒΙΟ ΠΟΛΥΤΕΧΝΕΙΟ.

**Code Specifications**

CYS National Annex to CYS EN 1991-1-1:2002. Eurocode1: Actions on buildings - Part 1- 1: General actions -Densities, self-weight, imposed loads for buildings. Nicosia: Eurocodes Committee, Scientific and Technical Chamber of Cyprus under a Ministry of Interior's Programme.

CYS National Annex to CYS EN 1998-1:2004. Eurocode8: Design of buildings for earthquake resistance - Part 1: General rules, seismic actions and rules for buildings. Nicosia: Eurocodes Committee, Scientific and Technical Chamber of Cyprus under a Ministry of Interior's Programme.

EN 1998-1:2004. Eurocode8: Design of buildings for earthquake resistance - Part 1: General rules, seismic actions and rules for buildings. Brussels: European Committee for Standardization.

# APPENDIX A

It is noted that the following written commands is just a brief sample of the utilized algorithm, and it does not correspond to the complete written algorithm that is needed to execute the parametric analyses for the considered cases, in this thesis.

```
import os

import sys

import comtypes.client

#Setting the following flag to False, a new instance of the program will be started

AttachToInstance = False

#Setting the following flag to False,the latest installed version of SAP2000 will be launched

SpecifyPath = False

#Specifying the path to SAP2000

ProgramPath = 'C:\Program Files\Computers and Structures\SAP2000 22\SAP2000.exe'

#Full path of the model

APIPath = 'C:\CSiAPI-SAP2000\diatrivi''

#If the desired folder it doesn't exist, it is created. Otherwise, the program continues

if not os.path.exists(APIPath):

try:

os.makedirs(APIPath)

except OSError:

pass

# Determination a variable which includes the full path with the specific name of the file

ModelPath = APIPath + os.sep + 'baseisolatedwithsprings-1.sdb'

#SAP2000 API object creation

if AttachToInstance:

#attach to a running instance of SAP2000
```

```
try:
#get the active SapObject
mySapObject = comtypes.client.GetActiveObject("CSI.SAP2000.API.SapObject")
except (OSError, comtypes.COMError):
print("No running instance of the program found or failed to attach.")
sys.exit(-1)
else:
#create API helper object
helper = comtypes.client.CreateObject('SAP2000v1.Helper')
helper = helper.QueryInterface(comtypes.gen.SAP2000v1.cHelper)
if SpecifyPath:
try:
#'create an instance of the SAPObject from the specified path
mySapObject = helper.CreateObject(ProgramPath)
except (OSError, comtypes.COMError):
print("Cannot start a new instance of the program from " + ProgramPath)
sys.exit(-1)
else:
try:
#create an instance of the SAPObject from the latest installed SAP2000
mySapObject = helper.CreateObjectProgID("CSI.SAP2000.API.SapObject")
except (OSError, comtypes.COMError):
print("Cannot start a new instance of the program.")
sys.exit(-1)
#Starting SAP2000 application via ApplicationStart() function
mySapObject.ApplicationStart()
#Creation of SapModel object
SapModel = mySapObject.SapModel
```

```
#Initializion of the model. The units to be used in the current file will be kN,m,C which they symbolized with number 6

SapModel.InitializeNewModel(6)

#Creation of a new blank model

ret = SapModel.File.NewBlank()

#Definition of materials properties

MATERIAL_CONCRETE = 2

ret = SapModel.PropMaterial.AddMaterial('C30/37',MATERIAL_CONCRETE,'Europe','EN 1992-1-1 per EN 206-1','C30/37')

#Definition of rectangular frame section property

ret = SapModel.PropFrame.SetRectangle('Col50/50', 'C30/37', 0.50, 0.50)

#Definition of frame section property modifiers

ColModValue = [1, 0.5, 0.5, 0.1, 0.5, 0.5, 1, 1]

ret = SapModel.PropFrame.SetModifiers('Col50/50', ColModValue)

#Definition of T frame section property for double-sided beam

#Definition of Γ frame section property for single-sided beam

#Definition of T,Γ frame section property modifiers

ret = SapModel.PropFrame.SetTee('AmphiplevridokosX', 'C30/37', 0.60,0.85,0.15,0.25)

ret = SapModel.PropFrame.SetTee('AmphiplevridokosY', 'C30/37', 0.60,0.73,0.15,0.25)

ret = SapModel.PropFrame.SetAngle('MonoplevridokosX', 'C30/37', 0.60,1.95,0.15,0.25)

ret = SapModel.PropFrame.SetAngle('MonoplevridokosY', 'C30/37', 0.60,1.61,0.15,0.25)

BeamModValue = [1, 0.5, 0.5, 0.1, 0.5, 0.5, 1, 1]

ret = SapModel.PropFrame.SetModifiers('AmphiplevridokosX', BeamModValue)

ret = SapModel.PropFrame.SetModifiers('AmphiplevridokosY', BeamModValue)

ret = SapModel.PropFrame.SetModifiers('MonoplevridokosX', BeamModValue)

ret = SapModel.PropFrame.SetModifiers('MonoplevridokosY', BeamModValue)

#Design of Model through .FrameObj.AddByCoord() function

#(Xi,Yi,Zi,Xj,Yj,Zj,element name,section name,name of element for the user,coordinate system)
```

```
# Ground Floor Columnmns

K11=' '

K21=' '

K31=' '

K41=' '

K51='

…

[K11,ret]= SapModel.FrameObj.AddByCoord(0,0,0,0,0,3,K11,'Col50/50','K11','Global')

[K21,ret]= SapModel.FrameObj.AddByCoord(5,0,0,5,0,3,K21,'Col50/50','K21','Global')

[K31,ret]= SapModel.FrameObj.AddByCoord(10,0,0,10,0,3,K31,'Col50/50','K31','Global')

[K41,ret]= SapModel.FrameObj.AddByCoord(15,0,0,15,0,3,K41,'Col50/50','K41','Global')

[K51,ret]= SapModel.FrameObj.AddByCoord(0,4,0,0,4,3,K51,'Col50/50','K51','Global')

…

# First Floor Columnmns

K12=' '

K22=' '

K32=' '

K42=' '

K52=' '

…

[K12,ret]= SapModel.FrameObj.AddByCoord(0,0,3,0,0,6,K12,'Col50/50','K12','Global')

[K22,ret]= SapModel.FrameObj.AddByCoord(5,0,3,5,0,6,K22,'Col50/50','K22','Global')

[K32,ret]= SapModel.FrameObj.AddByCoord(10,0,3,10,0,6,K32,'Col50/50','K32','Global')

[K42,ret]= SapModel.FrameObj.AddByCoord(15,0,3,15,0,6,K42,'Col50/50','K42','Global')

[K52,ret]= SapModel.FrameObj.AddByCoord(0,4,3,0,4,6,K52,'Col50/50','K52','Global')

…

#First Floor Beams

#Where necessary, the beams will be rotated to correctly determine the effective flange width
```

```
#with the function .FrameObj.SetLocalAxes()

D11=' '

D21=' '

D31=' '

D41=' '

D51=' '

…

[D11,ret]= SapModel.FrameObj.AddByCoord(5,0,3,0,0,3,D11,'MonoplevridokosX','D11','Global')

[D21,ret]= SapModel.FrameObj.AddByCoord(10,0,3,5,0,3,D21,'MonoplevridokosX','D21','Global')

[D31,ret]= SapModel.FrameObj.AddByCoord(15,0,3,10,0,3,D31,'MonoplevridokosX','D31','Global')

[D41,ret]= SapModel.FrameObj.AddByCoord(0,4,3,5,4,3,D41,'AmphiplevridokosX','D41','Global')

[D51,ret]= SapModel.FrameObj.AddByCoord(5,4,3,10,4,3,D51,'AmphiplevridokosX','D51','Global')

…

ret = SapModel.FrameObj.SetEndLengthOffset('D11',False,0.25,0.25,0.5,0)

ret = SapModel.FrameObj.SetEndLengthOffset('D21',False,0.25,0.25,0.5,0)

ret = SapModel.FrameObj.SetEndLengthOffset('D31',False,0.25,0.25,0.5,0)

ret = SapModel.FrameObj.SetEndLengthOffset('D41',False,0.25,0.25,0.5,0)

ret = SapModel.FrameObj.SetEndLengthOffset('D51',False,0.25,0.25,0.5,0)

#Second Floor Beams

D12=' '

D22=' '

D32=' '

D42=' '

D52=' '

…

[D12,ret]= SapModel.FrameObj.AddByCoord(5,0,6,0,0,6,D12,'MonoplevridokosX','D12','Global')

[D22,ret]= SapModel.FrameObj.AddByCoord(10,0,6,5,0,6,D22,'MonoplevridokosX','D22','Global')

[D32,ret]= SapModel.FrameObj.AddByCoord(15,0,6,10,0,6,D32,'MonoplevridokosX','D32','Global')
```

```
[D42,ret]= SapModel.FrameObj.AddByCoord(0,4,6,5,4,6,D42,'AmphiplevridokosX','D42','Global')

[D52,ret]= SapModel.FrameObj.AddByCoord(5,4,6,10,4,6,D52,'AmphiplevridokosX','D52','Global')

…

ret= SapModel.FrameObj.SetLocalAxes(D11,-180,0)

ret= SapModel.FrameObj.SetLocalAxes(D21,-180,0)

ret= SapModel.FrameObj.SetLocalAxes(D31,-180,0)

…

# Determination of base-isolation

# NRBs and LRBs

dofiso=[True,True,True,True,True,True]

fixediso=[False,False,False,False,False,False]

lineariso=[False,False,False,False,False,False]

nlineariso=[False,True,True,False,False,False]

kenrb=[1273048,1239,1239,21.58,21.58,21.58]

kelrb=[897048,2288,2288,21.56,21.56,21.56]

ceiso=[0,0,0,0,0,0]

kiso=[0,1200,1200,0,0,0]

yieldiso=[0,49.59,49.59,0,0,0]

ratioiso=[0,0.0364,0.0364,0,0,0]

dj2iso=0.0015

dj3iso=0.0015

ret=SapModel.PropLink.SetRubberIsolator('NRB',dofiso,fixediso,lineariso,kenrb,ceiso,kiso,yieldiso,ratioiso,dj2iso,dj3iso)

ret=SapModel.PropLink.SetRubberIsolator('LRB',dofiso,fixediso,nlineariso,kelrb,ceiso,kiso,yieldiso,ratioiso,dj2iso,dj3iso)

ret = SapModel.PropLink.SetWeightAndMass('NRB',1.158,0.118,0.032,0.032,0.032)

ret = SapModel.PropLink.SetWeightAndMass('LRB',1.167,0.119,0.032,0.032,0.032)

# Add Special points for soil springs
```

```
ret= SapModel.PointObj.AddCartesian(0,0,-1,'sp1','sp1','Global',True,0)

ret = SapModel.PointObj.SetSpecialPoint('sp1',True,0)

ret = SapModel.PointObj.AddCartesian(5,0,-1,'sp2','sp2','Global',True,0)

ret = SapModel.PointObj.SetSpecialPoint('sp2',True,0)

ret = SapModel.PointObj.AddCartesian(10,0,-1,'sp3','sp3','Global',True,0)

ret = SapModel.PointObj.SetSpecialPoint('sp3',True,0)

…

#Determination of (Base) Structural Supports

#Firsty, the base point of each column have to be located and then the type of each structural support is going to be determined by the function .PointObj.SetRestraint()

#AND Determination of diaphragm on each level

ret= SapModel.ConstraintDef.SetDiaphragm('DIAPH',3,'Global')

ret= SapModel.ConstraintDef.SetDiaphragm('DIAPH2',3,'Global')

Restraint = [False,False,False,False,False,False]

SpringStif = [46285714,46285714,54480000,6075000,6075000,10504688] #ROCK

# SpringStif = [15152,15152,19402,2164,2164,3242] #SAND

# SpringStif = [3767,3767,5067,565,565,782] #CLAY

PointName1= ' '

PointName01= ' '

PointName02= ' '

sp1= ' '

[sp1,ret] = SapModel.PointObj.GetSpecialPoint('sp1',True)

[PointName1,PointName01,ret] = SapModel.FrameObj.GetPoints(K11,PointName1,PointName01)

[PointName01,PointName02,ret] = SapModel.FrameObj.GetPoints(K12,PointName01,PointName02)

ret= SapModel.PointObj.SetConstraint(PointName01,'DIAPH',0,True)

ret= SapModel.PointObj.SetConstraint(PointName02,'DIAPH2',0,True)

ret = SapModel.PointObj.SetRestraint('sp1',Restraint)

ret = SapModel.PointObj.SetSpring('sp1',SpringStif,0,False,True)
```

```
PointName2= ' '

PointName21= ' '

PointName22= ' '

sp2= ' '

[sp2,ret] = SapModel.PointObj.GetSpecialPoint('sp2',True)

[PointName2,PointName21,ret] = SapModel.FrameObj.GetPoints(K21,PointName2,PointName21)

[PointName21,PointName22,ret] = SapModel.FrameObj.GetPoints(K22,PointName21,PointName22)

ret= SapModel.PointObj.SetConstraint(PointName21,'DIAPH',0,True)

ret= SapModel.PointObj.SetConstraint(PointName22,'DIAPH2',0,True)

ret = SapModel.PointObj.SetRestraint('sp2',Restraint)

ret = SapModel.PointObj.SetSpring('sp2',SpringStif,0,False,True)

…

#Assign seismic isolation to the base joints

ret = SapModel.LinkObj.AddByCoord(0,0,0,0,0,-1,'NRB1',False,'NRB','NRB1','Global')

ret = SapModel.LinkObj.AddByCoord(5,0,0,5,0,-1,'LRB2',False,'LRB','LRB2','Global')

ret = SapModel.LinkObj.AddByCoord(10,0,0,10,0,-1,'LRB3',False,'LRB','LRB3','Global')

ret = SapModel.LinkObj.AddByCoord(15,0,0,15,0,-1,'NRB4',False,'NRB','NRB4','Global')

ret = SapModel.LinkObj.AddByCoord(0,4,0,0,4,-1,'LRB5',False,'LRB','LRB5','Global')

ret = SapModel.LinkObj.AddByCoord(5,4,0,5,4,-1,'NRB6',False,'NRB','NRB6','Global')

ret = SapModel.LinkObj.AddByCoord(10,4,0,10,4,-1,'NRB7',False,'NRB','NRB7','Global')

ret = SapModel.LinkObj.AddByCoord(15,4,0,15,4,-1,'LRB8',False,'LRB','LRB8','Global')

ret = SapModel.LinkObj.AddByCoord(0,8,0,0,8,-1,'NRB9',False,'NRB','NRB9','Global')

ret = SapModel.LinkObj.AddByCoord(5,8,0,5,8,-1,'NRB10',False,'NRB','NRB10','Global')

…

# Determination of load type

#Load Patterns creation through .LoadPatterns.Add() function

ret = SapModel.LoadPatterns.ChangeName('DEAD','Idiovaros')

ret= SapModel.LoadPatterns.Add('Idiovaros',1,1,True)
```

```
ret= SapModel.LoadPatterns.Add('Monimo',1,0,True)

ret= SapModel.LoadPatterns.Add('Kinito',3,0,True)

ret= SapModel.LoadPatterns.Add('Ex_spectrum',5,0,True)

ret= SapModel.LoadPatterns.Add('Ey_spectrum',5,0,True)

ret= SapModel.LoadPatterns.Add('Ex_time',5,0,True)

ret= SapModel.LoadPatterns.Add('Ey_time',5,0,True)

# Design spectra creation with function .Func.FuncRS.SetEurocode82004_1()

ret=SapModel.Func.FuncRS.SetEurocode82004_1('SpectrumX',1,1,1,1,0.25,1,0.90,0.15,0.40,2,0.20,3.9,0.05)

ret=SapModel.Func.FuncRS.SetEurocode82004_1('SpectrumY',1,1,1,1,0.25,1,0.90,0.15,0.40,2,0.20,3.9,0.05)

# Time-History function

ret = SapModel.Func.FuncTH.SetFromFile_1('EQX','C:\FF\EQ6\\6X.txt',0,0,1,2,True)

ret = SapModel.Func.FuncTH.SetFromFile_1('EQY','C:\FF\EQ6\\6Y.txt',0,0,1,2,True

#Determination of Load Case

ret = SapModel.LoadCases.ModalEigen.SetNumberModes('MODAL',10,1)

#Response Spectrum X

ret = SapModel.LoadCases.ResponseSpectrum.SetCase('EX_spectrum')

ux = ['U1']

funx = ['SpectrumX']

sf = [9.81]

gl=['Global']

ang=[0]

ret = SapModel.LoadCases.ResponseSpectrum.SetLoads('EX_spectrum',1,ux,funx,sf,gl,ang)

ret = SapModel.LoadCases.ResponseSpectrum.SetModalComb_1('EX_spectrum',2,1,0,1,60)

#Response Spectrum Y

ret = SapModel.LoadCases.ResponseSpectrum.SetCase('EY_spectrum')

uy = ['U2']

funy = ['SpectrumY']

ret = SapModel.LoadCases.ResponseSpectrum.SetLoads('EY_spectrum',1,uy,funy,sf,gl,ang)
```

```
ret = SapModel.LoadCases.ResponseSpectrum.SetModalComb_1('EY_spectrum',2,1,0,1,60)

#Determination of Loads Combination

#1,35G+1,5Q

ret = SapModel.LoadCases.StaticLinear.SetCase('1.50G+1.35Q')

load_comb1=['Load','Load','Load']

loadname_comb1=['Idiovaros','Monimo','Kinito']

load_comb1_sf=[1.5,1.5,1.35]

ret=SapModel.LoadCases.StaticLinear.SetLoads('1.50G+1.35Q',3,load_comb1,loadname_comb1,load_comb
1_sf)

#1,00G+0,30Q

ret = SapModel.LoadCases.StaticLinear.SetCase('1.00G+0.30Q')

load_comb1=['Load','Load','Load']

loadname_comb1=['Idiovaros','Monimo','Kinito']

load_comb1_sf2=[1,1,0.30]

ret=SapModel.LoadCases.StaticLinear.SetLoads('1.00G+0.30Q',3,load_comb1,loadname_comb1,load_comb
1_sf2)

#Seismic loads with design spectra

#1,00Ex+0,30Ey

ret = SapModel.LoadCases.ResponseSpectrum.SetCase('1.00Ex+0.30Ey')

u_comb1=['U1','U2']

fun_comb1=['SpectrumX','SpectrumY']

sf_comb1=[9.81,2.943]

gl1=['Global','Global']

ang_comb1=[0,0]

ret=SapModel.LoadCases.ResponseSpectrum.SetLoads('1.00Ex+0.30Ey',2,u_comb1,fun_comb1,sf_comb1,gl
1,ang_comb1)

ret = SapModel.LoadCases.ResponseSpectrum.SetModalComb_1('1.00Ex+0.30Ey',2,1,0,1,60)

#1,00Ex-0,30Ey
```

```
ret = SapModel.LoadCases.ResponseSpectrum.SetCase('1.00Ex-0.30Ey')

u_comb1=['U1','U2']

fun_comb1=['SpectrumX','SpectrumY']

sf_comb1=[9.81,2.943]

gl1=['Global','Global']

ang_comb2=[0,180]

ret=SapModel.LoadCases.ResponseSpectrum.SetLoads('1.00Ex-
0.30Ey',2,u_comb1,fun_comb1,sf_comb1,gl1,ang_comb2)

ret = SapModel.LoadCases.ResponseSpectrum.SetModalComb_1('1.00Ex-0.30Ey',2,1,0,1,60)

…

# Time-History Seismic load cases

####################

#1,00Ext+0,30Eyt

ret = SapModel.LoadCases.DirHistNonlinear.SetCase('1.00Ext+0.30Eyt')

Loadty2=['Accel','Accel']

u_timecomb=['U1','U2']

fun_timecomb=['EQX','EQY']

sf_time2=[9.81,2.943]

tf_time2=[1,1]

af_time2=[0,0]

gl1=['Global','Global']

ang_time2=[0,0]

ret=SapModel.LoadCases.DirHistNonlinear.SetLoads('1.00Ext+0.30Eyt',2,Loadty2,u_timecomb,fun_timecom
b,sf_time2,tf_time2,af_time2,gl1,ang_time2)

ret = SapModel.LoadCases.DirHistNonlinear.SetTimeStep('1.00Ext+0.30Eyt',2200,0.02)

…

# Set Time Integration Method

ret = SapModel.LoadCases.DirHistNonlinear.SetTimeIntegration('1.00Ext+0.30Eyt',1,0,0.25,0.5,0,0)
```

```
#Determination of imposed loads
# slab self-weight, dead slab and masonries and live slab loads
# dead loads 1
ret=SapModel.FrameObj.SetLoadDistributed(D11,'Monimo',1,10,0,5,14.96,14.96,'Global',False,False,0)
ret=SapModel.FrameObj.SetLoadDistributed(D21,'Monimo',1,10,0,5,14.13,14.13,'Global',False,False,0)
ret=SapModel.FrameObj.SetLoadDistributed(D31,'Monimo',1,10,0,5,14.99,14.99,'Global',False,False,0)
ret=SapModel.FrameObj.SetLoadDistributed(D41,'Monimo',1,10,0,5,21.47,21.47,'Global',False,False,0)
ret=SapModel.FrameObj.SetLoadDistributed(D51,'Monimo',1,10,0,5,18.11,18.11,'Global',False,False,0)
…
#live loads 1
ret = SapModel.FrameObj.SetLoadDistributed(D11,'Kinito',1,10,0,5,1.76,1.76,'Global',False,False,0)
ret = SapModel.FrameObj.SetLoadDistributed(D21,'Kinito',1,10,0,5,1.44,1.44,'Global',False,False,0)
ret = SapModel.FrameObj.SetLoadDistributed(D31,'Kinito',1,10,0,5,1.77,1.77,'Global',False,False,0)
ret = SapModel.FrameObj.SetLoadDistributed(D41,'Kinito',1,10,0,5,5.78,5.78,'Global',False,False,0)
ret = SapModel.FrameObj.SetLoadDistributed(D51,'Kinito',1,10,0,5,4.5,4.5,'Global',False,False,0)
…
# Determination of Mass
# loadpat=['Idiovaros']
# loadpat_sf=[0]
loadpat=['Monimo','Kinito']
loadpat_sf=[1,0.3]
ret= SapModel.SourceMass.SetMassSource('MSSSRC1',True,True,True,True,2,loadpat,loadpat_sf)
# File Saving to the previously defined path
ret= SapModel.File.Save(ModelPath)
# Analysis
DOF=[True,True,True,True,True,True]
ret= SapModel.Analyze.SetActiveDOF(DOF)
# ret= SapModel.Analyze.SetRunCaseFlag('Idiovaros',True,True)
```

```
ret= SapModel.Results.Setup.SetOptionDirectHist(2) # entoli xronoistorias

ret= SapModel.Analyze.RunAnalysis()

…

#Exit Application

ret= mySapObject.ApplicationExit(True)
```